UNIVERSITY OF CALIFORNIA, SAN DIEGO

Cross layer design for the transmission of multimedia over wireless channels

A Dissertation submitted in partial satisfaction
of the requirements for the degree

Doctor of Philosophy

in

Electrical Engineering
(Communication Theory and Systems)

by

Hobin Kim

Committee in charge:

Professor Pamela C. Cosman, Co-chair
Professor Laurence B. Milstein, Co-chair
Professor William S. Hodgkiss
Professor Bhaskar D. Rao
Professor Ruth J. Williams

2011

The dissertation of Hobin Kim is approved and it is acceptable in quality and form for publication on microfilm and electronically:

Co-chair

Co-chair

University of California, San Diego

2011

DEDICATION

To my parents and my wife

TABLE OF CONTENTS

LIST OF FIGURES

LIST OF TABLES

ACKNOWLEDGEMENTS

It is my pleasure to thank many people who supported my Ph.D. study in UCSD for the last five years.

First of all, I would like to express my deep and sincere gratitude to my advisors, Profs. Pamela Cosman and Laurence Milstein, for their excellent guidance, caring, patience, and support. Prof. Cosman brought many interesting and practical problems in multimedia communication to my attention and taught me how to express my ideas efficiently in both presentations and published papers. She always helped me to see the big picture of my research and gave me clear guidance. Without her brilliant ideas and critical comments based on the wide research experiences from the data compression to the communication, this dissertation would not have been possible. Prof. Milstein is distinguished by his depth of knowledge in wireless communication and his powerful mathematical ability. His technical advice was essential to the completion of this dissertation.

My thanks also go to Dr. Ramesh Annavajjala from Mitsubishi Electric Research Labs, who is my friend as well as sincere mentor, and to Prof Sun Yong Kim and Prof. Minjoong Rim, who were visiting scholars at UCSD. Dr. Annavajjala helped me start my research at UCSD, and invited me to Mitsubishi Electric Resrach Labs to obtain industrial experience. Whenever I needed help, he gave me his inspiring ideas and advice. Prof. Kim and Prof. Rim also gave me lots of comments on the research. Their professional knowledge and experience in wireless communications helped me build my research background.

I would like to thank my dissertation committee members, Prof. Bhaskar Rao, Prof. William Hodgkiss and Prof. Ruth Williams for their invaluable time and feedback in my Ph.D. qualifying exam and defense exam. The suggestions from them have strengthened the dissertation.

I am also thankful to my friends in the lab for positive interactions. I want to thank Ting-Lan Lin and Mayank Tiwari, who introduced me to video coding. I also want to thank Seok-Ho Chang, Sheu-Sheu Tan, and Seongho Huh for sharing their knowledge and research.

I am thankful to all my friends in San Diego. Whenever my wife and I have encountered trouble, many sincere friends in San Diego helped us and encouraged me to pursue my study.

Most importantly, none of this would have been possible without the love and unconditional support of my family. Especially, I want to thank my mother Kyong Sook Shin and my father Ssang Su Kim for their encouragement and support to pursue my degree without any concerns. I also thank my other family members for bringing happiness and fun to the family.

Finally, I would like to thank my lovely wife Min Jung Kang for her dedication and support. Without her, it would have been much harder to complete my Ph.D. Whenever I became tired of research, she helped me refresh my brain and return to my workplace. I also thank our unborn baby, who made my wife and me so excited and happy.

Chapter II of this dissertation is partial a reprint of the material as it appears in H. Kim, R. Annavajjala, P.C. Cosman and L.B. Milstein, "Source-channel rate optimization for progressive image transmission over block fading relay channels", *IEEE Transactions on Communications*, vol. 58, No. 6, pp. 1631-1642, June 2010. I was the primary author and the co-authors Dr. Annavajjala, Prof. Cosman and Prof. Milstein directed and supervised the research which forms the basis for Chapters II.

Chapter III of this dissertation is a partial reprint of the material as it appears in H. Kim, P.C. Cosman and L.B. Milstein, "Superposition coding based cooperative communication with relay selection", *44th Asilomar Conference on Signals, Systems and Computers*, November, 2010. I was the primary author of this paper. Co-authors Prof. Cosman and Prof. Milstein directed and supervised the research which forms the basis for Chapter III.

Chapter IV of this dissertation is a partial reprint of the material as it appears in H. Kim, S.Y. Kim, P.C. Cosman and L.B. Milstein, "Motion-compensated scalable video transmission over MIMO wireless channels under imperfect channel estimation", *IEEE Global Communication Conference (Globecom)*, December, 2009. I was the primary author. Co-authors Prof. Kim, Prof. Cosman and Prof. Milstein directed and supervised the research which forms the basis for Chapter IV.

VITA

1977	Born, Masan, South Korea
Feb 2003	B.S., Department of Electrical, Electronic and Computer Engineering Hanyang University, Seoul, Korea
Dec 2004	M.S., Department of Electrical Engineering and Computer Science University of Michigan, Ann Arbor, MI
Jan 2005–Jun 2006	Senior Engineer LG Electronics Mobile Research, San Diego, CA
Jun 2007–Jun 2011	Research Assistant, University of California, San Diego
Summer 2008	Intern, Mitsubishi Electric Research Laboratory, Cambridge, MA
Jun 2011	Ph.D., Electrical Engineering (Communication Theory and Systems) University of California, San Diego

PUBLICATIONS

Journal Papers

H. Kim, R. Annavajjala, P. Cosman, L. Milstein, "Source-channel rate optimization for progressive image transmission over block fading relay channels", *IEEE Transactions on Communications*, Volume 58, Issue 6, pp. 1631-1642, Jun, 2010.

Conference Papers

H. Kim, P. Cosman, L. Milstein, "Motion-compensated scalable video transmission over MIMO wireless channels under imperfect channel estimation ", *IEEE Globecom 2009*

H. Kim, P. Cosman, L. Milstein, "Superposition coding based cooperative communication with relay selection", *44th Asilomar Conference on Signals, Systems and Computers*, 2010

S. Wang, H. Kim, B.K. Yi, S. Kwon, "On the feedback channel for MIMO beamforming", *IEEE WCNC 2008*

S. Wang, S.G. Kim, L-H. Sun, H. Kim, S.W. Lee, S.R. Subramanya, K.Y. Kim, B.K. Yi, "Semi-blind adaptive multiuser detection for asynchronous CDMA", *IEEE Electro Information Technology 2005*

ABSTRACT OF THE DISSERTATION

Cross layer design for the transmission of multimedia over wireless channels

by

Hobin Kim

Doctor of Philosophy in Electrical Engineering (Communication Theory and Systems)

University of California, San Diego, 2011

Professor Pamela C. Cosman, Co-chair

Professor Laurence B. Milstein, Co-chair

When we transmit multimedia through wireless channels, we need to protect source bits from channel noise. However, due to the constraints on the channel resources, source and channel bits should share the resources optimally in the sense of distortion or throughput. That is, the problem is how to allocate channel resources such as the bandwidth, diversity, or transmit power to the source and channel under system constraints. In addition, due to the unequal priority of source packets, performance can be improved by assigning unequal channel resources to the packets based on their priority. In this dissertation, we introduce an information-theoretic framework which allows us to analyze the system performance mathematically with unequal allocation of the channel resources with respect to the unequal priority of the source packets. By applying the information-theoretic framework, an algorithm to find the throughput-optimal unequal error protection (UEP) is derived.

The first example to apply this framework is the progressive image transmission over block fading channels with relay-assisted distributed spatial diversity. Assuming a progressive image coder with a constraint on the transmission bandwidth, we formulate a joint source-channel rate allocation scheme that maximizes

the expected source throughput. Specifically, using Gaussian as well as BPSK inputs on flat Rayleigh fading channels, we lower bound the average packet error rate by the corresponding mutual information outage probability, and derive the average throughput expression as a function of channel code rates as well as channel signal-to-noise ratio (SNR) for a frequency-division multiplexing-based system both without relaying and with a half-duplex relay using a decode-and-forward protocol. At high SNR, the optimization problem involves a convex function of the channel code rates, and we show that a known recursive algorithm can be used to predict the performance of both systems.

The second example is the layered transmission of a Gaussian source over multiple relays using superposition coding. At first, we analyze the outage probability and performance in terms of average throughput and distortion for decode-and-forward (DF) protocols with single-layer and superposed two-layer coding. For the superposition coding approach, we consider different power allocations to the base and enhancement layers. Then, we propose a simple protocol which assigns a pre-determined number of relays to individual layers instead of repeating the superposition coded packet at the relay. We also present numerical results based on the analysis to compare the performance.

We then consider a practical application where motion compensated fine granular scalable (MC-FGS) video is transmitted over multi-input multi-output (MIMO) wireless channels and the leaky and partial prediction schemes are applied in the enhancement layer of MC-FGS video to exploit the tradeoff between error propagation and coding efficiency. For reliable transmission, we propose UEP by considering a tradeoff between reliability and data rates, which is controlled by forward error correction (FEC) and MIMO mode selection to minimize the average distortion. In a high Doppler environment where it is hard to get an accurate channel estimate, we investigate the performance of the proposed MC-FGS video transmission scheme with joint control of both the leaky and partial prediction parameters and the UEP. In a slow fading channel where the channel throughput can be estimated at the transmitter, adaptive control of the prediction parameters is considered.

I

Introduction

Recently, the transmission of multimedia such as images and video over wireless channels has been in high demand, especially due to the explosive growth of mobile users. However, due to the fundamental limitations on mobile communication over wireless channels, such as power, bandwidth, mobility and fading, it becomes challenging to maintain the quality of service if a multimedia stream is transmitted. To achieve reliable and high-quality performance in wireless multimedia communications, cross-layer design, which allows interaction between the different protocol layers, was proposed [1][2][3][4].

A simplified protocol stack for cross layer design to transmit multimedia over wireless channels is shown in Fig. I.1, where the application, link, and physical layers are controlled jointly. To do that, the application layer provides information such as the rate-distortion (RD) function and unequal priority of the source bitstream, which can be based on performance metrics such as distortion or visibility. From the link layer, packet error rate (PER) is sent to the controller. Instantaneous or long-term averaged channel state information (CSI) or channel SNR is reported by the physical layer. In the cross-layer controller, all information from the source and channel are gathered, and then the appropriate parameters are decided and sent back to the individual layers. For example, source coding parameters such as source rate, quantization level [5] or intra refresh rate [6] can be

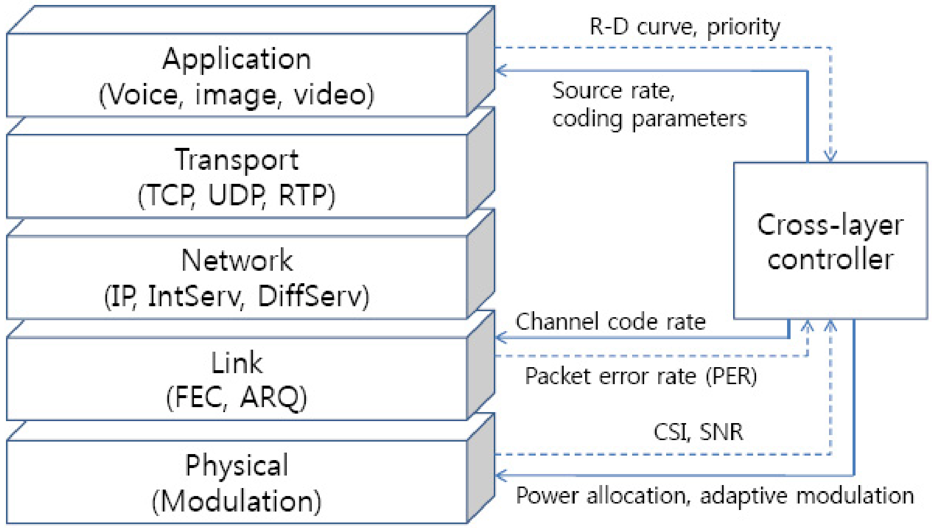

Figure I.1: Simplified protocol stack for cross layer design to transmit wireless multimedia.

controlled for the application layer. In the link and physical layers, the controller can determine unequal error protection (UEP) with various channel resources, such as forward error correction coding (FEC), diversity and transmit power. In the following, we introduce cross-layer designs in various systems for wireless multimedia transmission, along with the relevant literature.

I.A Information-theoretic framework for source-channel rate optimization

Usually, source packets in compressed images or video have unequal priority in terms of the quality, such as distortion or visibility. For example, in progressive image coders such as JPEG2000 [7], embedded zerotree wavelet (EZW) coding [8] and SPIHT [9] or scalable video coders such as MPEG-4 [10], decoding stops at the first packet error. That is, more distortion can be expected if the early packets are lost. Or, in video encoders such as MPEG-2 and H.264 [11], packets may have different visibility, which represents the video quality based on human visual perception. Therefore, it is reasonable to assign unequal levels of error protection to packets in transmission over lossy wireless channels. However, it becomes complicated to find the optimal allocation of the channel resources to the source packets.

Many studies have appeared on cross-layer design with a fixed transmission bandwidth. For example, in [12], the transmission of progressive images jointly with rate compatible punctured convolutional (RCPC) codes was proposed and investigated for binary symmetric channels. In [13], optimization using dynamic programming for a specific performance measure was proposed to choose block length as well as the appropriate channel code rate, where various performance measures such as mean-squared error (MSE), peak signal-to-noise ratio (PSNR), or the number of received source bits were considered. A more computationally efficient algorithm was proposed in [14], where the optimal UEP solution was computed recursively. As a more practical approach, in [15], a parametric procedure was proposed, where the exact bit error rate (BER) corresponding to each code rate was modelled empirically for certain channels. However, much of the previous research on source-channel rate allocation with forward error correction coding has focused on efficient algorithms to find the optimal UEP.

Information-theoretic approaches to joint source-channel bit allocation have also been considered. Both [16] and [17] considered layered transmission of successively refinable Gaussian sources over quasi-static fading channels, and the performance in terms of the distortion exponent was investigated using well-known rate-distortion expressions for a Gaussian source. In [18] and [19], joint source-channel coding was studied in multi-input multi-output (MIMO) or cooperative relay channels, and the performance was presented in the form of a distortion exponent, which represents the rate of decay of the end-to-end distortion with infinite SNR.

In Chapters II and III of this dissertation, we use an information-theoretic framework to analyze the source-channel rate allocation to maximize the throughput of a practical progressive image. This analysis provides an approximate bound on the system performance at high SNR in terms of average throughput.

I.B Cooperative relay networks

Relay transmission has been considered as an attractive technology to support high data rates in mobile environments, such as LTE-Advanced and Wi-MAX [20]. Since a cooperative relay system has an advantage over a single hop system due to the path-loss reduction in the source-relay and relay-destination paths, higher modulation schemes can be used for relay transmission. Due to this advantage, relay transmission was studied for multimedia applications, such as progressive image [21], video [22][23] or layered Gaussian sources [19].

In Fig. I.2, a two-hop relay channel with N relays is presented. Let's consider the transmission of a multimedia bitstream over the relay channel. In the first time slot, the source (S) broadcasts the bitstream to the N relays (R). Due to the different channel qualities from the source to the multiple relays, some relays may not decode the bitstream successfully. In the second time slot, only relays which succeed to decode the bitstream retransmit that based on the decode-and-forward (DF) protocol. Or, with the amplify-and-forward (AF) protocol, all relays amplify what they received and transmit them to the destination (D).

For the broadcast of a multimedia bitstream, superposition coding is widely used, for example in DVB-H [25] and MediaFlo [26], because it can provide different qualities of service (QoS) to the various users who may have different channel qualities. Moreover, by assigning unequal power between layers, unequal error protection can be achieved easily. Therefore, we consider superposition coding for the two-hop relay channel for wireless multimedia communication. Although superposition coding-based transmission over a relay channel is studied from the throughput [27] and resource allocation [28] perspectives, its effectiveness in the transmission of multimedia has not been studied, to the best of our knowledge.

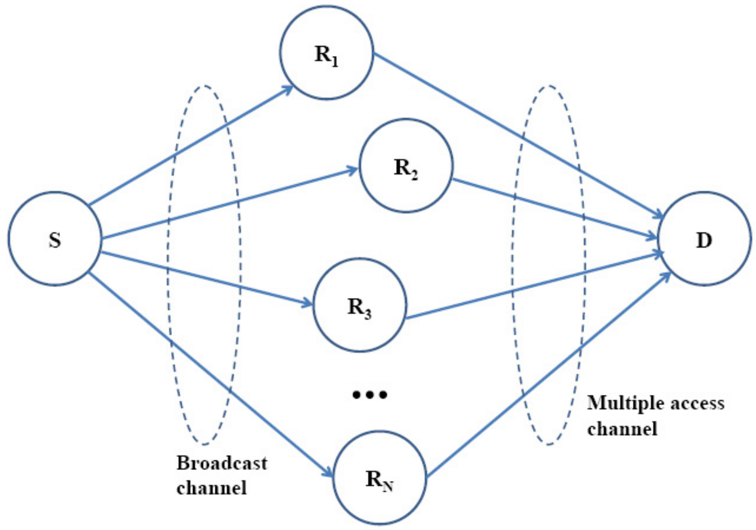

Figure I.2: Two-hop relay channel. Channels from source (S) to the N relays (R_1, R_2, $\cdots$, R_N) and from the N relays to the destination (D) are considered as *broadcast* and *multiple access channels*, respectively.

In this dissertation, we use a cooperative relay channel to transmit multimedia bitstreams, where superposition coding is applied. We first address the information theoretic framework to analyze the performance in terms of the distortion when a layered Gaussian source is assumed. Then, we compare the performance of various relay protocols based on decode-and-forward (DF) and relay selection.

I.C Scalable video transmission over MIMO wireless channels

Fine grain scalable (FGS) video was proposed to provide flexible video streaming which can adapt to dynamic channel conditions. It divides the compressed bitstream into a base layer (BL) and a progressively encoded enhancement layer (EL), where the EL can be truncated at any arbitrary point.

In the current state-of-the-art video codecs, motion compensated prediction (MCP) is widely used to enhance the compression efficiency. In MCP, the current frame is predicted from the previous frame by eliminating the temporal redundancy between frames. For applying MCP to FGS video coding, motion-compensated fine grain scalable (MC-FGS) video coding was proposed [29]. In MC-FGS video coding, a high quality reference frame can be reconstructed by using both the BL and the EL, and thus enhance the compression efficiency significantly. However, MC-FGS video coding suffers from error propagation if the portion of the EL used for prediction is lost at the decoder. In [29], to achieve a tradeoff between coding efficiency and error resilience, the amount of the EL used for prediction is controlled at the encoder.

In [30] and [31], this tradeoff is controlled by introducing partial and leaky predictions in their MCP loop. Specifically, in [31], the authors showed that partial knowledge of wireless channels, such as the coherence bandwidth and average channel SNR, can help to find the appropriate values for the partial and leaky prediction parameters, and this knowledge can be used in cross-layer design. In this dissertation, we apply the leaky and partial prediction parameters to MC-FGS video coding, which is transmitted over a MIMO wireless channel. Our goal is to develop a wireless video transmission system based on a cross-layer design, and compare the proposed system with a conventional system. In addition, adaptation of the video coding parameters such as leaky and partial prediction parameters based on the channel is considered when instantaneous channel state information is available.

I.D Thesis outline

In Chapter II, we provide the details of the information-theoretic framework to analyze the source-channel rate allocation, which is based on a block fading channel model. This mathematical expression is also applied in Chapter III for cooperative relay channels. We then present an algorithm to find the optimal UEP in the system with and without cooperative relays. We show that our proposed framework provides bounds for both the performance and the channel code rate.

In Chapter III, we discuss joint source channel coding in the cooperative relay system with superposition coding. We propose a simple relay dedication-based protocol and show the performance compared to the conventional DF-based protocol, both with and without superposition coding, in terms of the throughput and the distortion.

In Chapter IV, we consider a more practical system, where scalable video is transmitted over a MIMO channel. We propose a novel UEP method combined with FEC and MIMO mode selection, and consider the leaky and partial prediction parameters to achieve a tradeoff in compression efficiency and error resilience.

In the Conclusion, we summarize the contributions of this dissertation, and discuss potential future work. We note that partial conclusions are also given at the end of each individual chapter.

II

Source-channel rate optimization for progressive image transmission over block fading relay channels

II.A Introduction

In this chapter, we use an information-theoretic framework to analyze the source-channel rate allocation to maximize the throughput of a progressive image in a system either with or without a cooperative relay. This analysis provides an approximate bound on the system performance at high SNR in terms of average throughput, which may not be optimal in the sense of distortion. However, the throughput-optimal approach has some advantages over the distortion-optimal approach. First, the throughput-optimal approach can be analyzed mathematically without considering the source characteristics. And, the UEP solution can be found at the transmitter and receiver independently without any additional signaling between them, since the average channel gain, which is needed in the throughput-optimal approach, is known by both the transmitter and the receiver. Moreover, the throughput-optimal approach can allow one to find the distortion-optimal solution using a local search algorithm and the source statistics in linear time [32].

We study both Gaussian and symmetric BPSK inputs over block fading channels, and get the mutual information (MI) outage probability, which is a lower bound on the actual packet error rate (PER) of a BPSK-based system [33],[34]. Although there are well-known expressions for mutual information and outage probability for Gaussian inputs, a closed-form expression for the capacity when either PSK or QAM inputs is used is not known. However, both bounds and approximations have been widely studied (e.g.,[35][36][37][38]). In this paper, we use [36] to find an approximation for the MI outage probability for BPSK inputs. Then, we derive an average source throughput expression using MI outage probability and the progressive property of the source. We prove that this rate-optimization problem is a convex function of the channel code rates at high SNR, and the solution can be found by using a recursive algorithm introduced in [39]. Our predicted system performance and average channel code rates upper bound the simulation results.

The rest of this chapter is organized as follows. In Section II.B, we introduce the system model for the transmission of progressive images. Using both Gaussian and BPSK inputs, in Section II.C, we present expressions for the average source throughput for the baseline as well as the relay-based systems. In Section II.D, we provide a simple algorithm to determine the optimal channel code rates under a bandwidth constraint. Numerical and simulation results are presented in Section II.E, and we conclude this work in Section II.F.

II.B System model

We consider a general progressive image transmission system consisting of a single source and destination either with or without relays. The image source rate is denoted by $\mathcal{R}_s$ pixels/sec. If we assume r_s bits-per-pixel (bpp), then the total source rate is $\mathcal{R}_s r_s$ bits/sec. The source bit stream is packetized into M packets, which are protected by suitable channel codes. All the packets are assumed to have equal channel codeword length, n. The total bandwidth available for the source is W Hz, whereas the duration of a code symbol is denoted by T_s. Assuming a Nyquist pulse-shaping filter at the transmitter, we have

$$W = \frac{1+\beta}{T_s}, \tag{II.1}$$

where β is the roll-off factor of the pulse-shaping filter.

We assume the channels between all the nodes are random, independent, and constant over the packet duration. The coherence bandwidth is assumed to be the same as the bandwidth of a sub-channel, where the bandwidth of a sub-channel is defined as W/N and N is the number of relays. We assume Rayleigh fading, so the square of the fading amplitude follows an exponential distribution, and the additive noise is independent and identical distributed (i.i.d.) white Gaussian and independent for each channel. We assume that the receivers of the relays and the destination know the instantaneous channel realizations, and the transmitters of the source and the relays know only the mean channel gain.

The destination combines the received channel code symbols on the N sub-channels using maximal ratio combining (MRC). We assume that the system is able to detect any errors and halts decoding of subsequent packets following an erroneous packet.

II.B.1 Baseline System

In the baseline system, the transmission bandwidth W is equally divided into N uncorrelated sub-bands and the source repeats each packet over the N sub-channels. The bit duration of each sub-channel is $T_{s_1} = NT_s$. If K_j denotes the number of information bits in the jth packet, where $j = 1, \ldots, M$, then the channel code rate of the jth packet is $r_c^{\mathrm{B}}(j) = K_j/n$, where n is the packet length in bits. The total transmission time for a given image is $M \times n \times T_{s_1}$. In this time, the total number of source bits generated is $\mathcal{R}_s r_s M n T_{s_1}$ which is assumed to be equal to $\sum_{j=1}^{M} K_j = n \sum_{j=1}^{M} r_c^{\mathrm{B}}(j)$. That is, we have the rate constraint

$$n \sum_{j=1}^{M} r_c^{\mathrm{B}}(j) = \mathcal{R}_s r_s M n T_{s_1} = N \mathcal{R}_s r_s M n \frac{1+\beta}{W} \leq Mn. \tag{II.2}$$

Since K_j information bits are transmitted in the jth packet, the average time duration to transmit a single information bit, $T_b^{\mathrm{B}}(j)$, is computed as

$$T_b^{\mathrm{B}}(j) = \frac{nT_{s_1}}{K_j}.$$

If $R_b^{\mathrm{B}}(j) = 1/T_b^{\mathrm{B}}(j)$ denotes the information bit rate for the jth packet, then, we have

$$R_b^{\mathrm{B}}(j) = \frac{K_j}{n}\frac{1}{T_{s_1}} = \frac{r_c^{\mathrm{B}}(j)}{NT_s} = \tilde{r}_c^{\mathrm{B}}(j)\frac{W}{N}, \tag{II.3}$$

where $\tilde{r}_c^{\mathrm{B}}(j) = r_c^{\mathrm{B}}(j)/(1+\beta)$.

Let $\alpha_{j,l}$ denote the channel fading amplitude experienced by the jth packet on the lth sub-channel. We assume that the $\alpha_{j,l}$, for $j = 1, \ldots, M$ and $l = 1, \ldots, N$, are i.i.d. Rayleigh random variables, with second moment $E[\alpha_{j,l}^2] = \Omega_1$. The total average transmission power budget at the source is P_T. Therefore, the average power per sub-channel is $P_1 = P_T/N$.

II.B.2 Half-duplex Relay System

We assume N relay nodes, each of them and the source occupying a bandwidth of W/N, as presented in Fig. II.1. The source transmits each packet sequentially through one of N sub-channels. Each packet is received by the destination as well as by all the N relays. The packets are assumed to be further protected by suitable cyclic redundancy check (CRC) codes to aid verification of their integrity. With this, only those relay nodes that successfully decode the source packets re-encode and forward them to the destination. For simplicity, we assume that the probability of undetected error is very low, and can be ignored. The destination combines all the packets that it receives from the source and the relay nodes in an appropriate manner before proceeding with channel decoding. For the lth packet, we denote by $\alpha_{sd,l}$ the fading amplitude on the path from the source to the destination, $\alpha_{sr,l}^j$ the fading amplitude on the path from the source to the jth relay node, and $\alpha_{rd,l}^j$ the fading amplitude on the path from the jth relay node to the destination. Similar to the baseline system, we assume that $\alpha_{sd,l}$, $\alpha_{sr,l}^j$ and $\alpha_{rd,l}^j$,

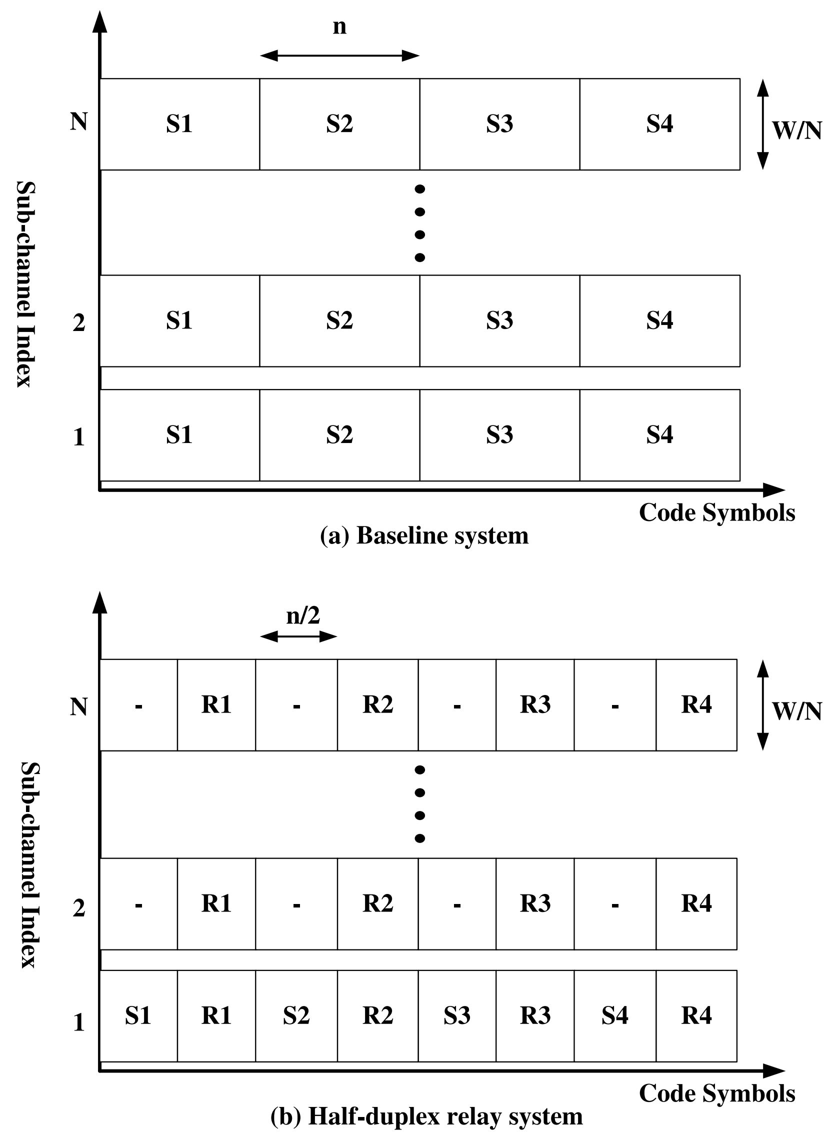

Figure II.1: (a) Baseline system and (b) half-duplex relay system, where Si and Ri are the ith packet transmission at the source and the relay, respectively.

for $j = 1, \ldots, N$ and $l = 1, \ldots, M$, are independent and Rayleigh distributed, with second moments $E[\alpha_{sd,l}^2] = \Omega_{sd}$, $E[(\alpha_{sr,l}^j)^2] = \Omega_{sr}^j$ and $E[(\alpha_{rd,l}^j)^2] = \Omega_{rd}^j$.

If we denote by L_j the number of information bits in the jth packet, then the code rate of the jth packet with cooperation is $r_c^{\mathrm{CoOp}}(j) = L_j/n$, $j = 1, \ldots, M$. In the half duplex relay system, where the relays transmit and receive in different time slots, $2M$ time slots are required to transmit M packets. Since the bit duration of the half duplex relay system, T_{s_2}, is equal to that of the baseline system, the length of each time slot is $(n/2)T_{s_2} = (n/2)NT_s$, which is half of a packet transmission time. This leads to the following rate constraint with cooperation :

$$\sum_{j=1}^{M} L_j = \mathcal{R}_s r_s M T_{s_2} n/2 \leq Mn/2 \quad \Rightarrow \frac{1}{M}\sum_{j=1}^{M} r_c^{\mathrm{CoOp}}(j) = \frac{1}{2} N \mathcal{R}_s r_s T_s \leq \frac{1}{2}, \tag{II.4}$$

where the effective channel code rate of the jth packet, $r_c^{\mathrm{CoOp}}(j) = L_j/n$. If we denote by P_s the average transmit power of the source, and by P_j the average transmit power of the jth relay node, then we have the following energy constraint:

$$P_s(n/2)T_{s2} + \sum_{j=1}^{N} P_j(n/2)T_{s2} = P_T n T_{s1} \quad \Rightarrow P_s + \sum_{j=1}^{N} P_j = 2P_T, \tag{II.5}$$

where P_T is the average transmission power of the source without cooperation.

II.C Throughput performance analysis

In this section, by assuming large block lengths and block fading of the channel over the packet duration nT_{s_1}, we lower bound the actual PER by the channel mutual information (MI) outage probability [40], which is defined [41] as the probability that the instantaneous MI observed by a packet, which is a random variable (r.v.), is below the attempted information bit rate. Then, we derive the average throughput expression for each system using the MI outage probability.

II.C.1 Gaussian Inputs

II.C.1.a Baseline System

Let π_j^{B} denote the MI outage probability for the jth packet, which is a lower bound of the PER, at the destination. For the jth packet, the MI (in bits/sec) is

$$\mathrm{MI}^{\mathrm{B}}(j) = \frac{W}{N} \log_2 \left(1 + \sum_{l=1}^{N} \frac{P_1}{N_0 \frac{W}{N}} \alpha_{j,l}^2 \right). \tag{II.6}$$

The corresponding MI outage probability is

$$\begin{aligned} \pi_j^{\mathrm{B}} &= \mathrm{Prob}\left(\mathrm{MI}^{\mathrm{B}}(j) < R_{b,j}^{\mathrm{B}} \right) \\ &= \mathrm{Prob}\left(\frac{W}{N} \log_2 \left(1 + \sum_{l=1}^{N} \frac{P_1}{N_0 \frac{W}{N}} \alpha_{j,l}^2 \right) \le \frac{W \tilde{r}_c^{\mathrm{B}}(j)}{N} \right) \\ &= \mathrm{Prob}\left(\sum_{l=1}^{N} \frac{\alpha_{j,l}^2}{\Omega_1} \le \frac{2^{\tilde{r}_c^{\mathrm{B}}(j)} - 1}{\overline{\Gamma}} \right) \\ &= \gamma_{\mathrm{inc}}\left(\frac{2^{\tilde{r}_c^{\mathrm{B}}(j)} - 1}{\overline{\Gamma}}, N \right), \end{aligned} \tag{II.7}$$

where we have used the fact that $\zeta \triangleq \sum_{l=1}^{N} \alpha_{j,l}^2 / \Omega_1$ is a Gamma-distributed r.v. with probability density function (PDF)

$$f_\zeta(x) = \frac{e^{-x} x^{N-1}}{\Gamma(N)} \quad x \ge 0, \tag{II.8}$$

and where $\Gamma(n) = \int\limits_{u=0}^{\infty} e^{-u} u^{n-1} du$ is the standard Gamma function [42], and $\gamma_{\mathrm{inc}}(x, n)$ in (II.7) is the incomplete Gamma function, which is defined as [42]

$$\gamma_{\mathrm{inc}}(x, n) \triangleq \frac{1}{\Gamma(n)} \int\limits_{u=0}^{x} e^{-u} u^{n-1} du. \tag{II.9}$$

In (II.7) $\overline{\Gamma} = P_1 \Omega_1 N / (N_0 W) = P_T \Omega_1 / (N_0 W)$ is the average received signal-to-noise ratio (SNR) per sub-channel.

Due to the progressive nature of the source, only the packets decoded successfully until the first decoding failure are used by the source decoder for reconstructing the source. Let us denote by $\mathsf{S}_k^{\mathrm{B}}$ the probability of successfully receiving k source packets at the input of the source decoder. Then, we have

$$\begin{aligned}
\mathsf{S}_0^{\mathrm{B}} &= \pi_1^{\mathrm{B}} \\
\mathsf{S}_k^{\mathrm{B}} &= \pi_{k+1}^{\mathrm{B}} \prod_{i=1}^{k} (1-\pi_i^{\mathrm{B}}) \quad k=1,\ldots,M-1 \qquad \text{(II.10)} \\
\mathsf{S}_M^{\mathrm{B}} &= \prod_{i=1}^{M} (1-\pi_i^{\mathrm{B}}).
\end{aligned}$$

The average number of source bits successfully decoded by the source decoder in the baseline system is

$$\begin{aligned}
\overline{\mathcal{T}}_{\mathrm{B}}(\underline{r}_c^{\mathrm{BL}}) &= \sum_{j=1}^{M} \left(\sum_{i=1}^{j} K_i \right) \mathsf{S}_j^{\mathrm{B}} \\
&= n(1+\beta) \sum_{j=1}^{M} \left(\sum_{i=1}^{j} \tilde{r}_c^{\mathrm{B}}(i) \right) \mathsf{S}_j^{\mathrm{B}}, \qquad \text{(II.11)}
\end{aligned}$$

where $\underline{r}_c^{\mathrm{BL}} = \left(\tilde{r}_c^{\mathrm{B}}(1),\ldots,\tilde{r}_c^{\mathrm{B}}(M)\right)$. The source-channel rate allocation problem for the baseline system can then be stated as

$$\begin{aligned}
&\text{maximize} \quad \overline{\mathcal{T}}_{\mathrm{B}}(\underline{r}_c^{\mathrm{BL}}) \qquad \text{(II.12)} \\
&\text{subject to} \quad \sum_{j=1}^{M} \tilde{r}_c^{\mathrm{B}}(j) \le \frac{M}{1+\beta}. \qquad \text{(II.13)}
\end{aligned}$$

II.C.1.b Half-duplex Relay System

We denote by $q(i,j)$ the probability of decoding error of the jth packet at the ith relay node, which is computed as follows: Let $\mathrm{MI}(i,j)$ denote the MI of the jth packet at the ith relay, then

$$\begin{aligned}
\mathrm{MI}(i,j) &= \frac{W}{N} \log_2 \left(1 + \frac{P_s}{N_0 \frac{W}{N}} (\alpha_{sr,j}^i)^2 \right) \\
&= \frac{W}{N} \log_2 \left(1 + \overline{\gamma}_{sr}^i N \frac{\left(\alpha_{sr,j}^i\right)^2}{\Omega_{sr}^i} \right), \qquad \text{(II.14)}
\end{aligned}$$

where $\overline{\gamma}_{sr}^i = \frac{P_s}{N_0 W} \Omega_{sr}^i$, $i=1,\ldots,N$. The transmission rate of the jth packet with cooperation is $R_b^{\mathrm{CoOp}}(j) = 2\tilde{r}_c^{\mathrm{CoOp}}(j) W/N$, where $\tilde{r}_c^{\mathrm{CoOp}}(j) = r_c^{\mathrm{CoOp}}(j)/(1+\beta)$.

Then,

$$\begin{aligned} q(i,j) &= \text{Prob}\left(\text{MI}(i,j) < R_b^{\text{CoOp}}(j)\right) \\ &= \text{Prob}\left(\frac{\left(\alpha_{sr,j}^i\right)^2}{\Omega_{sr}^i} < \frac{2^{2\tilde{r}_c^{\text{CoOp}}(j)}-1}{\overline{\gamma}_{sr}^i N}\right) \\ &= \gamma_{\text{inc}}\left(\frac{2^{2\tilde{r}_c^{\text{CoOp}}(j)}-1}{\overline{\gamma}_{sr}^i N}, 1\right), \end{aligned} \tag{II.15}$$

which follows from the fact that $(\alpha_{sr,j}^i)^2/\Omega_{sr}^i$ is exponentially-distributed with unit mean.

Let $\mathcal{D}_j$ denote the set of relay nodes that successfully decode the jth source packet. Then the probability that relays in the set $\mathcal{D}_j$ are only able to decode the jth source packet is

$$\text{Prob}(\mathcal{D}_j) = \left\{\prod_{i\in\mathcal{D}_j}(1-q(i,j))\right\} \times \left\{\prod_{k\notin\mathcal{D}_j} q(k,j)\right\} \tag{II.16}$$

owing to the independence of the decoding errors at the relays, which is attributed to the spatial independence of the channel fading.

At the destination, we assume that each source packet is maximal-ratio combined. Then, the MI of the jth packet at the destination, conditioned on $\mathcal{D}_j$, is

$$\begin{aligned} \text{MI}(\mathcal{D}_j) &= \frac{W}{N}\log_2\left(1 + \frac{P_s}{N_0\frac{W}{N}}\alpha_{sd,j}^2 + \sum_{l\in\mathcal{D}_j}\frac{P_l}{N_0\frac{W}{N}}(\alpha_{rd,j}^l)^2\right) \\ &= \frac{W}{N}\log_2\left(1 + N\overline{\gamma}_{sd}(\alpha_{sd,j})^2/\Omega_{sd} + N\sum_{l\in\mathcal{D}_j}\overline{\gamma}_{rd}^l(\alpha_{rd,j}^l)^2/\Omega_{rd}^l\right), \end{aligned} \tag{II.17}$$

where $\overline{\gamma}_{rd}^l = \frac{P_l}{N_0 W}\Omega_{rd}^l$, $l = 1,\ldots,N$. Conditioned on $\mathcal{D}_j$, the probability of jth packet error at the destination is

$$\begin{aligned} \pi_j^{\text{CoOp}}(\mathcal{D}_j) &= \text{Prob}\left(\text{MI}(\mathcal{D}_j) < \frac{2\tilde{r}_c^{\text{CoOp}}(j)W}{N}\right) \\ &= \text{Prob}\left(\overline{\gamma}_{sd}(\alpha_{sd,j})^2/\Omega_{sd} + \sum_{l\in\mathcal{D}_j}\overline{\gamma}_{rd}^l(\alpha_{rd,j}^l)^2/\Omega_{rd}^l < \frac{2^{2\tilde{r}_c^{\text{CoOp}}(j)}-1}{N}\right). \end{aligned} \tag{II.18}$$

To simplify (II.18) further, define

$$Z(\mathcal{D}_j) \triangleq \overline{\gamma}_{sd}(\alpha_{sd,j})^2/\Omega_{sd} + \sum_{l\in\mathcal{D}_j} \overline{\gamma}_{rd}^l(\alpha_{rd,j}^l)^2/\Omega_{rd}^l. \tag{II.19}$$

Assuming $\overline{\gamma}_{sd}$, $\overline{\gamma}_{rd}^l$, $\forall\, l \in \mathcal{D}_j$, are all distinct, and using the moment generating function approach, it is easy to show that the PDF of $Z(\mathcal{D}_j)$ is given by

$$f_{Z(\mathcal{D}_j)}(z) = \lambda_0(\mathcal{D}_j)\frac{1}{\overline{\gamma}_{sd}}\exp\left(-\frac{z}{\overline{\gamma}_{sd}}\right) + \sum_{l\in\mathcal{D}_j}\lambda_l(\mathcal{D}_j)\frac{1}{\overline{\gamma}_{rd}^l}\exp\left(-\frac{z}{\overline{\gamma}_{rd}^l}\right), \tag{II.20}$$

where

$$\lambda_0(\mathcal{D}_j) = \prod_{l\in\mathcal{D}_j}\frac{\overline{\gamma}_{sd}}{\overline{\gamma}_{sd}-\overline{\gamma}_{rd}^l} \tag{II.21}$$

$$\text{and}\quad \lambda_l(\mathcal{D}_j) = \frac{\overline{\gamma}_{rd}^l}{\overline{\gamma}_{rd}^l-\overline{\gamma}_{sd}} \times \prod_{m\in\mathcal{D}_j, m\neq l}\frac{\overline{\gamma}_{rd}^l}{\overline{\gamma}_{rd}^l-\overline{\gamma}_{rd}^m}. \tag{II.22}$$

Upon using (II.20) in (II.18), we arrive at

$$\begin{aligned}\pi_j^{\mathrm{CoOp}}(\mathcal{D}_j) &= \lambda_0(\mathcal{D}_j)\gamma_{\mathrm{inc}}\left(\frac{2^{2\tilde{r}_c^{\mathrm{CoOp}}(j)}-1}{\overline{\gamma}_{sd}N}, 1\right)\\ &\quad + \sum_{l\in\mathcal{D}_j}\lambda_l(\mathcal{D}_j)\gamma_{\mathrm{inc}}\left(\frac{2^{2\tilde{r}_c^{\mathrm{CoOp}}(j)}-1}{\overline{\gamma}_{rd}^l N}, 1\right).\end{aligned} \tag{II.23}$$

Finally, upon averaging (II.23) over all possible decoding sets, the average probability of error for the jth packet is

$$\pi_j^{\mathrm{CoOp}} = \sum_{\mathcal{D}_j}\mathrm{Prob}(\mathcal{D}_j)\pi_j^{\mathrm{CoOp}}(\mathcal{D}_j). \tag{II.24}$$

Once π_j^{CoOp} is found, the probability of successfully receiving k packets at the input of the source decoder with cooperation, $\mathsf{P}_k^{\mathrm{CoOp}}$, can be expressed in a form similar to (II.10), where the π_j^{B} in (II.10) is replaced by π_j^{CoOp} of (II.24).

The average number of source bits successfully decoded by the source decoder with cooperation is

$$\begin{aligned}\overline{\mathcal{T}}_{\mathrm{CoOp}}(\underline{r}_c^{\mathrm{CoOp}}) &= \sum_{j=1}^{M}\left(\sum_{i=1}^{j}L_i\right)\mathsf{P}_j^{\mathrm{CoOp}}\\ &= n(1+\beta)\sum_{j=1}^{M}\left(\sum_{i=1}^{j}\tilde{r}_c^{\mathrm{CoOp}}(i)\right)\mathsf{P}_j^{\mathrm{CoOp}},\end{aligned} \tag{II.25}$$

where $\underline{r}_c^{\text{CoOp}} = \left(\tilde{r}_c^{\text{CoOp}}(1), \ldots, \tilde{r}_c^{\text{CoOp}}(M)\right)$. The source-channel rate allocation problem with half-duplex relayed transmission can then be stated as follows :

$$\text{maximize} \quad \overline{\mathcal{T}}_{\text{CoOp}}(\underline{r}_c^{\text{CoOp}}) \tag{II.26}$$

$$\text{subject to} \quad \sum_{j=1}^{M} \tilde{r}_c^{\text{CoOp}}(j) \leq \frac{M}{2(1+\beta)}. \tag{II.27}$$

II.C.2 BPSK Inputs

In order to apply the results of an information-theoretic analysis to practical system design, BPSK inputs are considered. Although a closed-form expression for the symmetric capacity with respect to BPSK inputs is not known, it is possible to compute the symmetric capacity numerically. However, in this paper, we use both bounds and an approximation for symmetric capacity instead of numerical computation. Both upper and lower bounds for the symmetric capacity were derived by Baccarelli in [35], and approximations were proposed in [36], [37], and [38]. In this paper, the upper bound of [35] and the approximation in [36] of the symmetric capacity for BPSK inputs are used to find an upper bound on the average throughput of the rate-optimal UEP for the system. From (10) in [35], an upper bound for the MI of the baseline system is

$$\text{MI}^{\text{B}}_{BPSK}(j) < \frac{W}{N}\left(1 - \log_2\left(1 + \exp\left(-2\sum_{l=1}^{N} \frac{P_1}{N_0 \frac{W}{N}} \alpha_{j,l}^2\right)\right)\right), \tag{II.28}$$

and the upper bounds of MIs for the relay system are

$$\text{MI}_{BPSK}(i,j) < \frac{W}{N}\left(1 - \log_2\left(1 + \exp\left(-2\frac{P_s}{N_0 \frac{W}{N}} (\alpha_{sr,j}^i)^2\right)\right)\right), \tag{II.29}$$

and

$$\begin{aligned} &\text{MI}_{BPSK}(\mathcal{D}_j) \\ &< \frac{W}{N}\left(1 - \log_2\left(1 + \exp\left(-2\frac{P_s}{N_0 \frac{W}{N}} \alpha_{sd,j}^2 - 2\sum_{l \in \mathcal{D}_j} \frac{P_l}{N_0 \frac{W}{N}} (\alpha_{rd,j}^l)^2\right)\right)\right). \end{aligned} \tag{II.30}$$

From (9) in [36], the approximation of the MI for the baseline system is

$$\mathrm{MI}^{\mathrm{B}}_{BPSK}(j) \approx \frac{W}{N}\left(1 - \exp\left(-2b\sum_{l=1}^{N}\frac{P_1}{N_0\frac{W}{N}}\alpha_{j,l}^2\right)\right), \tag{II.31}$$

and the approximations of MIs for the relay system are

$$\mathrm{MI}_{BPSK}(i,j) \approx \frac{W}{N}\left(1 - \exp\left(-2b\frac{P_s}{N_0\frac{W}{N}}(\alpha_{sr,j}^i)^2\right)\right), \tag{II.32}$$

and

$$\mathrm{MI}_{BPSK}(\mathcal{D}_j) \approx \frac{W}{N}\left(1 - \exp\left(- 2b\frac{P_s}{N_0\frac{W}{N}}\alpha_{sd,j}^2 - 2b\sum_{l\in\mathcal{D}_j}\frac{P_l}{N_0\frac{W}{N}}(\alpha_{rd,j}^l)^2\right)\right), \tag{II.33}$$

where b is a parameter that equals 0.6573 for BPSK inputs [36]. The approximated average throughput expressions of each system with respect to BPSK inputs can be derived in the same manner as those with Gaussian inputs, so details are not presented here.

II.D Optimum source-channel rate allocation

In this section, we discuss an algorithm to find the optimal source-channel rate allocation to maximize the average throughput of each system. In [39], a recursive algorithm to find the throughput-optimal solution was proposed. We show that the same algorithm can find the throughput-optimal solution for our information-theoretic framework. All objective functions for baseline as well as relay systems are concave over $\underline{r}_c^{\mathrm{BL}}$ or $\underline{r}_c^{\mathrm{CoOp}}$ at high SNR, which can be proved by showing that the Hessian matrix of the objective function is negative definite. The detailed concavity proof is presented in the appendices. Then, the optimal UEP can be found by M partial differentiations as follows :

$$\frac{\partial\overline{\mathcal{T}}_M((\underline{r}_c))}{\partial r_c(i)} = 0 \quad i = 1, \ldots, M. \tag{II.34}$$

If there is no solution for the ith equation, then the ith element of the optimal UEP is min$\{R\}$ or max$\{R\}$, where R is the set of possible code rates. In particular,

$$\frac{\partial \overline{\mathcal{T}}_M((\underline{r}_c))}{\partial r_c(M)} = (1-\pi_M) - r_c(M)\frac{\partial \pi_M}{\partial r_c(M)} = 0, \tag{II.35}$$

where π_M is the MI outage probability of the Mth packet, presented in (II.7) and (II.23). That is, we can find the optimum rate of the last packet first, and then find the rate of the $(M-1)$th packet recursively. Therefore, we can find the rate-optimal UEP policy, $\underline{r}_c^* = (r_c^*(1), r_c^*(2), \cdots, r_c^*(M))$, using the algorithm of [39]:

1. Set $i = 1$ and $r_c^*(M) = \arg\max_{r_c(M)\in\mathcal{R}} \overline{\mathcal{T}}_1(r_c(M))$ for all $r_c(M) \in (0, 1]$
2. If $i = M$, then $\underline{r}_c^* = (r_c^*(1), r_c^*(2), \cdots, r_c^*(M))$ and stop.
3. Set $i = i + 1$ and $r_c^*(M-i+1) = \arg\max_{r_c(M-i+1)\in(0,r_c(M-i)]} \overline{\mathcal{T}}_i\Big(r_c(M-i+1), r_c^*(M-i), \cdots, r_c^*(M)\Big)$. Go to step 2,

where $\overline{\mathcal{T}}_i((\underline{r}_c))$ is the average throughput expression of the last i packets. Note that, at low SNR, this algorithm will find a sub-optimal UEP policy since the convexity of the average throughput was not proved.

II.E A practical system design example and simulation results

In this section, we consider a BPSK-based practical embedded image transmission system with and without cooperative relays and then present the results of joint source-channel rate allocation based on the analysis as well as simulations. For a practical system, an algorithm to find a rate-optimal UEP policy can be found in [14] [39] when the PER of a specific channel coding scheme is known.

II.E.1 Simulation Setup

For the simulation, we use SPIHT to encode Lena image with 0.4 bpp of source rate. For channel encoding, RCPC and RCPT codes are considered. The RCPC codes have constraint length 3 and generator polynomial (23, 35) in octal. The rate of the mother code is 1/4, and the length of the codeword is fixed to 1000 bits, which is also the length of a packet, L. We consider 13 punctured code rates, R_{RCPC}={8/32, 8/30, 8/28, 8/26, 8/24, 8/22, 8/20, 8/18, 8/16, 8/14, 8/12, 8/10, 8/9}. Since we assumed fixed packet length, there are 13 different source block sizes corresponding to code rates. For RCPT codes, the encoder consists of two identical recursive systematic convolutional (RSC) coders with memory of 2 and generator polynomial (7,5) in octal. The rate of the mother code is 1/3 and the codeword length is 1000 bits. We also consider 9 punctured code rates, R_{RCPT}={8/24, 8/22, 8/20, 8/18, 8/16, 8/14, 8/12, 8/10, 8/9}. We use soft output Viterbi decoding with 10 iterations. Regarding the bit budget, we assume the total number of packets, M, is fixed at 100, so the optimization must find the code rates of 100 different packets which maximize average throughput. The channel is assumed to be block fading, so the channel gain is constant within a packet, but independent packet by packet. For the half duplex relay system, we assume a single relay is located halfway between the source and destination, and the path loss exponent is set to 4. For a comparison of two systems, we assume they have same bandwidth, transmission time and energy. In the baseline system, the total transmit power is equally allocated to the subchannels, but in the half-duplex relay system, twice the total transmit power of the baseline system is equally allocated to the source as well as to the relay to make them have the same transmit energy, as shown in (II.5).

II.E.2 Simulation Results

In this subsection, we provide simulation results and compare them with the analytical results. Although any real number between 0 and 1 can be a code

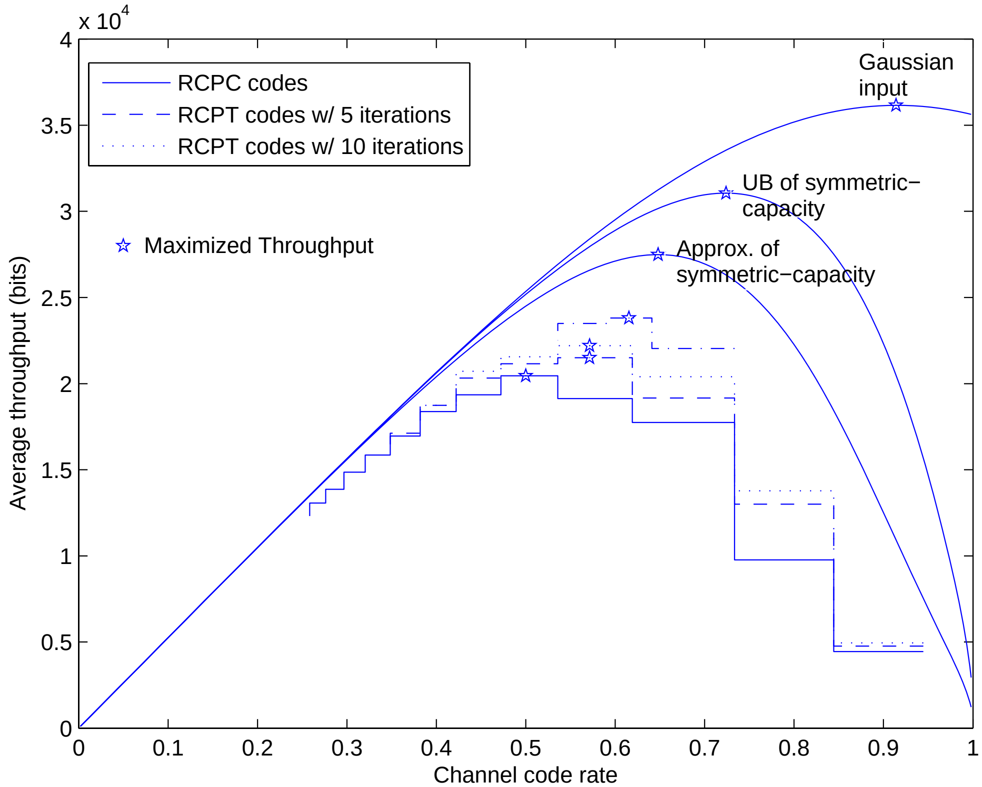

Figure II.2: EEP channel code rate profile of the baseline system at SNR of 4 dB, where three independent sub-channels are assumed.

rate theoretically, we restrict the possible code rate for the analysis to be bounded by the minimum and maximum code rates of the RCPC or RCPT codes in order to get comparable results. In Fig. II.2, the average throughputs of the rate-optimal EEP for the baseline system are presented, where RCPC and RCPT codes are considered. As explained in [43], the iterative decoding performance of the RCPT code approaches the maximum-likelihood (ML) bound as the number of iterations increases. Therefore, Fig. II.2 shows that the rate-optimal EEP channel code rate approaches the analytical bound as better channel coding schemes are used. In the figure, the three solid curves represent the analytically-derived average throughputs, which are computed by using the MI outage probability of the Gaussian and BPSK inputs. For Gaussian inputs, the rate-optimal EEP code rate is approxi-

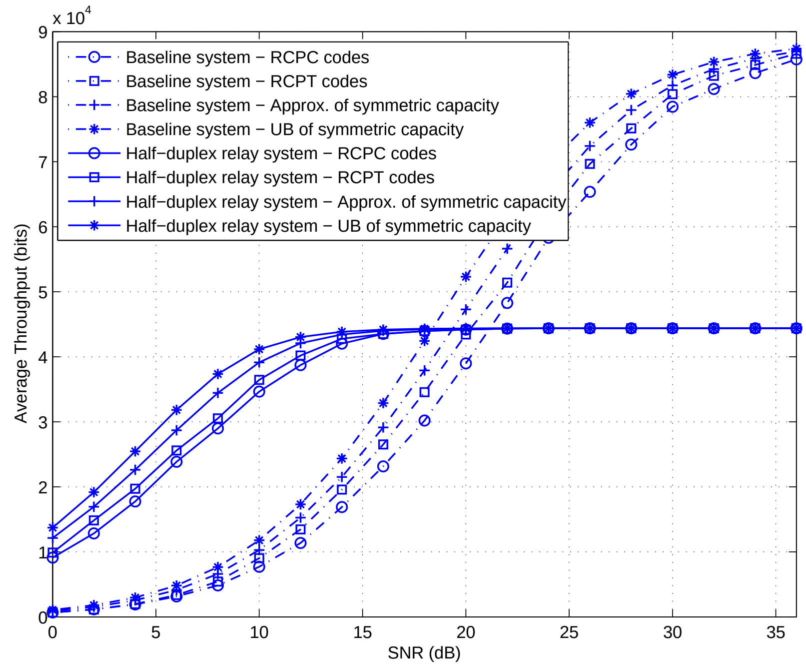

Figure II.3: Average throughput of baseline system and half duplex relay system.

mately 0.9. However, for BPSK inputs, the rate is reduced to 0.65. On the other hand, the rate-optimal EEP channel code rate for the RCPC codes is 8/16 and the channel code rate for the RCPT codes is 8/14 with 5 iterations, 8/14 with 10 iterations, and 8/13 with 100 iterations, so the optimal code rate is approaching 0.65 asymptotically. The average throughputs and PSNRs of rate-optimal UEP policies for the baseline and the half-duplex relay systems are presented in Fig. II.3 and II.4. Due to the path loss reduction, as well as the cooperative diversity gain, the half duplex relay system is better than the baseline system, especially at SNR around 12 dB. However, the average throughput of the half-duplex relay system saturates at intermediate SNRs. In contrast, the throughput of the baseline system is significantly enhanced as SNR increases and the crossover of the two curves appears at around 20 dB, which is caused by the loss in the spectral efficiency of the half-duplex relay system. The same trend is observed for average PSNR. In Figs. II.5 and II.6, average code rates of UEP policies for the two systems are

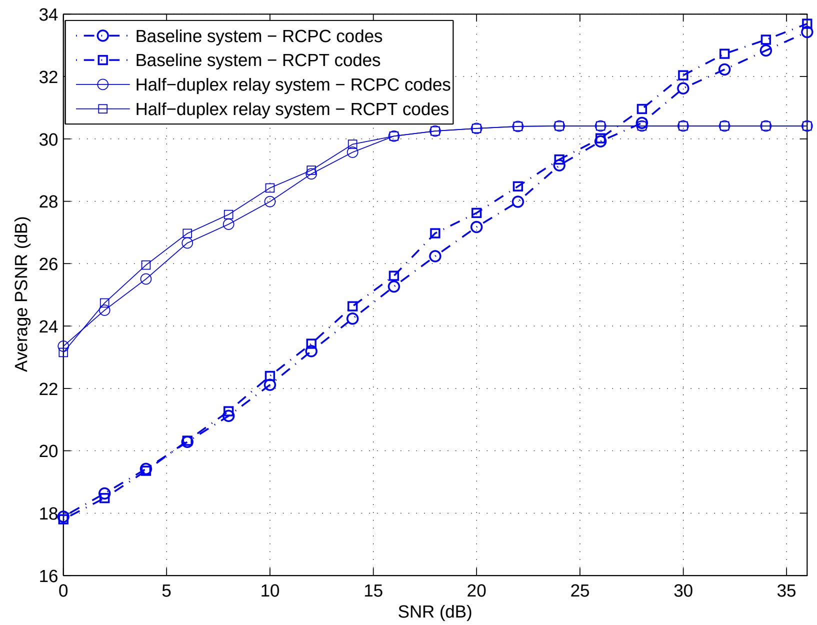

Figure II.4: Average PSNR of baseline system and half duplex relay system.

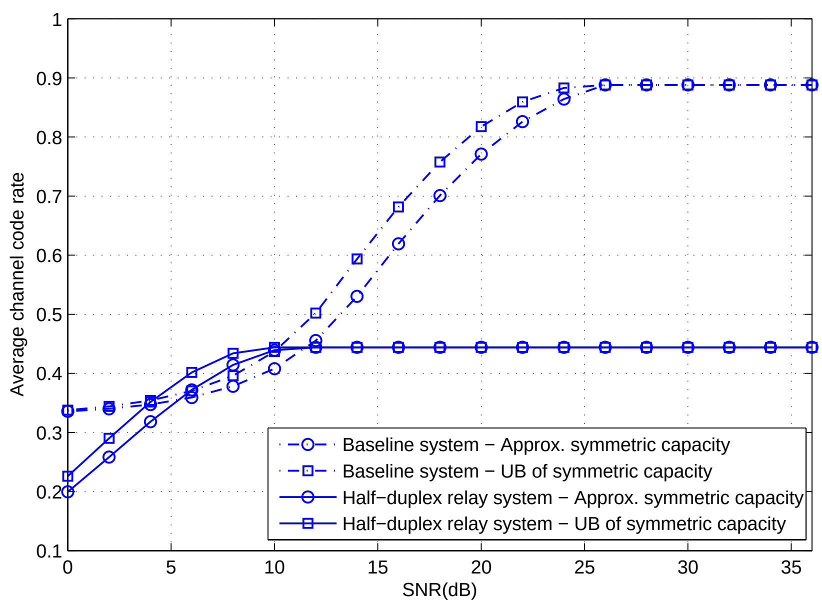

Figure II.5: Average channel code rate of baseline system and half duplex relay system. Effective code rate is presented, where effective code rate is defined as the ratio of the number of information bits and the length of packet.

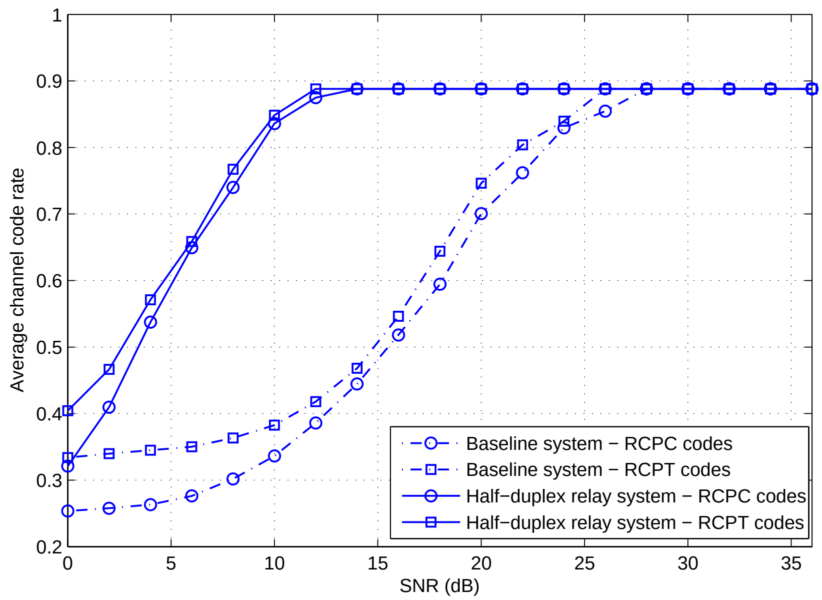

Figure II.6: Average RCPC and RCPT channel code rate of baseline system and half duplex relay system. For the half duplex relay system, code rate per time slot is presented.

presented. Fig. II.5 shows the effective code rate, r_c, where the effective code rate is defined as the ratio of the number of information bits per packet to the packet length. In the half-duplex relay system, the packet consists of two time slots, where the second time slot is the repetition of the first slot if the relay decodes the first time slot successfully. Therefore, even though the two systems have the same channel code rates, the number of information bits per packet in the half-duplex relay system is half of that in the baseline system, and the effective code rate of the half duplex relay system cannot be greater than $1/2 \max\{R\}$, as shown in Fig. II.5. Interestingly, the average code rate for the half-duplex relay system is fixed at 4/9 after 12 dB of channel SNR. This is mainly caused by the high diversity gain of the relay system, which allows for a higher code rate. Fig. II.6 presents the average RCPC and RCPT code rates, where the code rate of the half-duplex relay system represents the code rate per time slot, not per packet. As shown in this figure, the average code rates corresponding to the half duplex relay system converge to $\max\{R\}$ at an SNR around 14 dB. That is, when channel SNR is greater than 14 dB, the half duplex relay system can choose the highest code rate for all packets and then rate-optimal UEP becomes EEP. Finally, the rate-optimal UEP profiles of the baseline system at an SNR of 18 dB are presented in Fig. II.7. The UEP profiles of the RCPC and RCPT codes are found using the corresponding PER and the algorithm of [39], while the two curves above represent UEP profiles computed by using approximated MI outage probability and its lower bound. The stepwise UEP profiles are also presented by rounding the UEP profiles of the MI outage probability to the nearest RCPC and RCPT code rates. As can be seen, in most packets, the analytically-derived UEP channel code rates are higher than the UEP channel code rates of the RCPC and RCPT codes, since the MI outage probability lower bounds the PER. This can help in finding the rate-optimal UEP for a specific channel coding scheme by reducing the possible code-rate set.

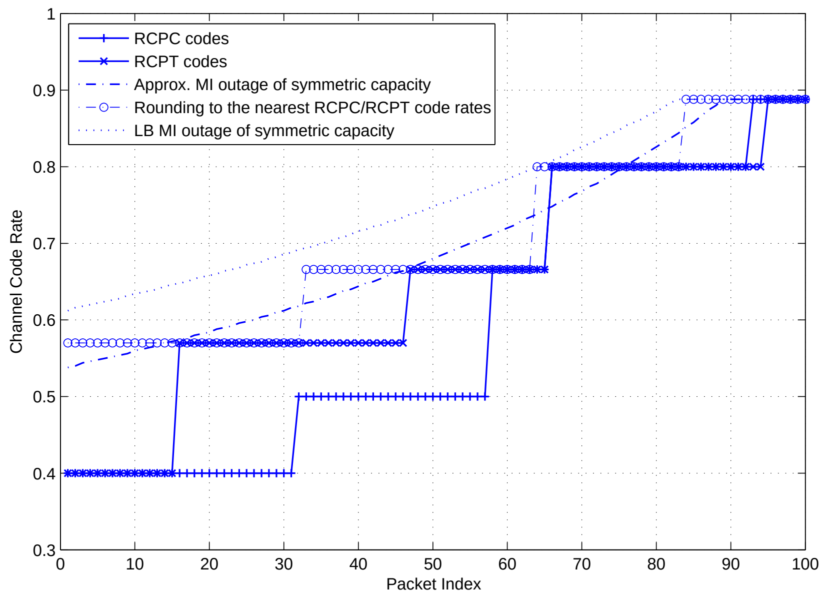

Figure II.7: Channel code rate profile of the baseline system at 18 dB

II.F Conclusion

We studied source channel rate allocation for a general progressive image transmission system over a block fading relay channel. In particular, we derived the outage probability for the baseline and the half-duplex relay systems with Gaussian as well as BPSK inputs. We then derived the average throughput expressions using the channel MI outage probability, which is a lower bound on the PER. To solve the optimization problem, we proved the concavity of the objective functions at high SNR and then found the solution using the recursive algorithm from [39]. We compared the average throughput and the rate-optimal UEP code rates found from the analysis with those obtained from simulations of a BPSK-based system. Numerical results indicated that our information-theoretic system model yielded an approximate upper bound at high SNR on the system performance for the actual BPSK-based system with capacity achieving channel coding.

II.G Acknowledgements

This work was supported in part by the Center for Wireless Communications at UCSD, LG Electronics, and the UC Discovery Grant Program.

III

Superposition coding for cooperative communication with relay selection

III.A Introduction

Previously, we studied the cross-layer design for the transmission of progressive images over cooperative relay channels with focusing on the performance analysis and the derivation of the algorithm to find UEP with multiple DF protocol based relays. In this chapter, we extend the cross-layer design for the cooperative relay channel especially in the relay protocol perspective. That is, to enhance the performance, a relay-selection-based protocol can be considered instead of a conventional DF protocol. To do that, we still consider a block fading relay channel to transmit a Gaussian source which is successively refinable. In addition, to support the layered transmission of the source, superposition coding, which has been useful for a broadcast channel [33] [44], is considered.

In a broadcast channel, the transmitter cannot adapt to an individual node's channel gain. Instead, it may be required that all nodes have some minimum performance. By assigning high priority data, which can achieve a specified quality, to the base layer of the superposition coding, most nodes can achieve at least some minimum pre-specified performance, even if they have poor channel conditions. However, for nodes with good channel conditions, signals can be decoded with better performance. In [27], superposition coding is applied to relay communication to improve the throughput between the source and the destination, where the relay transmits a single layer which is re-encoded with a different codebook. Optimal power and rate allocation in two-level superposition coding based relaying schemes are studied by Goparaju et al [28]. An information theoretic approach for this problem is studied in [19], where the authors considered joint source-channel coding for cooperative relaying systems with superposition coding when channel state information is only known at the receiver and quasi-static channels are assumed. They investigated the performance in terms of the distortion exponent to quantify the decay rate of the expected distortion. In this chapter, we analyze the performance of the system both with and without superposition coding in terms of the average distortion. Then, we propose a simple algorithm where the superposition coding is used for the channel from the source to the relays, which is a broadcast channel. A pre-determined number of relays are dedicated to the base layer and to the enhancement layer in the transmission from the relays to the destination, which is not a broadcast channel.

The rest of this chapter is organized as follows. In Sections III.B and III.C, the system model and the performance analysis of three different protocols based on DF are presented. Numerical results are shown in Section III.D. Finally, in Section III.E, conclusions are presented.

III.B System Model and Performance Analysis - SISO

In this chapter, we consider a single source, a single destination, and multiple relays. A Gaussian source is transmitted. Assuming that the total bandwidth is divided into N equiwidth, disjoint channels as shown in Fig. III.1, the transmissions of source and relay nodes are orthogonal in the time and frequency domains. We assume half-duplex and DF relays, so only those relay nodes that successfully decode the source packet will re-encode and forward it to the destination. A direct link (DL) between source and destination is not assumed. We consider a block fading channel, where the fading coefficients are only known at the corresponding receivers of the relay and destination nodes.

We assume power constraints on both the source and relay nodes. If the transmit power from the source node is P_T, then we assume that the maximum transmit power per relay node is P_T/N, where N is the total number of relays. We consider the following three protocols for relays to transmit the packet:

III.B.1 Case 1 : Repetition-based conventional single layer transmission

As presented in [21], the relay transmits a packet if the packet is decoded successfully at the relay. If not, the relay is silent. To analyze the performance, we assume that a successively refinable Gaussian source is transmitted. We derive information-theoretic expressions of the average throughput and the expected distortion as functions of the outage probability. In Case 1, the Gaussian source is transmitted in a single layer.

We denote by α_{sr}^j the fading amplitude on the path from the source to the jth relay node, and by α_{rd}^j the fading amplitude on the path from the jth relay node to the destination. We assume that α_{sr}^j and α_{rd}^j, for $j = 1, ..., N$, are independent and Rayleigh distributed, with second moments $E[(\alpha_{sr}^j)^2] = \Omega_{sr}^j$ and $E[(\alpha_{rd}^j)^2] = \Omega_{rd}^j$. Then, the mutual information (MI), conditioned on the channel gain, and the outage probability for the channel from the source to the jth relay

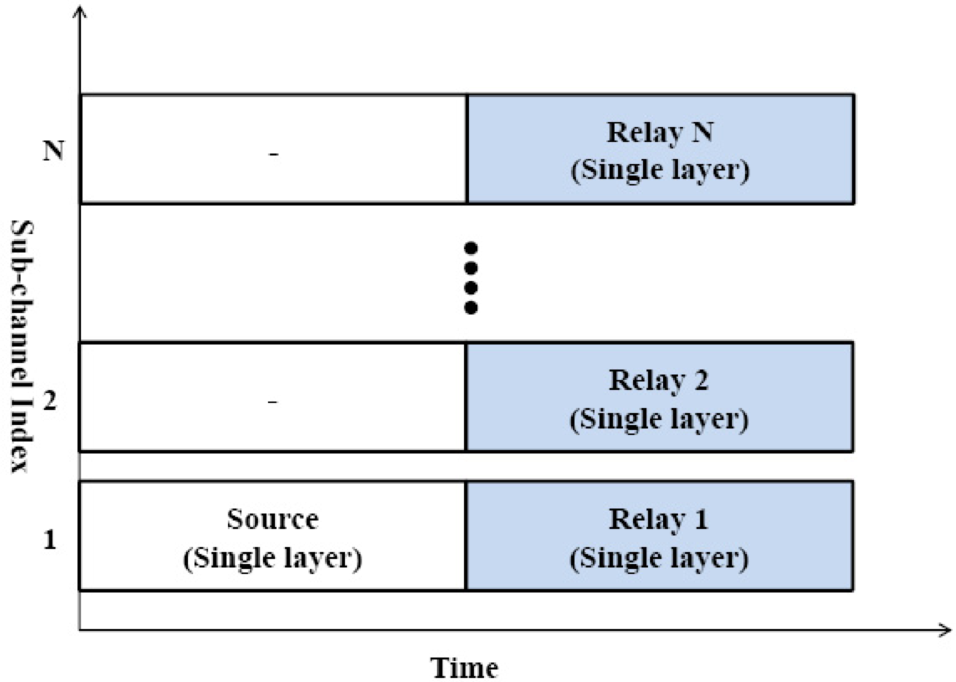

Figure III.1: Case 1 : Repetition-based conventional single layer transmission.

with given rate R can be represented as [21] [45]

$$\begin{aligned} \mathrm{MI}(j) &= \frac{1}{2}\log_2\Big(1+\frac{P_T}{\sigma_N^2}(\alpha_{sr}^j)^2\Big) && \text{(III.1)} \\ \pi_{r_j}(R) &= \mathrm{Prob}\Big(\mathrm{MI}(j)<R\Big) \\ &= \mathrm{Prob}\Big(\frac{1}{2}\log_2\Big(1+\frac{P_T}{\sigma_N^2}(\alpha_{sr}^j)^2\Big)<2R\Big) \\ &= \mathrm{Prob}\Big(\frac{P_T}{\sigma_N^2}(\alpha_{sr}^j)^2<2R\Big) \\ &= \gamma_{\mathrm{inc}}\Big(\frac{2^2R-1}{\frac{P_T}{\sigma_N^2}\Omega_{sr}^j},1\Big), && \text{(III.2)} \end{aligned}$$

respectively, where γ_{inc} is the incomplete Gamma function, which is defined as [42]

$$\gamma_{\mathrm{inc}} \triangleq \frac{1}{\int_{\mu=0}^{\infty} e^{-\mu}\mu^{n-1}d\mu}\int_{\mu=0}^{x} e^{-\mu}\mu^{n-1}d\mu. \qquad \text{(III.3)}$$

Note that MI is normalized by W, which is the bandwidth of a subchannel, throughout this chapter. The single-sided power spectral density of the additive Gaussian noise is denoted by N_0, so that the noise power in a bandwidth W is $\sigma_N^2 = N_0W$.

We assume there are N relays and that P_T, which is the total transmit power from the source, is equally allocated to the relays. Then, the relays which decode the packet successfully will transmit the packet to the destination. At the destination, all packets are maximal-ratio combined and then decoded. Let Φ_k denote the possible set of relay nodes which successfully decode the source packet, where $k = 1, ..., 2^N$. The probability of the set Φ_k is

$$\text{Prob}(\Phi_k) = \prod_{i \in \Phi_k} (1 - \pi_{r_i}(R)) \prod_{j \notin \Phi_k} \pi_{r_j}(R), \tag{III.4}$$

where independence of the decoding errors at the relays, due to the spatial independence of the channel fading, is assumed. At the destination, the MI and the outage probability, conditioned on Φ_k, are

$$\begin{aligned} \text{MI}_d(\Phi_k) &= \frac{1}{2}\log_2\Big(1 + \sum_{l \in \Phi_k} \frac{P_T/N}{\sigma_N^2}(\alpha_{rd}^l)^2\Big) && \text{(III.5)} \\ \pi_d(R, \Phi_k) &= \sum_{l \in \Phi_k} \lambda(\Phi_k)\gamma_{\text{inc}}\big(\frac{2^2R - 1}{\frac{P_T/N}{\sigma_N^2}\Omega_{rd}^l}, 1\big), && \text{(III.6)} \end{aligned}$$

respectively, where $\lambda(\Phi_k)$ is defined as [21]

$$\lambda(\Phi_k) = \prod_{m \in \Phi_k, m \neq l} \frac{\Omega_{rd}^l}{\Omega_{rd}^l - \Omega_{rd}^m}. \tag{III.7}$$

For simplicity, we assume channels from relays to destination have identical statistics. Then,

$$\pi_d(R, \Phi_k) = \gamma_{\text{inc}}\big(\frac{2^2R - 1}{\frac{P_T/N}{\sigma_N^2}\Omega_{rd}}, |\Phi_k|\big), \tag{III.8}$$

where Ω_{rd} represents the mean channel gain from relays to destination, and $|\Phi_k|$ is the number of relays in the set Φ_k. Finally, on averaging (III.6) over all possible decoding sets, the outage probability is

$$\pi_d(R) = \sum_{\Phi_k} \text{Prob}(\Phi_k)\pi_d(R, \Phi_k). \tag{III.9}$$

With (III.9), the average throughput at the destination can be computed as

$$E[T(R)] = 0 \cdot \pi_d(R) + R(1 - \pi_d(R)). \tag{III.10}$$

To obtain the expected distortion, we use the well-known distortion-rate function for the unit variance Gaussian source presented in [33] as

$$D(R) = 2^{-2R}. \tag{III.11}$$

Based on this function, the expected distortion can be computed as

$$E[D(R)] = 2^0 \cdot \pi_d(R) + 2^{-2R}(1 - \pi_d(R)). \tag{III.12}$$

III.B.2 Case 2 : Repetition-based superposition coding

In this case, the base and enhancement layers are multiplexed using superposition coding, where the base layer (BL) and enhancement layer (EL) are generated by partitioning the successively refinable Gaussian source bitstream and the EL cannot be decoded without the BL. Since the priority of the BL is higher than that of the EL, more power can be assigned to the BL, which will be discussed later. At the relay, the BL is decoded first. To do that, the EL is considered as interference. If the BL is decoded successfully, then it is subtracted from the received signal to decode the EL. If a relay decodes both layers successfully, then both layers are superposed and transmitted. However if a relay decodes only the BL, then it will transmit the BL only. Since the EL cannot be used to reconstruct the source without the BL, we ignore the case where only the EL is available. Relays with good channel conditions will likely decode both the BL and the EL, while other relays, with poor channel condition, may decode nothing, or the BL only. Therefore, at the destination, maximal ratio combining (MRC) cannot be used over all received signals.

For Case 2, we will find the outage probability for the BL and EL separately. Since the Gaussian source is successively refinable, the source cannot be reconstructed from the EL alone. As explained previously, at first, decoding is done for the BL. Then the EL is decoded after subtracting the BL from the received signal. We define β as the power allocation parameter for the BL, so that βP_T is allocated to the BL and $(1-\beta)P_T$ is allocated to the EL, where P_T represents the

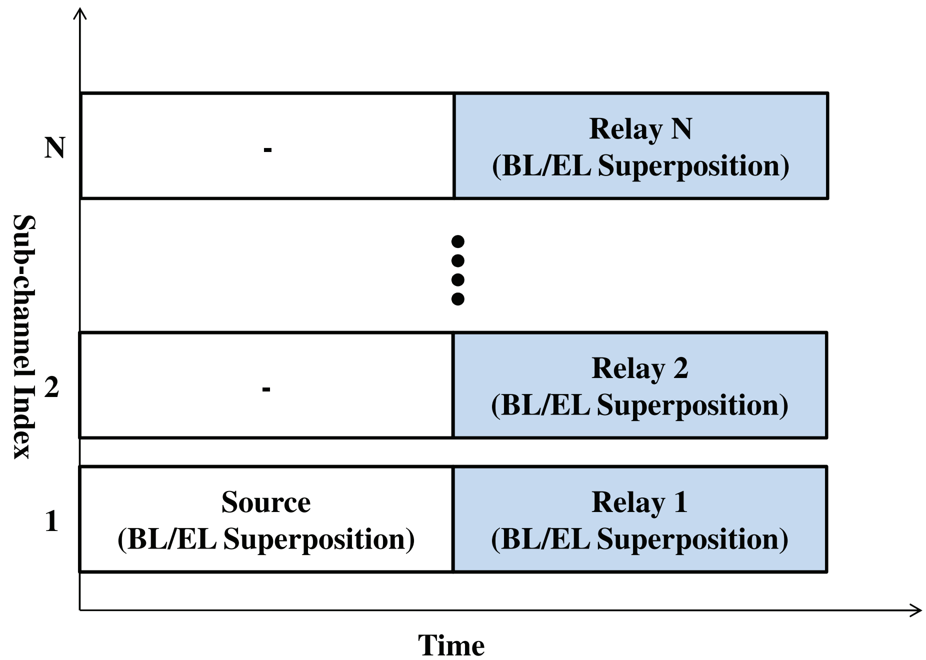

Figure III.2: Case 2 : Repetition-based superposition coding.

total transmit power from a single source. The MI, conditioned on the channel gain, for the BL from the source to the jth relay can be represented as

$$\mathrm{MI}_{BL}(j) = \frac{1}{2}\log_2\Big(1 + \frac{\beta P_T(\alpha_{sr}^j)^2}{\sigma_N^2 + (1-\beta)P_T(\alpha_{sr}^j)^2}\Big), \tag{III.13}$$

where $(1-\beta)P_T(\alpha_{sr}^j)^2$ represents the power of the interference caused by the EL. The corresponding outage probability for the BL from the source to the jth relay is given by

$$
\begin{aligned}
&\pi_{r_j,\mathrm{BL}}(R_{\mathrm{BL}}) \\
&= \mathrm{Prob}\Big(\mathrm{MI}_{\mathrm{BL}}(j) < R_{\mathrm{BL}}\Big) \\
&= \mathrm{Prob}\Big(\frac{\beta P_T(\alpha_{sr}^j)^2}{\sigma_N^2 + (1-\beta)P_T(\alpha_{sr}^j)^2} < 2^{2R_{\mathrm{BL}}} - 1\Big) \\
&= \mathrm{Prob}\big(\beta P_T(\alpha_{sr}^j)^2 - (1-\beta)P_T(\alpha_{sr}^j)^2(2^{2R_{\mathrm{BL}}}-1) < \sigma_N^2(2^{2R_{\mathrm{BL}}}-1)\big) \\
&= \begin{cases} \mathrm{Prob}\Big(\frac{(\alpha_{sr}^j)^2}{\Omega_{sr}^j} < \frac{\sigma_N^2(2^{2R_{\mathrm{BL}}}-1)}{\Omega_{sr}^j P_T(\beta+(\beta-1)(2^{2R_{\mathrm{BL}}}-1))}\Big), & \text{if } (1+(\beta-1)2^{2R_{\mathrm{BL}}}) > 0 \\ \mathrm{Prob}\Big(\frac{(\alpha_{sr}^j)^2}{\Omega_{sr}^j} > \frac{\sigma_N^2(2^{2R_{\mathrm{BL}}}-1)}{\Omega_{sr}^j P_T(\beta+(\beta-1)(2^{2R_{\mathrm{BL}}}-1))}\Big), & \text{if } (1+(\beta-1)2^{2R_{\mathrm{BL}}}) \le 0 \end{cases} \\
&= \begin{cases} \gamma_{\mathrm{inc}}\Big(\frac{2^{2R_{\mathrm{BL}}}-1}{\frac{P_T}{\sigma_N^2}\sigma_{sr}^j(1+(\beta-1)2^{2R_{\mathrm{BL}}})}\Big), & \text{if } (1+(\beta-1)2^{2R_{\mathrm{BL}}}) > 0 \\ 1, & \text{if } (1+(\beta-1)2^{2R_{\mathrm{BL}}}) \le 0 \end{cases}
\end{aligned} \tag{III.14}
$$

When the BL is decoded successfully and subtracted from the received signal, the MI and outage probability for the EL are

$$
\mathrm{MI}_{\mathrm{EL}}(j) = \frac{1}{2}\log_2\big(1 + \frac{(1-\beta)P_T(\alpha_{sr}^j)^2}{\sigma_N^2}\big) \tag{III.15}
$$

$$
\pi_{r_j,EL}(R_{\mathrm{EL}}) = \gamma_{\mathrm{inc}}\big(\frac{2^{2R_{\mathrm{EL}}}-1}{\frac{P_T}{\sigma_N^2}\Omega_{sr}^j(1-\beta)}, 1\big), \tag{III.16}
$$

respectively. If we assume all channels from source to relays have identical statistics, then

$$
\pi_{r,\mathrm{BL}}(R_{\mathrm{BL}}) = \gamma_{\mathrm{inc}}\Big(\frac{2^{2R_{\mathrm{BL}}}-1}{\frac{P_T}{\sigma_N^2}\Omega_{sr}(1+(\beta-1)2^{2R_{\mathrm{BL}}})}\Big) \tag{III.17}
$$

$$
\pi_{r,\mathrm{EL}}(R_{\mathrm{EL}}) = \gamma_{\mathrm{inc}}\Big(\frac{2^{2R_{\mathrm{EL}}}-1}{\frac{P_T}{\sigma_N^2}\Omega_{sr}(1-\beta)}\Big). \tag{III.18}
$$

As opposed to Case 1, the signals transmitted from relays may not be combined in Case 2. For example, if some relays decode both the BL and EL, but others decode only the BL, then MRC cannot be applied for all the received signals at the destination. Except for the cases where all relays decode both the BL and the EL, or the BL only, we have the following decoding procedure at the destination :

1. If there are any relays transmitting only the BL, they will be used to decode the BL at the destination. If there is no relay transmitting only the BL, decoding is done for the BL by considering the EL as interference.

2. The EL is decoded after subtracting the BL from the received signal.

Let Θ_k and Ψ_k denote the sets of relays which successfully decode only the BL, or both the BL and the EL, respectively, where $\Theta_k \cap \Psi_k = \emptyset$. If we define y_k and z_k as the numbers of relays in the sets Θ_k and Ψ_k, respectively, the joint probability of Θ_k and Ψ_k is

$$\begin{aligned}\mathrm{Prob}(\Theta_k, \Psi_k) &= (\pi_{r,\mathrm{BL}}(R_{\mathrm{BL}}))^{N-y_k-z_k}\big((1-\pi_{r,\mathrm{BL}}(R_{\mathrm{BL}})\pi_{r,\mathrm{EL}}(R_{\mathrm{EL}}))\big)^{y_k} \\ &\quad \cdot\big((1-\pi_{r,\mathrm{BL}}(R_{\mathrm{BL}}))(1-\pi_{r,\mathrm{EL}}(R_{\mathrm{EL}}))\big)^{z_k}. \qquad \text{(III.19)}\end{aligned}$$

Based on the decoding procedure for Case 2, the MI and outage probability for the BL at the destination, conditioned on (Θ_k, Ψ_k), are

$$\mathrm{MI}_{d,\mathrm{BL}}(\Theta_k, \Psi_k) = \begin{cases} \frac{1}{2}\log_2\Big(1+\sum_{l\in\Theta_k}\frac{P_T/N}{\sigma_N^2}(\alpha_{rd}^l)^2\Big), & y_k > 0 \\ \frac{1}{2}\log_2\Big(1+\frac{\beta P_T/N(\sum_{l\in\Psi_k}(\alpha_{rd}^l)^2)}{\sigma_N^2+(1-\beta)P_T/N(\sum_{l\in\Psi_k}(\alpha_{rd}^l)^2)}\Big), & y_k = 0, \end{cases} \qquad \text{(III.20)}$$

$$\pi_{d,\mathrm{BL}}(R_{\mathrm{BL}}, \Theta_k, \Psi_k)$$
$$= \begin{cases} \gamma_{\mathrm{inc}}\Big(\frac{2^{2R_{\mathrm{BL}}}-1}{\frac{P_T/N}{\sigma_N^2}\Omega_{rd}}, y_k\Big), & y_k > 0 \\ \gamma_{\mathrm{inc}}\Big(\frac{2^{2R_{\mathrm{BL}}}-1}{\frac{P_T/N}{\sigma_N^2}\Omega_{rd}(1+(\beta-1)2^{2R_{\mathrm{BL}}})}, z_k\Big), & y_k = 0 \text{ and } (1+(\beta-1)2^{2R_{\mathrm{BL}}}) > 0 \\ 1, & y_k = 0 \text{ and } (1+(\beta-1)2^{2R_{\mathrm{BL}}}) \leq 0, \end{cases}$$
(III.21)

respectively. If $y_k = z_k = 0$, then there is no transmission from relays to destination, so the outage probability is not defined. After perfect subtraction of the BL from the received signal, the EL outage probability at the destination, conditioned on (Θ_k, Ψ_k), is

$$\pi_{d,\mathrm{EL}}(R_{\mathrm{EL}}, \Theta_k, \Psi_k) = \gamma_{\mathrm{inc}}\big(\frac{2^{2R_{\mathrm{EL}}}-1}{\frac{P_T/N}{\sigma_N^2}\Omega_{rd}(1-\beta)}, z_k\big). \qquad \text{(III.22)}$$

The outage probabilities, after averaging over all possible decoding sets, (Θ_k, Ψ_k) for the BL and the EL, are

$$\pi_{d,\mathrm{BL}}(R_{\mathrm{BL}}) = \sum_{(\Theta_k,\Psi_k)} \mathrm{Prob}(\Theta_k, \Psi_k)\pi_{d,\mathrm{BL}}(R_{\mathrm{BL}}, \Theta_k, \Psi_k) \qquad \text{(III.23)}$$

$$\pi_{d,\mathrm{EL}}(R_{\mathrm{EL}}) = \sum_{(\Theta_k,\Psi_k)} \mathrm{Prob}(\Theta_k, \Psi_k)\pi_{d,\mathrm{EL}}(R_{\mathrm{EL}}, \Theta_k, \Psi_k), \qquad \text{(III.24)}$$

respectively. Then the average throughput can be computed as

$$\begin{aligned} E[T(R_{\mathrm{BL}}, R_{\mathrm{EL}})] &= 0 \cdot \pi_{d,\mathrm{BL}}(R_{\mathrm{BL}}) + R_{\mathrm{BL}}(1-\pi_{d,\mathrm{BL}}(R_{\mathrm{BL}}))\pi_{d,\mathrm{EL}}(R_{\mathrm{EL}}) \\ &\quad +(R_{\mathrm{BL}}+R_{\mathrm{EL}})(1-\pi_{d,\mathrm{BL}}(R_{\mathrm{BL}}))(1-\pi_{d,\mathrm{EL}}(R_{\mathrm{EL}})), \end{aligned} \tag{III.25}$$

and the expected distortion is given by

$$\begin{aligned} E[D(R_{\mathrm{BL}}, R_{\mathrm{EL}})] &= 1 \cdot \pi_{d,\mathrm{BL}}(R_{\mathrm{BL}}) + 2^{-2R_{\mathrm{BL}}}(1-\pi_{d,\mathrm{BL}}(R_{\mathrm{BL}}))\pi_{d,\mathrm{EL}}(R_{\mathrm{EL}}) \\ &\quad +2^{-2(R_{\mathrm{BL}}+R_{\mathrm{EL}})}(1-\pi_{d,\mathrm{BL}}(R_{\mathrm{BL}}))(1-\pi_{d,\mathrm{EL}}(R_{\mathrm{EL}})). \end{aligned} \tag{III.26}$$

III.B.3 Case 3 : Relay dedication-based superposition coding

The decoding procedure of this protocol at the relays is exactly the same as that of Case 2. However, in this case, we assume all relays can communicate with each other to know whether other relays decode the BL and EL successfully. Based on that, we dedicate specific relays to the BL or the EL, instead of transmitting the superposed signal. By doing that, the BL or EL avoids the interference caused by the other layer at the destination.

For Case 3, the outage probability from the source to the relays is exactly the same as for Case 2. However, from the relays to the destination, the outage is dependent on the number of relays dedicated to a specific layer. Assume at most M relays are assigned to the BL. If there are more than M relays which decode both the BL and the EL, then only M relays transmit the BL and the others transmit the EL. However, if there are fewer than M relays which decode the BL or both the BL and the EL, then all relays transmit only the BL. Then, the following decoding procedure is applied to Case 3, where y_k and z_k represent the number of relays which successfully decode only the BL, or both the BL and the EL, respectively :

1. If $(y_k + z_k) \leq M$, all relays transmit only the BL.

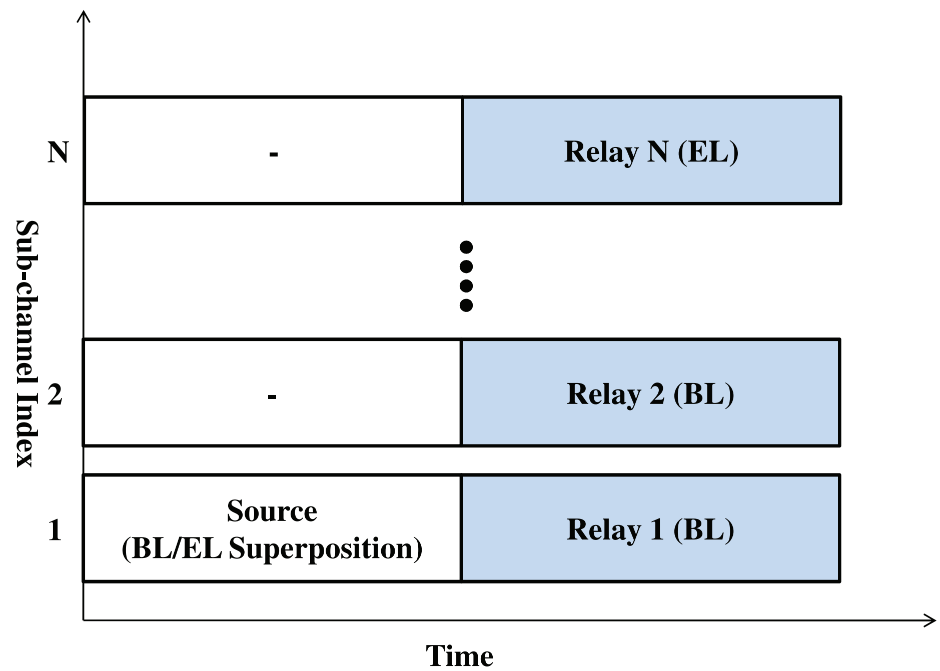

Figure III.3: Case 3 : Relay dedication-based superposition coding.

2. If $(y_k + z_k) > M$, but $y_k \leq M$, then the y_k relays which decode only the BL and the $(M - y_k)$ relays which decode both layers are dedicated to transmit only the BL. The remaining $(z_k - (M - y_k))$ relays which have both BL and EL transmit only the EL.

3. If $y_k > M$, then the z_k relays which have both layers transmit only the EL. The other y_k relays transmit only the BL.

If we denote $L = y_k + z_k - M$ for a given (Θ_k, Ψ_k), the outage probability for the BL from the relays to the destination is

$$\pi_{d,\mathrm{BL}}(R_{\mathrm{BL}}, \Theta_k, \Psi_k) = \begin{cases} \gamma_{\mathrm{inc}}\left(\frac{2^{2R_{\mathrm{BL}}}-1}{\frac{P_T/N}{\sigma_N^2}\Omega_{rd}}, y_k + z_k\right), & L \leq 0 \\ \gamma_{\mathrm{inc}}\left(\frac{2^{2R_{\mathrm{BL}}}-1}{\frac{P_T/N}{\sigma_N^2}\Omega_{rd}}, y_k\right), & L > 0 \text{ and } y_k > M \\ \gamma_{\mathrm{inc}}\left(\frac{2^{2R_{\mathrm{BL}}}-1}{\frac{P_T/N}{\sigma_N^2}\Omega_{rd}}, M\right), & L > 0 \text{ and } y_k \leq M, \end{cases} \quad \text{(III.27)}$$

and the outage probability for the EL is

$$\pi_{d,\mathrm{EL}}(R_{\mathrm{EL}}, \Theta_k, \Psi_k) = \begin{cases} \gamma_{\mathrm{inc}}\Big(\frac{2^{2R_{\mathrm{EL}}-1}}{\frac{P_T/N}{\sigma_N^2}\Omega_{rd}}, z_k\Big), & L > 0 \text{ and } y_k > M \\ \gamma_{\mathrm{inc}}\Big(\frac{2^{2R_{\mathrm{EL}}-1}}{\frac{P_T/N}{\sigma_N^2}\Omega_{rd}}, L\Big), & L > 0 \text{ and } y_k \leq M. \end{cases} \tag{III.28}$$

Note that there is no EL transmission from relays to the destination if $L \leq 0$. The average throughput and distortion for Case 3 are exactly the same as those presented in (III.25) and (III.26) for Case 2, except for the expression of outage probability.

III.C System model and performance analysis - MIMO

In this section, we assume that a single source and multiple relays have a single antenna each, and the destination has multiple antennas. As opposed to the previous SISO scenario, we assume all relays share a single channel by applying multiplexing schemes such as superposition coding as well as spatial multiplexing for the transmission of multiple layers. Since there are multiple receive antennas at the destination, spatial multiplexing or spatial diversity can be used in the relay-to-destination links consisting of virtual MIMO, based on the relay protocols.

III.C.1 Case 1 : Repetition-based conventional single layer transmission

We consider the same system model presented in the previous section for the SISO scenario, except that there are multiple antennas at the destination and all relays share a single channel. Therefore, for the link from the source to the relays, we have the same analysis for the MI and outage probability. For the links between the relays and the destination, we denote by α_{rd}^{ij} the fading amplitude on the path from the jth relay node to the ith receive antenna at the destination. Then, at the destination, the MI, conditioned on Φ_k, is

$$\mathrm{MI}_d(\Phi_k) = \frac{1}{2}\log_2\Big(1 + \sum_{i=1}^{M_R} \frac{P_T/N}{\sigma_N^2}(\sum_{j\in\Phi_k} \alpha_{rd}^{ij})^2\Big), \tag{III.29}$$

where M_R represents the number of receive antennas at the destination and the received SNR computation follows the approach presented in [46]. Assuming that the channels from the relays to the destination have identical statistics, the outage probability is

$$\pi_d(R, \Phi_k) = \gamma_{\text{inc}}\Big(\frac{2^2R - 1}{\frac{P_T/N}{\sigma_N^2}|\Phi_k|\Omega_{rd}}, M_R\Big). \tag{III.30}$$

III.C.2 Cases 2 and 3 : Repetition and relay dedication-based superposition coding

As shown in the previous section, not all relays necessarily transmit the same data to the destination when superposition coding is applied. That is, some relays transmit only the BL, but the others can transmit superposed BL/EL or EL only. However, individual antennas at the destination can receive both layers, since a single channel is shared by all relays. To combine the received signals at the individual antenna, we apply optimum combining [47], which maximizes the received SINR, where the EL is considered as co-channel interference when the BL is decoded first. With optimum combining, the received SINR is computed as [47]

$$\nu = \frac{P_T}{N}(C_D A(\Theta_k, \Phi_k))^{\dagger} R_I^{-1}(C_D A(\Theta_k, \Phi_k)), \tag{III.31}$$

where R_I denotes the short-term covariance matrix of the Gaussian noise and interference, and is given by

$$R_I = \sigma_N^2 I_{M_R} + \frac{P_T}{N}(C_D B(\Theta_k, \Phi_k))(C_D B(\Theta_k, \Phi_k))^{\dagger}. \tag{III.32}$$

In (III.32), C_D is the matrix of fading amplitudes from the relays to the multiple antennas at the destination, given by

$$C_D = \begin{pmatrix} \alpha_{rd}^{11} & \alpha_{rd}^{12} & \cdots & \alpha_{rd}^{1N} \\ \alpha_{rd}^{21} & \alpha_{rd}^{22} & \cdots & \alpha_{rd}^{2N} \\ \vdots & \vdots & \ddots & \vdots \\ \alpha_{rd}^{M_R1} & \alpha_{rd}^{M_R2} & \cdots & \alpha_{rd}^{M_RN} \end{pmatrix}, \tag{III.33}$$

and $A(\Theta_k, \Phi_k)$ and $B(\Theta_k, \Phi_k)$ are the vectors representing how much power is assigned to the BL and the EL, respectively, at the relay. For example, in the protocol of 'Repetition-based superposition coding', $\sqrt{\beta}P_T/N$ and $\sqrt{1-\beta}P_T/N$ are the assigned powers to the BL and the EL, respectively, if the relay decodes both BL and EL. Then, the MI and outage probability for the BL at the destination, conditioned on (Θ_k, Φ_k), are given by

$$\begin{aligned} \mathrm{MI}_{d,\mathrm{BL}}(\Theta_k, \Phi_k) &= \frac{1}{2}\log_2(1+\nu) \\ \pi_{d,\mathrm{BL}}(R_{\mathrm{BL}}, \Theta_k, \Phi_k) &= \mathrm{Prob}(\nu < 2^{2R_{\mathrm{BL}}} - 1), \end{aligned} \tag{III.34}$$

respectively. Due to the lack of a closed-form expression for the outage probability, the numerical results shown in the next section are based on a simulation.

III.D Numerical Results

In this section, we present numerical results based on the previous analysis. To generate the results, we consider either two or four relays located midway between the source and destination. All relays have the same mean channel gain to the destination. For the SISO scenario, in Fig. III.4, the expected throughputs for Cases 1, 2, and 3 are presented using (III.10) and (III.25). With two relays, we assign a single relay to the BL and the other to the EL to implement Case 3. As shown in the figure, Case 3 outperforms the other protocols in terms of the expected throughput. In particular, Cases 1 and 2 have almost the same throughput, where both of them are based on the DF protocol in the relays. The expected distortions for the three different protocols are shown in Fig. III.5. This shows that layered transmission with superposition coding can reduce the expected distortion, compared to single layer transmission, even with a conventional DF protocol. And, from the expected distortion of Cases 2 and 3, we need to assign higher order diversity to the BL to reduce the expected distortion.

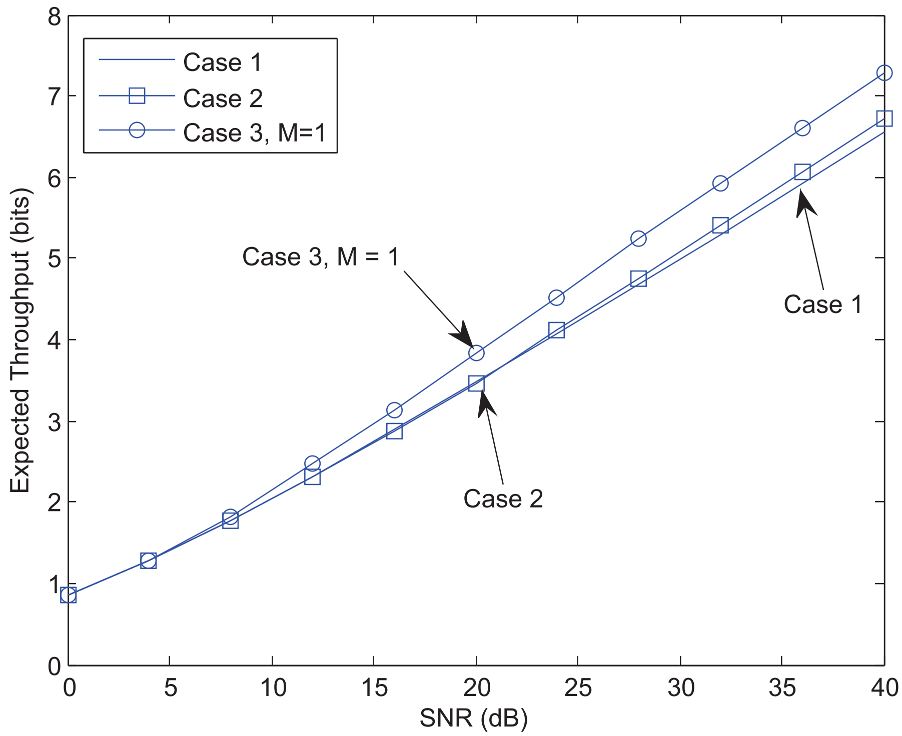

Figure III.4: Expected throughput with 2 relays and 1 receive antenna at the destination.

In Fig. III.6, the expected throughputs for Cases 1, 2, and 3 are shown, where four relays and a single receive antenna at the destination are considered. For Case 3, we consider $M = 1, 2, 3$. That is, one, two, or three relays are assigned to the BL. As shown, in terms of the expected throughput, Case 3 with $M = 2$ achieves the best performance. However, Case 2, which is based on the DF protocol and superposition coding, still does not enhance the throughput compared to Case 1, which is also shown in Fig. 4. The expected distortion is also presented in Fig. III.7, where Case 3 with $M = 2$ has the minimum distortion. Over most of the SNR range, Case 3 with $M = 3$ has comparable performance to Case 3 with $M = 2$. However, if $M = 1$, the expected distortion becomes worse than that of Case 2, where the relay repeats the superposed signal to the destination. This shows that the number of relays assigned to the BL needs to be at least 2 to reduce the expected distortion.

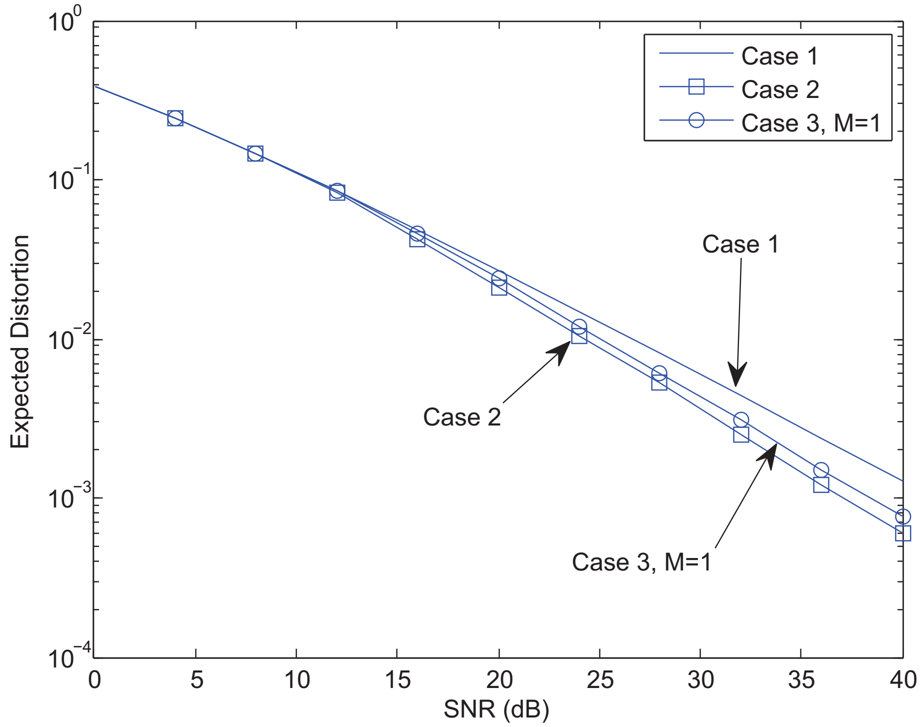

Figure III.5: Expected distortion with 2 relays and 1 receive antenna at the destination.

In Figs. III.8, III.9, III.10, and III.11, numerical results for the MIMO scenario are presented, where we assume two receive antennas at the destination and a single channel shared by all relays. Due to the lack of a closed-form expression for the outage probability in the link between the relays and the destination, we found the outage probability by simulation. In Fig. III.8 and III.9, the expected throughputs and distortions for the various protocols with two receive antennas are presented, where we consider two relays. As shown in Figs. III.4 and III.5 for SISO, Case 3 yields higher throughput than the other protocols, and Case 2 yields lower distortion than the other protocols. In particular, Case 3 shows poor distortion compared to Case 2. This is mainly caused by the loss of unequal resource assignment in the transmission through the link between the relays and the destination. That is, when there are only two relays, one of them transmits the BL and one transmits the EL, so the layers are getting equal resources. To

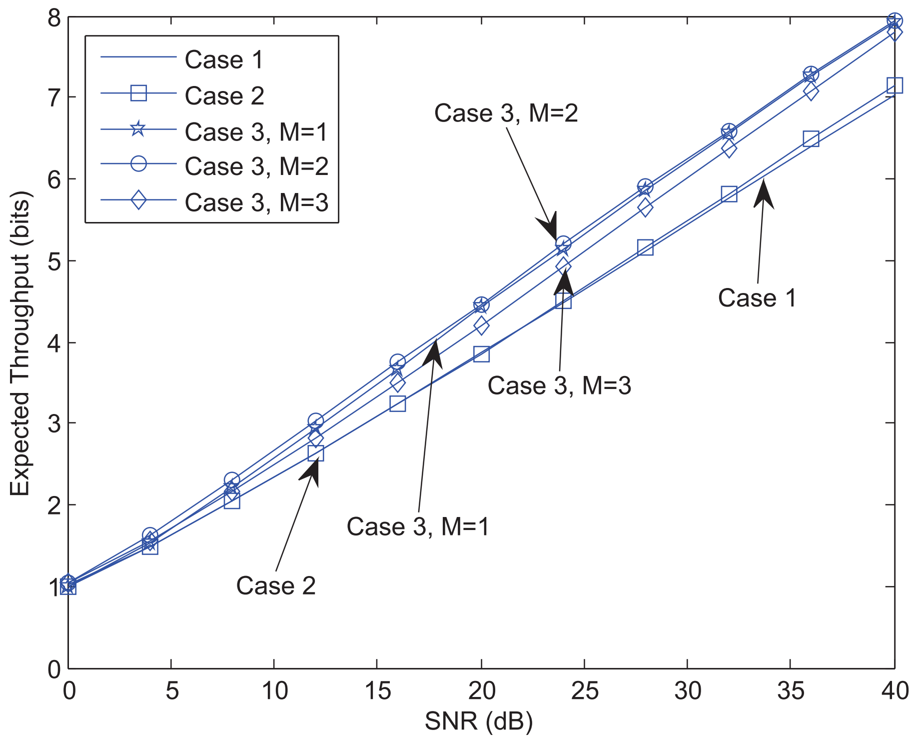

Figure III.6: Expected throughput with 4 relays and 1 receive antenna at the destination.

exploit the unequal resource assignment of the relay dedication-based protocol, we consider four relays as shown in Figs. III.10 and III.11. We see that Case 3 with $M = 2$ is the best among all the protocols considered in terms of the expected throughput as well as distortion.

III.E Conclusion

In this work, we consider the transmission of a Gaussian source over multiple relays. We consider three different protocols, which are based on the DF, with or without superposition coding. In the first protocol, a single layer source is transmitted and the relay repeats the source packet if it is decoded correctly. With superposition coding, the second protocol allows the relays to transmit either only the BL or both layers to the destination. Then, we propose a simple protocol to

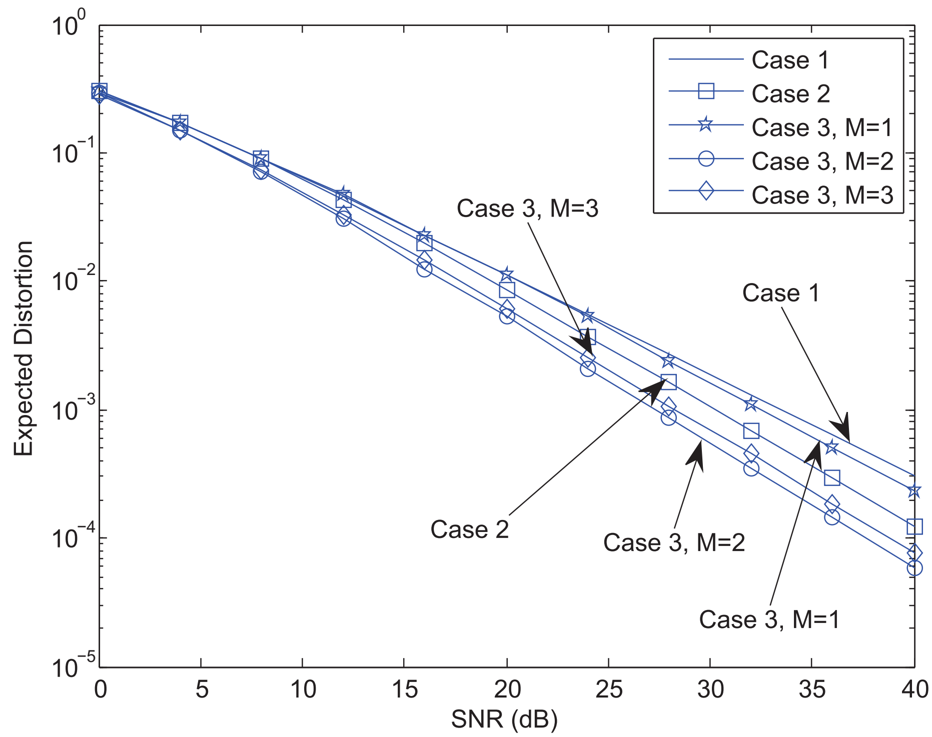

Figure III.7: Expected distortion with 4 relays and 1 receive antenna at the destination.

assign dedicated relays to the BL and the EL. The key point of the third protocol is that the superposition coding is used for the channel from the source to the multiple relays, which can be considered as a broadcast channel, and then specific relays are dedicated to the BL and the EL in the transmission from the relays to the destination, which is not a broadcast channel, to avoid the interference present in the superposition coding. Even though this simple protocol may not achieve the full diversity order for the superposed BL and EL at the destination, unequal diversity order can be assigned to the layers. We also present numerical results based on an information-theoretic approach for two different scenarios equipped with single or multiple antennas at the destination, and show that there is a reduction in the expected distortion by using the protocol based on relay dedication to specific layers for both scenarios.

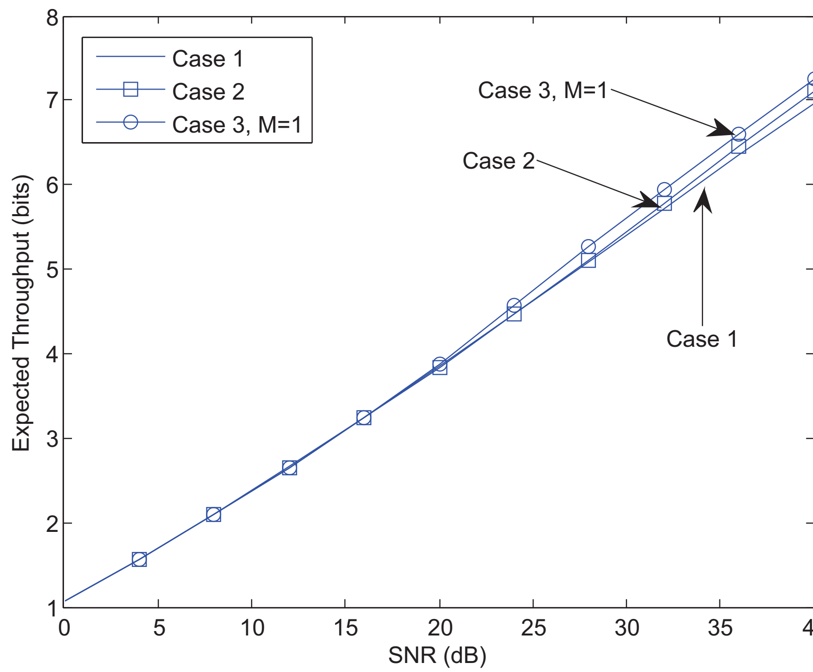

Figure III.8: Expected throughput with 2 relays and 2 receive antennas at the destination.

III.F Acknowledgements

This work was supported in part by the Center for Wireless Communications at UCSD, LG Electronics and the UC Discovery Grant Program.

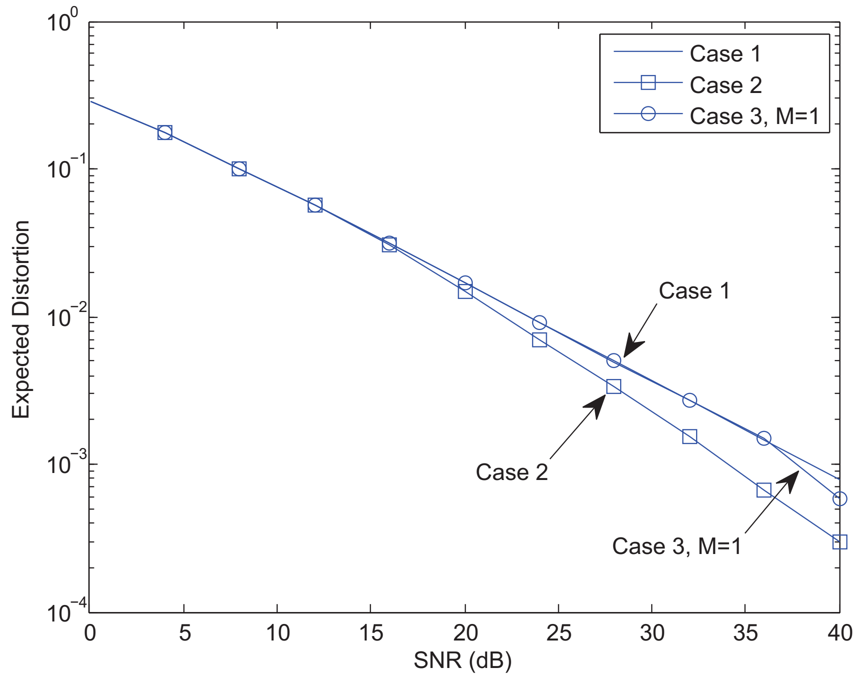

Figure III.9: Expected distortion with 2 relays and 2 receive antennas at the destination.

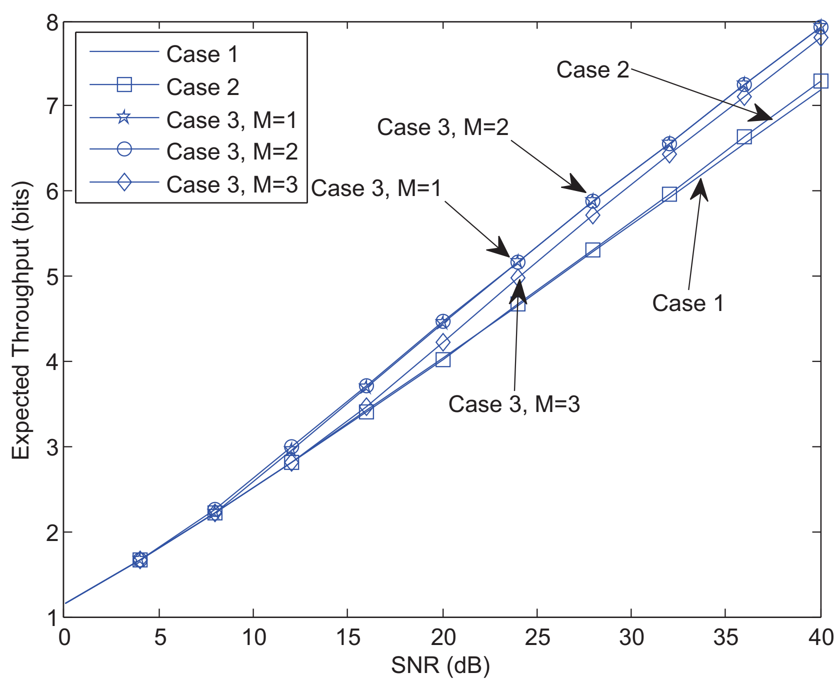

Figure III.10: Expected throughput with 4 relays and 2 receive antennas at the destination.

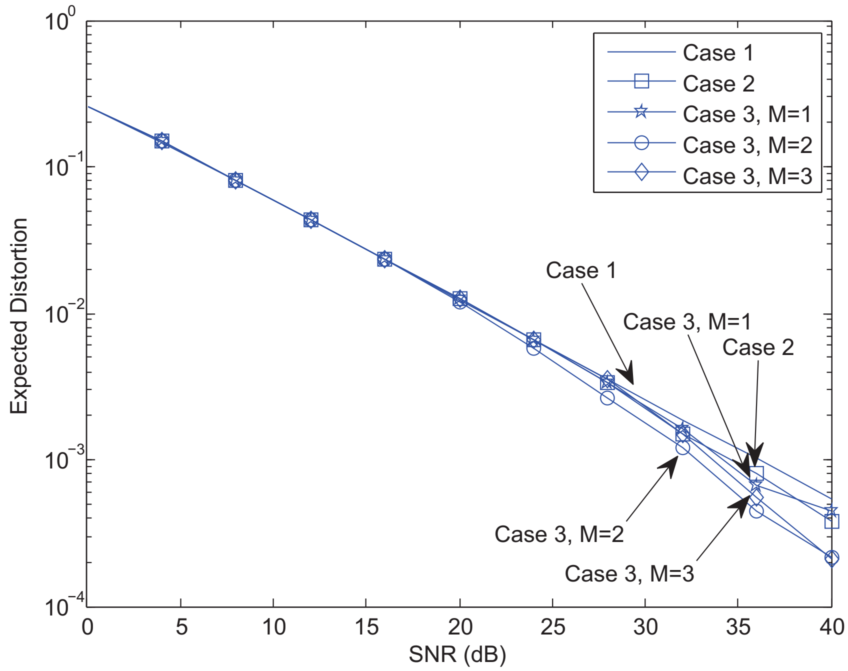

Figure III.11: Expected distortion with 4 relays and 2 receive antennas at the destination.

IV

Motion-compensated scalable video transmission over MIMO wireless channels

IV.A Introduction

Fine granularity scalable (FGS) video coding is suitable for mobile users with variable channel bandwidth, since it makes decoding possible even in the case of partial loss of the bitstream, where the FGS bitstream is encoded in a progressive manner. For example, in MPEG-4 FGS video coding, the base layer (BL) contains the most important information, such as coding modes and motion vectors. A scalable enhancement layer (EL) is generated using bit-plane coding on the DCT coefficients. When the BL is transmitted reliably, the scalable EL bitstream can be decoded, even though it is truncated at any point.

In motion compensated prediction (MCP) of conventional MPEG-4 FGS coding, the current BL and EL are only predicted from the BL of the previous frame. By excluding the EL from the MCP loop, MPEG-4 FGS coding can avoid error propagation which can be caused by the corruption of the EL. However, this can decrease the coding efficiency due to the use of a low quality reference frame. To enhance the compression efficiency, motion compensated fine granularity scalable (MC-FGS) coding was proposed in [29]. In this video coding scheme, a high quality reference is generated using the EL as well as the BL, which allows the system to achieve a high coding efficiency. However, the loss of the EL can result in severe error propagation, since there can be a mismatch (drift) between the reconstructed references at the encoder and the decoder.

In [48], progressive FGS (PFGS) was introduced to improve the coding efficiency and alleviate error propagation simultaneously. For higher coding efficiency, PFGS uses a separate prediction loop that contains a high quality reference frame in the encoding of the EL video. In order to address the drift problem, PFGS keeps a prediction path from the BL to the least significant bitplanes of the EL across several frames to ensure graceful recovery from errors over a few frames. Robust FGS (RFGS) [30] uses a different approach to control the tradeoff between the coding efficiency and the error propagation, where the two distinct parameters of leaky and partial prediction are used jointly. UEP can also be used to enhance the error resilience of MC-FGS by reducing the loss probability of the EL to be used for the reconstruction of the reference. As in [31], different numbers of parity bits are allocated to the packets of the EL according to their impact on average distortion.

In this chapter, we study the transmission of an MC-FGS bitstream over a MIMO channel with joint control of the UEP and the prediction parameters. Specifically, we propose a UEP policy consisting of FEC and MIMO mode selection to exploit the fundamental tradeoff between spatial diversity and multiplexing. Originally, the idea of combining cooperative diversity gain with UEP for a progressive image bitstream was proposed by Kwasinski in [49], where additional diversity was applied to high priority packets. We extend this to a MIMO system which can provide higher diversity orders. That is, for each packet, we choose an appropriate MIMO mode and FEC code rate to minimize average distortion.

The rest of this chapter is organized as follows. In Section IV.B, the source and channel models are described. The UEP scheme, based on a tradeoff between reliability and data rate, is proposed in Section IV.C. In Section IV.D, we provide simulation results and a discussion regarding the selection of the prediction parameters based on the instantaneous channel information which can be fed back to the transmitter. Finally, in Section IV.E, conclusions are presented.

IV.B System Model

IV.B.1 Source Model

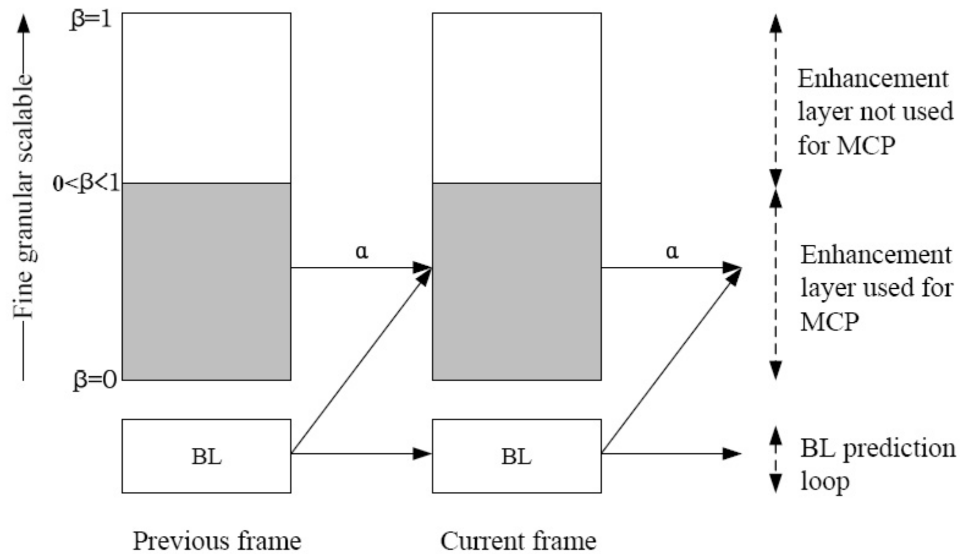

Figure IV.1: A motion compensated FGS coder with leaky and partial prediction.

We consider an MC-FGS video coder employing leaky and partial prediction, as introduced in [30] and [31]. In conventional MC-FGS video coding, both the BL and EL are used to reconstruct a high-quality reference. However, this can result in error propagation. To compensate for the error propagation, RFGS introduced leaky prediction as presented in Fig. IV.1, where the EL is scaled by the leaky prediction parameter, $\alpha \in [0, 1]$, before it is incorporated into the MCP loop. That is, at the encoder, the reference for the prediction of the current EL at time n, $\hat{F}_n^{EL,enc}$, is a weighted sum of the previous BL, F_{n-1}^{BL} and EL, F_{n-1}^{EL}, i.e.,

[31]

$$\hat{F}_n^{EL,enc} = (1-\alpha)F_{n-1}^{BL} + \alpha F_{n-1}^{EL}. \tag{IV.1}$$

Therefore, if the leaky prediction parameter is set to 0, the scheme becomes the MPEG-4 FGS video coding, where the EL is entirely excluded from the MCP loop. In contrast, if the leaky prediction parameter is fixed at unity, then it works as MC-FGS video coding. However, by choosing the parameter less than unity, the effect of error propagation can be reduced at the price of coding efficiency.

In partial prediction, the encoder designates the amount of the EL to be used for the reconstruction of the reference frame in the MCP loop. For example, the encoder could designate the number of bitplanes to be used. By including more bitplanes of the EL into the MCP loop, better coding efficiency can be achieved. However, if the instantaneous channel bandwidth cannot support the number of bitplanes used in the MCP loop, then it can result in error propagation. Therefore, the partial prediction parameter needs to be chosen based on knowledge of the channel bandwidth. In this paper, we allow an arbitrary number of symbols in the EL bitstream to be used in the MCP loop. Because the EL of MC-FGS coding can be truncated at any point, we do not need to operate with the coarse granularity of whole bitplanes, but can operate with the fine granularity of individual symbols. We define the partial prediction parameter, β, to be the ratio of the number of EL symbols used for MCP and the maximum number of EL symbols for that frame. Then, (IV.1) can be represented as

$$\hat{F}_n^{EL,enc,\beta} = (1-\alpha)F_{n-1}^{BL} + \alpha F_{n-1}^{EL,\beta}, \tag{IV.2}$$

where $\hat{F}_n^{EL,enc,\beta}$ is the reference for the prediction of the current EL with partial prediction, and $F_{n-1}^{EL,\beta}$ is the partially reconstructed EL of the previous frame at the encoder.

IV.B.2 Channel Model

In this paper, we assume an $M_r \times M_t$ wireless MIMO channel, where M_r and M_t represent the number of receive and transmit antennas, respectively. Assuming perfect matched filter reception, we can use the following discrete-time channel model :

$$r[l] = H[l]s[l] + n[l], \tag{IV.3}$$

where $r[l]$ represents the $M_r \times 1$ received signal vector, $s[l]$ is the $M_t \times 1$ transmitted signal vector, and $n[l]$ is the $M_r \times 1$ independent and identically distributed (i.i.d.) additive Gaussian noise vector for the l-th symbol. $H[l]$ is the $M_r \times M_t$ MIMO channel coefficients matrix, whose elements are i.i.d. zero-mean complex Gaussian random variables with variance σ_h^2. We consider a high Doppler environment, which results in rapidly time-varying channels. Given the Doppler spread, to model the channel estimation error, we consider the following system :

- Pilot symbol assisted modulation (PSAM) [50]
- Orthogonal pilot symbols for each transmit antenna
- Channel estimation using the K nearest pilot samples in conjunction with a Wiener filter.

If we denote the estimation error of the channel from the jth transmit antenna to the ith receive antenna by $\varepsilon_{ij}[l]$, then it can be modelled as a complex Gaussian random variable, and its variance, $\sigma_\varepsilon^2[l]$, can be expressed as [50]

$$\sigma_\varepsilon^2[l] = 1 - w^\dagger[l]R^{-1}w[l], \tag{IV.4}$$

where R represents the $K \times K$ autocorrelation matrix of the nearest K received pilot samples, $w[l]$ is the $K \times 1$ cross-covariance vector between the received pilot samples and $h_{ij}[l]$, and we assume $\sigma_h^2 = 1$. Note that $w[l]$ and R are dependent on the pilot signal-to-noise ratio (SNR), Doppler spread, and pilot spacing. In this

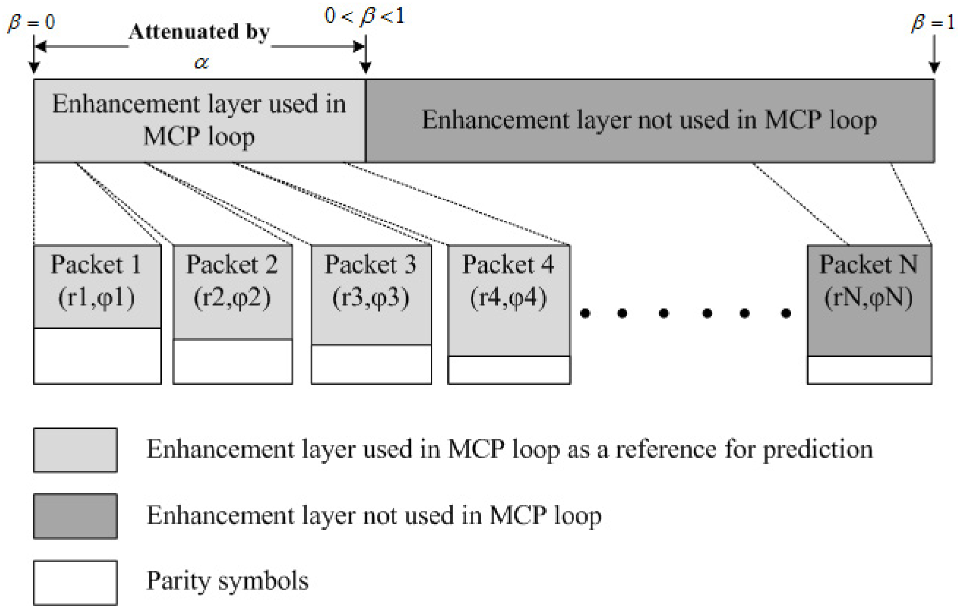

Figure IV.2: Packetization of the MC-FGS enhancement layer.

chapter, we assume that the pilot SNR and its spacing are selected to be equal to the data symbol SNR and the channel coherence time, respectively.

By the assumption that all MIMO channels are independent, channel estimation errors in the MIMO system can be modelled as a matrix consisting of i.i.d. complex Gaussian random variables with the variance of (IV.4). To maximize the signal-to-interference-and-noise ratio (SINR) under the condition of imperfect channel estimation, we consider the modified minimum-mean-squared-error (MMSE) detection scheme proposed in [51]. We assume BPSK modulation, and that N packets, whose size is fixed at m symbols, are allocated to a frame of the FGS enhancement layer bitstream, as presented in Fig. IV.2. Note that each packet is protected by FEC. For the transmission of the packet, we choose either spatial diversity, spatial multiplexing or a hybrid of the two. We have a total transmit power constraint to make the system consume a constant power for any selection of MIMO modes. The specific MIMO mode (multiplexing, diversity, hybrid) is chosen at the transmitter on a packet by packet basis in order to minimize distortion. The selection of UEP and MIMO mode per packet is performed at the transmitter because the source statistics and encoder characteristics are known and are based on the average channel gain.

IV.B.2.a Spatial Diversity

Spatial diversity is achieved by transmitting and receiving symbol streams with the same information content through multiple transmit and receive antennas. There are various ways to implement spatial diversity, but quasi-orthogonal space time block coding (QOSTBC) [52] is considered in this chapter.

IV.B.2.b Spatial Multiplexing

Spatial multiplexing makes it possible to increase the transmission rate proportional to $min(M_t, M_r)$ without allocating additional bandwidth or transmit power [53]. Spatial multiplexing can be achieved by transmitting different data streams through multiple transmit antennas over independently fading channels. However, under the constraint of the fixed total transmit power, spatial multiplexing assigns less energy per bit compared to spatial diversity.

IV.B.2.c Hybrid Mode

We consider the hybrid mode to have twice the data rate and half the diversity order, as compared to the spatial diversity mode. For the purpose of simulation, we implement Double Space Time Transmit Diversity (D-STTD), as proposed in [54].

IV.C Unequal Error Protection with FEC and MIMO Mode Selection

In this section, we investigate how to find a UEP policy for the FGS EL to minimize the average distortion by choosing the FEC code rate and the appropriate MIMO mode in a fast varying channel. For BL, we assume the lowest

FEC code rate spatial diversity are assigned to guarantee the reliable delivery. We assume that N fixed size packets are available for the transmission of the FGS EL in a frame, where the packet length is equal to the duration of m symbols. For the ith packet, the channel code rate and MIMO mode are denoted r_i and ϕ_i, respectively, where r_i is chosen from the possible channel code rate set and ϕ_i represents one of the MIMO modes. If we denote the packet error rate of the ith packet by $p_i(r_i, \phi_i)$, then the probability that the first k packets are received successfully and the first packet error happens at packet $(k+1)$ is

$$\begin{aligned} \pi_k &\triangleq \text{Pr(first packet error occurs at packet } k{+}1) \\ &= \begin{cases} p_1(r_1, \phi_1), & k{=}0 \\ \prod_{j=1}^{k}(1 - p_j(r_j, \phi_j))p_{k+1}(r_{k+1}, \phi_{k+1}), & 0 < k < N \\ \prod_{j=1}^{N}(1 - p_j(r_j, \phi_j)), & k{=}N. \end{cases} \end{aligned} \tag{IV.5}$$

When the first k packets are successfully received, the number of information bits available at the receiver is $\sum_{j=1}^{k} r_j M_j$, where M_j represents the total number of symbols in the jth packet, which is determined by the MIMO mode. Assume that the rate-distortion function of the source input is available at the transmitter. Then, the average distortion, $E[D(\alpha, \beta)]$, can be computed as

$$E[D(\alpha, \beta)] = D(0, \alpha, \beta)\pi_0 + \sum_{k=1}^{N} D(\sum_{j=1}^{k} r_j M_j, \alpha, \beta)\pi_k, \tag{IV.6}$$

where α and β are the leaky and partial prediction parameters, respectively, and $D(R, \alpha, \beta)$ is the distortion of the decoded MC-FGS video when the entire base layer and R bits of enhancement layer are received successfully.

At this point, we focus on the choice of $\underline{r} = [r_1, r_2, \cdots, r_N]$ and $\underline{\phi} = [\phi_1, \phi_2, \cdots, \phi_N]$ for minimizing $E[D(\alpha, \beta)]$, given α and β. In [39], the authors proposed a local search algorithm to get a sub-optimal distortion-minimizing UEP policy when the length of the channel codeword is fixed. By using this algorithm, we can get a sub-optimal rate allocation and MIMO mode selection to transmit the FGS enhancement layer bitstream. To do this, we define the effective code rate,

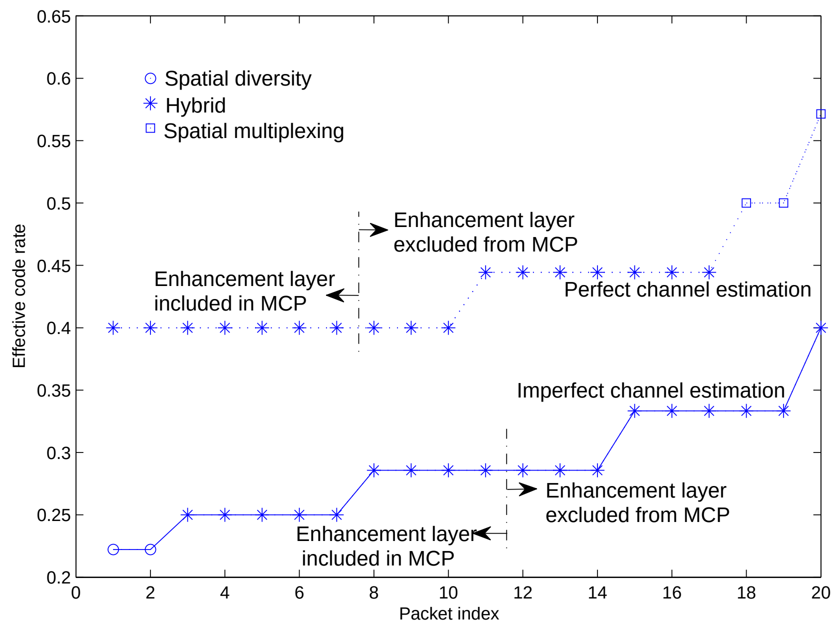

Figure IV.3: UEP policy and MIMO mode selection for the *"Foreman"* sequence where $\alpha = 1.0$ and $\beta = 0.15$. Total transmit signal to noise power ratio is fixed at 8 dB.

s_i, as the ratio of the number of information symbols to the maximum number of transmitted symbols in a packet, where the maximum number of transmitted symbols is defined as that in a packet where spatial multiplexing is used. For example, in a 4×4 MIMO system, $4 \times m$ symbols can be transmitted with spatial multiplexing. Then, the effective code rate of the ith packet, s_i, is given by

$$s_i = \begin{cases} r_i/4, & \text{if spatial diversity is used} \\ r_i/2, & \text{if hybrid mode is used} \\ r_i, & \text{if spatial multiplexing is used.} \end{cases}$$

The computational complexity of finding $\underline{s} = [s_1, s_2, s_3, \cdots, s_N]$ using an existing local search algorithm from [39] is lower than the complexity of finding $\underline{r}$ and $\underline{\phi}$ separately. The performance is the same either way, and is sub-optimal.

In Fig. IV.3, the UEP policy and MIMO mode selection versus packet index are shown for the *"Foreman"* sequence, with $\alpha = 1$ and $\beta = 0.15$. Average channel SNR, P_T/σ_n^2, is fixed at 8 dB, where P_T is the total transmit power. Then, for perfect channel estimation, the first 8 packets transmit the enhancement layer used for MCP. Since this part of the enhancement layer can result in error propagation if lost, additional protection is required. When there is imperfect channel estimation, more diversity gain and a lower channel code rate are required to protect the enhancement layer used for MCP, where the first 12 packets are involved. In particular, to reduce the loss probability for the beginning of the bitstream, spatial diversity is applied for the first 2 packets.

IV.D Selection of Leaky and Partial Prediction Parameters

In this section, we discuss the selection of leaky and partial prediction parameters based on the available channel information at the transmitter. In [30] and [55], an analysis of error propagation with leaky prediction was presented. According to these analyses, at the encoder, the EL bitstream is generated by subtracting the BL residue, $(F_n^{BL} - F_{n-1}^{BL})$, and the high quality reference frame, $\hat{F}_n^{EL,enc,\beta}$, from the original frame, F_n. That is, the following residue is progressively encoded as an EL of the current frame,

$$\epsilon_n^{EL} = F_n - (F_n^{BL} - F_{n-1}^{BL}) - \hat{F}_n^{EL,enc,\beta}.$$

Note that the progressively encoded EL can be truncated anywhere. For example, in MPEG-4 FGS, the EL is encoded using bit-plane coding, and less significant bits can be discarded, at the cost of lower quality. When transmitted, the EL bitstream can be truncated due to a limitation of channel bandwidth or transmit power. We denote the reconstructed EL residue at the encoder using the transmitted EL bitstream as $\hat{\epsilon}_n^{EL}$. At the receiver, additional truncation can occur in the EL bitstream caused by channel error. Then, $\hat{\epsilon}_n^{EL}$ and $\tilde{\epsilon}_n^{EL}$, which represents the reconstructed EL residue at the decoder, are the coarsely quantized versions of ϵ_n^{EL} due to the truncation of the original EL bitstream at the encoder and decoder. We

Table IV.1: The symbol definitions

	Encoder	Decoder
Original/reconstructed frame	F_n	$\tilde{F}_n$
BL reconstructed frame	F_n^{BL}	F_n^{BL}
Original EL residue	ϵ_n^{EL}	$-$
Reconstructed EL residue	$\hat{\epsilon}_n^{EL}$	$\tilde{\epsilon}_n^{EL}$
Partially reconstructed EL residue	$\epsilon_n^{EL,\beta}$	$\tilde{\epsilon}_n^{EL,\beta}$
High quality reference frame	$\hat{F}_n^{EL,enc,\beta}$	$\tilde{F}_n^{EL,dec,\beta}$
Partially reconstructed frame	$F_n^{EL,\beta}$	$\tilde{F}_n^{EL,\beta}$

assume no mismatch for the BL at the encoder and decoder. The reconstructed frame at the decoder, $\tilde{F}_n$, is given by

$$\tilde{F}_n = \tilde{\epsilon}_n^{EL} + (F_n^{BL} - F_{n-1}^{BL}) + \tilde{F}_n^{EL,dec,\beta},$$

where $\tilde{F}_n^{EL,dec,\beta}$ is the high quality EL reference for frame n at the decoder. That is,

$$\tilde{F}_n^{EL,dec,\beta} = (1-\alpha)F_{n-1}^{BL} + \alpha\tilde{F}_{n-1}^{EL,\beta}. \tag{IV.7}$$

Hence,

$$\tilde{F}_n = \tilde{\epsilon}_n^{EL} + \alpha(\tilde{F}_{n-1}^{EL,\beta} - F_{n-1}^{BL}) + F_n^{BL}, \tag{IV.8}$$

where $\tilde{F}_{n-1}^{EL,\beta}$ is the reconstructed $(n-1)$-st frame using the BL and a partial EL specified by β, which is stored in the buffer at the decoder. Therefore,

$$\tilde{F}_{n-1}^{EL,\beta} = \tilde{\epsilon}_{n-1}^{EL,\beta} + (F_{n-1}^{BL} - F_{n-2}^{BL}) + \tilde{F}_{n-1}^{EL,dec,\beta}, \tag{IV.9}$$

where $\tilde{\epsilon}_{n-1}^{EL,\beta}$ represents the reconstructed partial EL residue at the $(n-1)$-st frame at the decoder. This may not be the same as the reconstructed partial EL residue at the encoder, $\epsilon_{n-1}^{EL,\beta}$, if the successfully received number of EL bits is less than the amount of partial EL specified by β. Also, the partially reconstructed $(n-1)$-st frame at the encoder, $F_{n-1}^{EL,\beta}$, is

$$F_{n-1}^{EL,\beta} = \epsilon_{n-1}^{EL,\beta} + (F_{n-1}^{BL} - F_{n-2}^{BL}) + \hat{F}_{n-1}^{EL,enc,\beta}. \tag{IV.10}$$

The error between the original frame at the encoder, F_n, and the reconstructed frame at the decoder, $\tilde{F}_n$, is

$$
\begin{aligned}
F_n - \tilde{F}_n &= \epsilon_n^{EL} - \tilde{\epsilon}_n^{EL} + \hat{F}_n^{EL,enc,\beta} - \tilde{F}_n^{EL,dec,\beta} \\
&= \epsilon_n^{EL} - \tilde{\epsilon}_n^{EL} + \alpha(F_{n-1}^{EL,\beta} - \tilde{F}_{n-1}^{EL,\beta}). \qquad \text{(IV.11)}
\end{aligned}
$$

Note that the difference between $F_{n-1}^{EL,\beta}$ and $\tilde{F}_{n-1}^{EL,\beta}$ results in reference mismatch while reconstructing the current frame. From (IV.9) and (IV.10), $(F_{n-1}^{EL,\beta} - \tilde{F}_{n-1}^{EL,\beta})$ can be represented as

$$
F_{n-1}^{EL,\beta} - \tilde{F}_{n-1}^{EL,\beta} = \epsilon_{n-1}^{EL,\beta} - \tilde{\epsilon}_{n-1}^{EL,\beta} + \alpha(F_{n-2}^{EL,\beta} - \tilde{F}_{n-2}^{EL,\beta}). \qquad \text{(IV.12)}
$$

Then, the distortion of the n-th frame, $D_n(\underline{R}, \alpha, \beta)$, is

$$
\begin{aligned}
D_n(\underline{R}, \alpha, \beta) &= E[(F_n - \tilde{F}_n)^2] \\
&= E[(\epsilon_n^{EL} - \tilde{\epsilon}_n^{EL} + \alpha(F_{n-1}^{EL,\beta} - \tilde{F}_{n-1}^{EL,\beta}))^2],
\end{aligned}
$$

where $\underline{R}$ is an $(n \times 1)$ vector of the throughputs from the first to the n-th frames. If we assume $(\epsilon_n^{EL} - \tilde{\epsilon}_n^{EL})$, which depends on the channels corresponding to the n-th frame, is independent of $(F_{n-1}^{EL,\beta} - \tilde{F}_{n-1}^{EL,\beta})$ for rapidly varying channels, the above expression becomes

$$
\begin{aligned}
D_n(\underline{R}, \alpha, \beta) &= E[(\epsilon_n^{EL} - \tilde{\epsilon}_n^{EL})^2] \\
&\quad + 2\alpha E[\epsilon_n^{EL} - \tilde{\epsilon}_n^{EL}] E[F_{n-1}^{EL,\beta} - \tilde{F}_{n-1}^{EL,\beta}] \\
&\quad + \alpha^2 E[(F_{n-1}^{EL,\beta} - \tilde{F}_{n-1}^{EL,\beta})^2]. \qquad \text{(IV.13)}
\end{aligned}
$$

In [56], the residue between the original frame and the reconstructed frame in the BL was well modelled as a zero-mean generalized Gaussian random variable. And, in MC-FGS, to eliminate the temporal redundancy, the previous frame's residue is subtracted from that of the current frame, either partially or entirely. Since both residues are considered as zero-mean generalized Gaussian random variables, the difference between them, ϵ_n^{EL}, can also be considered a zero-mean generalized Gaussian random variable. Note that $\tilde{\epsilon}_n^{EL}$ is the quantized

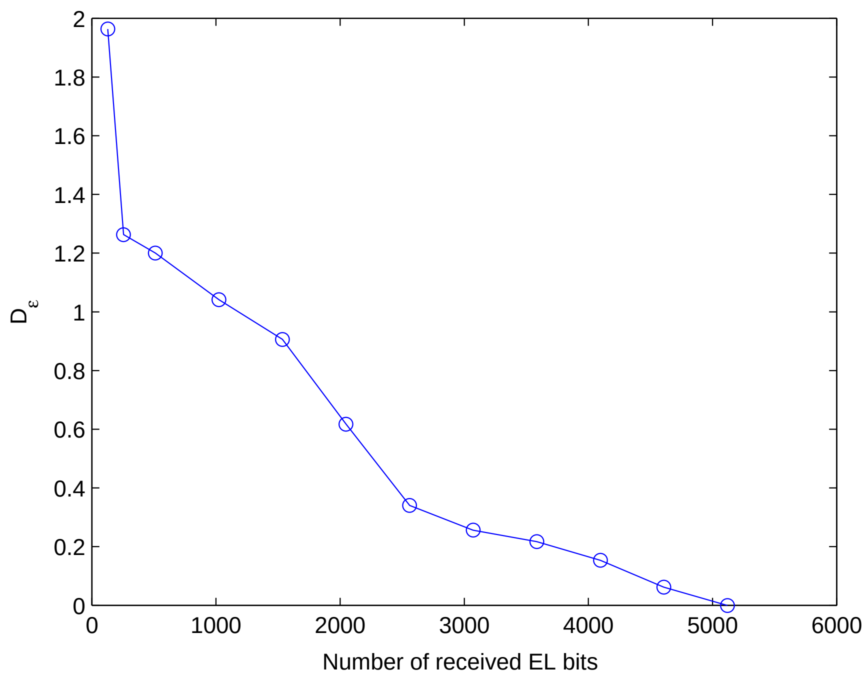

Figure IV.4: Distortion corresponding to the reference mismatch, D_ϵ, where $\alpha =$ 1.0 and the amount of the EL-MCP is 5120 bits.

version of ϵ_n^{EL}, and the distributions of both variables are symmetric around zero. Therefore, the mean of ϵ_n^{EL} and $\tilde{\epsilon}_n^{EL}$ will be zero and (IV.13) can be represented as

$$\begin{aligned} D_n(\underline{R}, \alpha, \beta) &= E[(\epsilon_n^{EL} - \tilde{\epsilon}_n^{EL})^2] + \alpha^2 E[(F_{n-1}^{EL,\beta} - \tilde{F}_{n-1}^{EL,\beta})^2] \\ &= E[(\epsilon_n^{EL} - \tilde{\epsilon}_n^{EL})^2] \\ &\quad + \alpha^2 E[(\alpha(F_{n-2}^{EL,\beta} - \tilde{F}_{n-2}^{EL,\beta}) + \epsilon_{n-1}^{EL,\beta} - \tilde{\epsilon}_{n-1}^{EL,\beta})^2]. \end{aligned} \quad \text{(IV.14)}$$

We define $D_\epsilon(R_{n-1}, \beta)$ as

$$D_\epsilon(R_{n-1}, \beta) = E[(\epsilon_{n-1}^{EL,\beta} - \tilde{\epsilon}_{n-1}^{EL,\beta})^2], \quad \text{(IV.15)}$$

where R_{n-1} is the number of successfully received bits for the EL at the $(n-1)$-st frame and $D_\epsilon(R_{n-1}, \beta)$ becomes zero if R_{n-1} is larger than the amount of the EL specified by β. With (IV.12) and (IV.15),

$$\begin{aligned} D_n(\underline{R}, \alpha, \beta) \quad = \quad & E[(\epsilon_n^{EL} - \tilde{\epsilon}_n^{EL})^2] \\ & + \alpha^{2(n-1)} E[(F_1^{EL,\beta} - \tilde{F}_1^{EL,\beta})^2] \\ & + \sum_{i=1}^{n-2} \alpha^{2i} D_\epsilon(R_{n-i}, \beta), \end{aligned} \tag{IV.16}$$

where the second term results from the partial EL reference mismatch at the first frame, and the last term represents the accumulated distortion caused by the reconstructed EL reference mismatch from the subsequent frames. It follows from (IV.2) that large α and β provide better coding efficiency. However, in (IV.16), when α is chosen to be large, the error resilience becomes worse, since the accumulated distortion, $E[(F_1^{EL,\beta} - \tilde{F}_1^{EL,\beta})^2]$ and $\sum_{i=1}^{n-2} D_\epsilon(R_{n-i}, \beta)$ will not decay rapidly. By choosing a large β, the probability that the second and third terms are greater than zero will be increased. In Fig. IV.4, we present the actual value of D_ϵ for the 10-th frame in the *"Foreman"* video sequence when 5120 bits in the EL bitstream are used for MCP. As seen, if the number of successfully received bits is more than that, D_ϵ becomes zero. However, as the amount of the received EL reduces, D_ϵ increases with the amount of reference mismatch. Therefore, to select the prediction parameters, α and β, to appropriately trade off coding efficiency and error resilience capability, the statistics of R_{n-i} need to be considered.

In the following, we have two different strategies to select α and β based on the available channel information. If accurate instantaneous channel information is available at the transmitter to choose β based on the expected number of successfully received EL bits to avoid reference mismatch, then α can be chosen to be unity, since the probability of error propagation will be reduced. However, in a high Doppler environment, where instantaneous channel information may not be available, the average channel information will be used to decide the parameters, where these parameters will be maintained for multiple frames.

IV.D.1 Selection of fixed α and β - Fast fading channel

In a high Doppler environment, it is hard to get instantaneous channel information at the transmitter. Instead, we use the average channel SNR to select the prediction parameters, as introduced previously to decide UEP. Due to the lack of an analytical approach for the leaky and partial prediction schemes, we find the prediction parameters based on simulation. For the simulation, we use MC-FGS video, which is implemented with an H.264 TML-9 codec for the base layer and an MPEG-4 FGS codec for the EL. Both partial and leaky prediction schemes are incorporated in the enhancement layer MCP loop. The first 150 frames of the video sequence, consisting of a single intra-frame (I-frame) and 149 predicted frames (P-frames), are encoded. Before transmitting the bitstream through the MIMO wireless channel, the bitstream is packetized and channel-encoded by rate compatible punctured convolutional (RCPC) codes. In this chapter, we assume that the base layer is delivered without any errors. However, for the EL bitstream, its UEP policy and leaky/partial prediction parameters are jointly selected. We fix the size of a packet at 256 BPSK symbols, and each frame is encoded using 20 packets. A 4x4 MIMO antenna configuration is considered, and a MMSEz detection scheme is used for all the MIMO modes. We consider Jakes' model with a normalized Doppler frequency of 10^{-2}, which is smaller than the transmission time for a frame, for the Rayleigh fading channel.

In Fig. IV.5, the average PSNR versus various partial prediction parameters is shown when the leaky prediction parameter is fixed at 0.7 and 1.0, under both perfect and imperfect channel estimation. Given the average channel SNR, the optimal selection of the partial prediction parameter, β, is highlighted by the square (□). For all scenarios, it is seen that a larger β can be chosen as the average received SNR increases. This is because a higher channel SNR can enhance the number of successfully received bits, R_j, for the frame and allow the use of larger β without increasing $D_\epsilon(R_j, \beta)$. If we compare Fig. IV.5(a) with Fig. IV.5(b), it can be observed that imperfect channel estimation results in decreasing partial

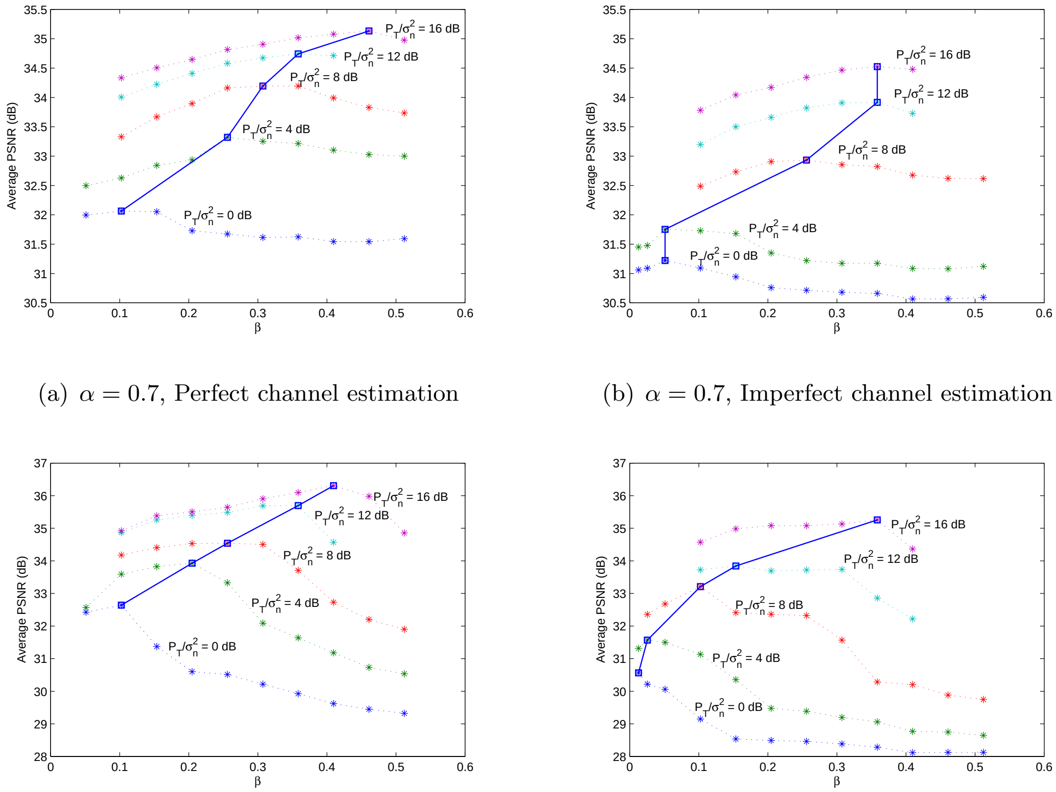

(a) $\alpha = 0.7$, Perfect channel estimation

(b) $\alpha = 0.7$, Imperfect channel estimation

(c) $\alpha = 1.0$, Perfect channel estimation

(d) $\alpha = 1.0$, Imperfect channel estimation

Figure IV.5: Average PSNR performance versus β for the *"Foreman"* sequence. The leaky prediction parameter is fixed at 0.7 and 1.0, and both perfect and imperfect channel estimation are considered.

prediction parameters. However, the choice of β is not sensitive, since the propagated error can be forced to decay by choosing $\alpha < 1$. In contrast, in Fig. IV.5(c) and Fig. IV.5(d) with α set to 1, the performance is more sensitive to the choice of β. Because the propagated error is not being forced to decay, a small value of β is preferred, compared to the case of $\alpha = 0.7$. If we choose a larger β than the optimal one, the corresponding performance is significantly degraded due to the lack of error resilience capability.

In Fig. IV.6, the average PSNR performance of the MC-FGS video with partial and leaky prediction is compared to that of a conventional FGS video under

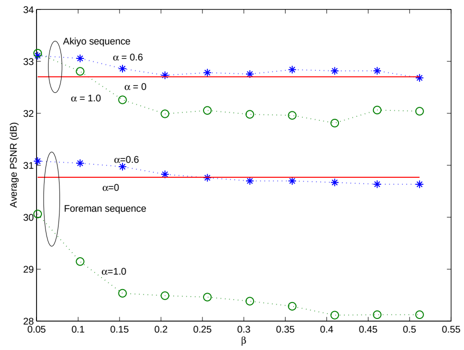

(a) $P_T/\sigma_n^2 = 0$ dB

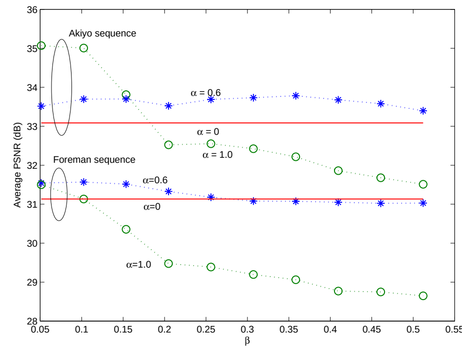

(b) $P_T/\sigma_n^2 = 4$ dB

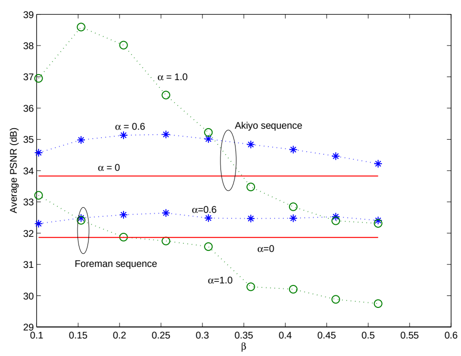

(c) $P_T/\sigma_n^2 = 8$ dB

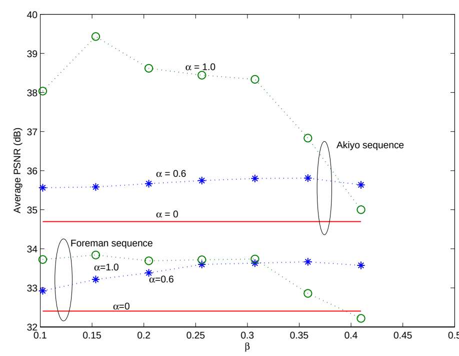

(d) $P_T/\sigma_n^2 = 12$ dB

Figure IV.6: Average PSNR performance versus β for the *"Foreman"* and *"Akiyo"* sequences where P_T/σ_n^2 represents the ratio of the total transmit power and noise variance. The solid line represents the average PSNR without using MC-FGS. Imperfect channel estimation is considered.

imperfect channel estimation for *"Foreman"* and *"Akiyo"* video sequences. As a point of comparison, we also implement conventional FGS video coding without partial and leaky prediction by setting α to 0. At low SNR, the MC-FGS video coding does not provide significant gain over conventional FGS video coding, since it suffers from error propagation even though a small value of β is chosen. However, by choosing a small α, performance can be enhanced by reducing the propagated error. As the channel SNR increases, MC-FGS outperforms conventional FGS, even if a large value of β is used.

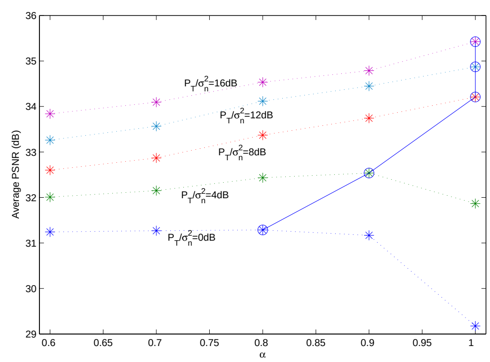

(a) $\beta = .15$

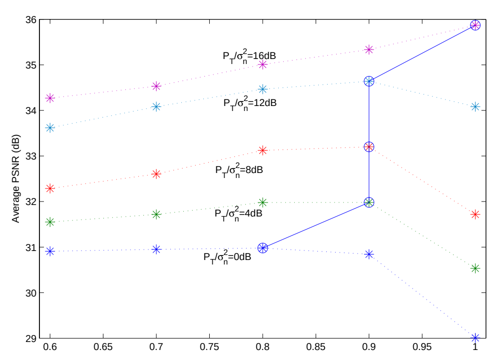

(b) $\beta = .35$

Figure IV.7: Average PSNR performance versus α for *"Foreman"*. The partial prediction parameter is fixed at 0.15 and 0.35, and imperfect channel estimation is considered.

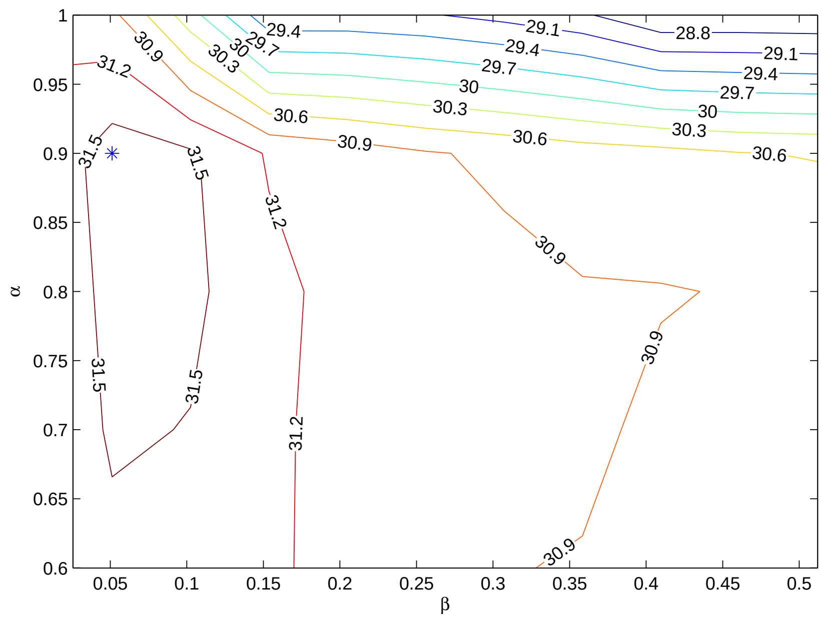

Figure IV.8: Contour plot of the PSNR performance for different (β, α) with the average channel SNR of 0 dB, where the normalized Doppler frequency $f_{nd} = 10^{-2}$.

In Fig. IV.7, the average PSNR versus various leaky prediction parameters is shown when the partial prediction parameter is fixed at a specific value. As can be seen, as a larger value of β is chosen, relatively smaller α needs to be selected. For example, at 8 dB of average channel SNR, if β is 0.15, then the best performance is achieved when α is chosen to be unity. In contrast, for the same conditions, if β is 0.35, then α is required to be less than unity because 8 dB of channel SNR is not enough to reliably deliver the amount of EL designated by β of 0.35. In addition, higher channel SNR allows the use of a higher α, and achieves a better compression efficiency, since the EL can be delivered more reliably.

In Fig. IV.8, we show a contour plot of constant PSNR performance when choosing α and β jointly when the average channel SNR is fixed at 0 dB. Each contour represents a constant PSNR achieved by different combinations of α and β. Note that we indicated the optimal pair of parameters with the symbol (*). In Figs. IV.9 and IV.10, the same contour plots with 8 and 16 dB of average channel

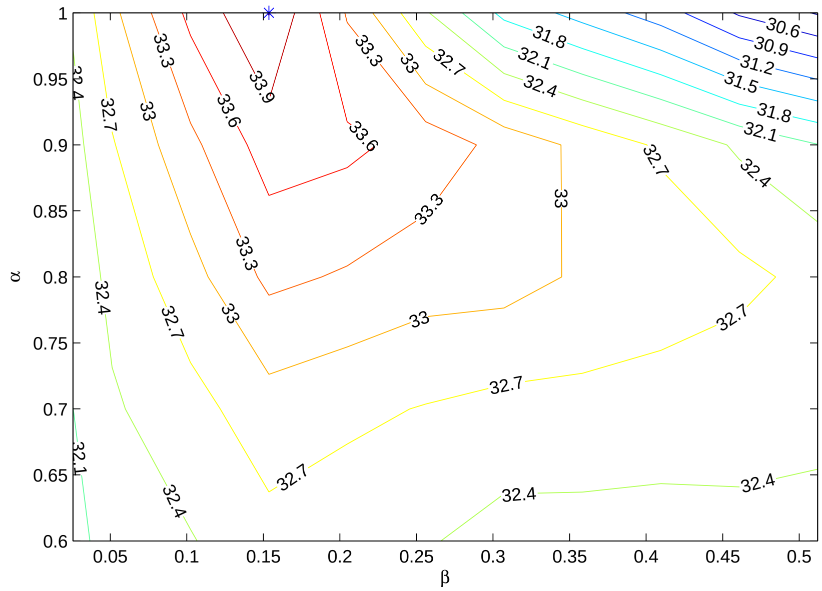

Figure IV.9: Contour plot of the PSNR performance for different (β, α) with the average channel SNR of 8 dB, where the normalized Doppler frequency $f_{nd} = 10^{-2}$.

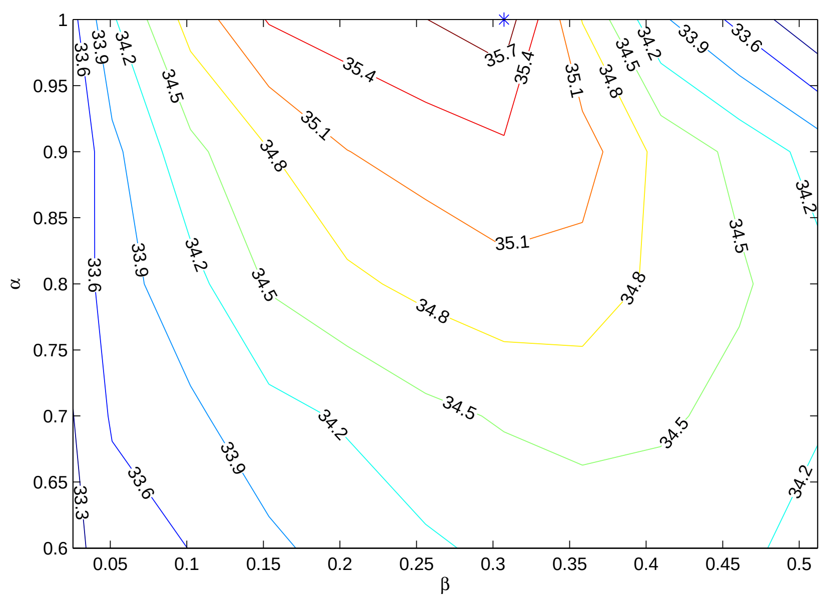

Figure IV.10: Contour plot of the PSNR performance for different (β, α) with the average channel SNR of 16 dB, where the normalized Doppler frequency $f_{nd} = 10^{-2}$.

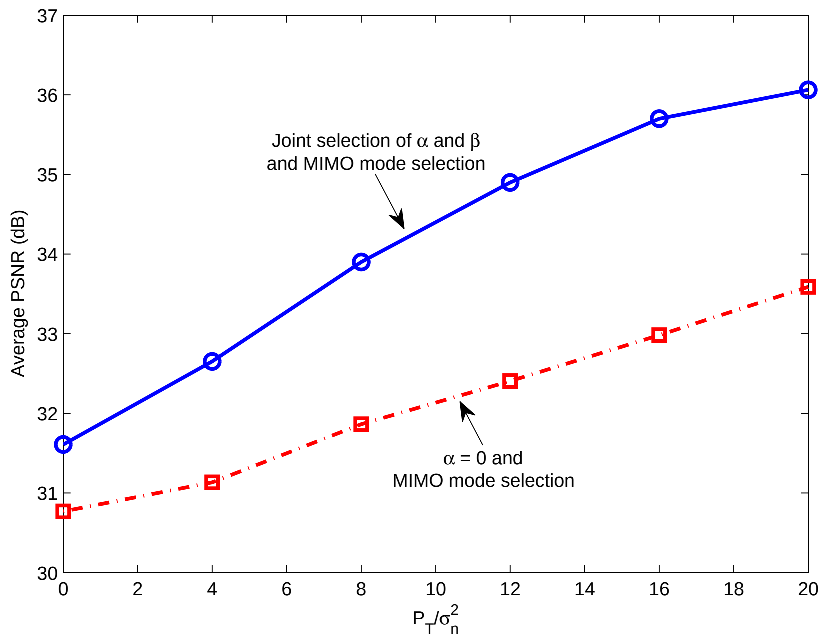

Figure IV.11: Comparison of average PSNR for the conventional FGS and MC-FGS video coding with fixed α and β under imperfect channel estimation, where the normalized Doppler frequency $f_{nd} = 10^{-2}$.

SNR are presented. Compared to the previous figure, the optimal values of both α and β are increased. In particular, the figures show that β is closely related to the average channel SNR.

In Fig. IV.11, the PSNR performance of conventional FGS video coding is compared with that of MC-FGS video coding using the leaky and partial predictions. For both systems, UEP and MIMO mode selection are applied. In the conventional FGS video coding, the FGS EL is excluded from MCP, so error propagation due to the corruption of the EL is entirely prohibited. Instead, it can suffer from poor compression efficiency. Our simulation results show that the leaky and partial predictions can result in a significant gain over a conventional FGS over a wide range of channel SNR in fast fading channels by controlling the tradeoff between compression efficiency and error resilience. In Fig. IV.12, the PSNR performances for MC-FGS video coding with and without MIMO mode

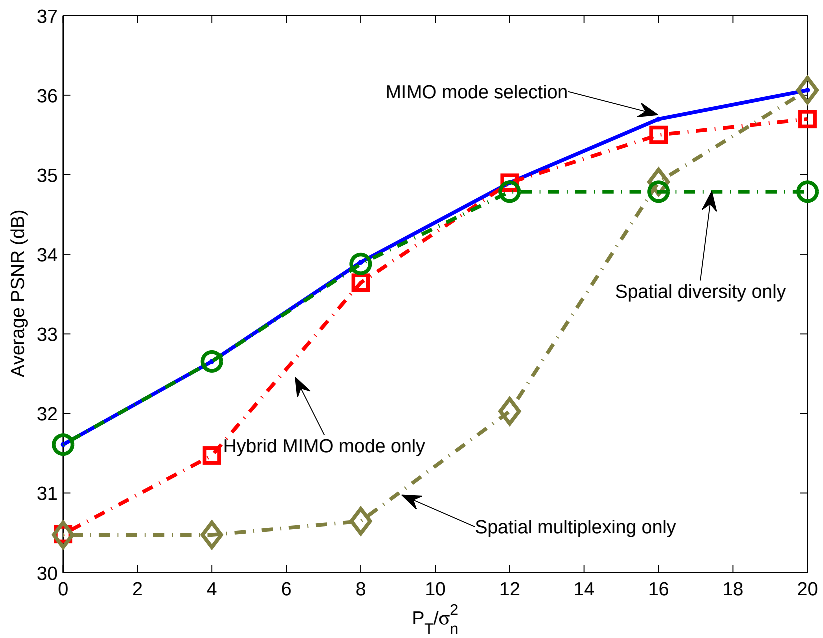

Figure IV.12: Comparison of average PSNR for the MIMO mode selection and single MIMO mode with fixed α and β under imperfect channel estimation, where the normalized Doppler frequency $f_{nd} = 10^{-2}$.

selection are presented. Note that, at low SNR, the selected MIMO mode for all packets is spatial diversity. Therefore, the performance of MIMO mode selection is equivalent to that of spatial diversity only. For the same reason, at high SNR, the performance of MIMO mode selection is the same as that of spatial multiplexing. However, in the intermediate region, different MIMO modes can be assigned based on the packet's priority, as seen in Fig. IV.3, and MIMO mode selection provides better performance than any single choice of MIMO mode.

IV.D.2 Adaptive selection of β - Slow fading channel

Previously, we saw that β is closely related to the average channel SNR or, equivalently, the number of successfully received bits. That is, if the number of successfully received EL bits is less than the amount of the EL specified by β, then reference mismatch between encoder and decoder can result. Therefore, if the transmitter can estimate the instantaneous throughput for the frame which is encoded currently, then it can be used to choose a value of β to avoid reference mismatch. In this section, by utilizing channel feedback from the decoder, we propose adaptive selection of β. To do that, we assume a slowly varying channel, where the channel is highly correlated over multiple frames.

Before the encoding of the n-th frame, it is assumed that the instantaneous channel information corresponding to the transmission of frame $(n-1)$ is available at the encoder. Then, based on this instantaneous channel information, we decide the appropriate β. At this point, we are not assuming adaptive UEP based on the instantaneous channel information in order to avoid high computational complexity to find the UEP policy frame-by-frame. That is, the UEP is only dependent on the average channel SNR and is kept fixed for some pre-determined number of frames (in our simulation, 150 frames). Then, the transmitter finds the distribution of the throughput, T, when the instantaneous channel information, especially the instantaneous received SNR per bitstream, is given, where the instantaneous received SNR per bitstream is defined as the SNR at the receiver

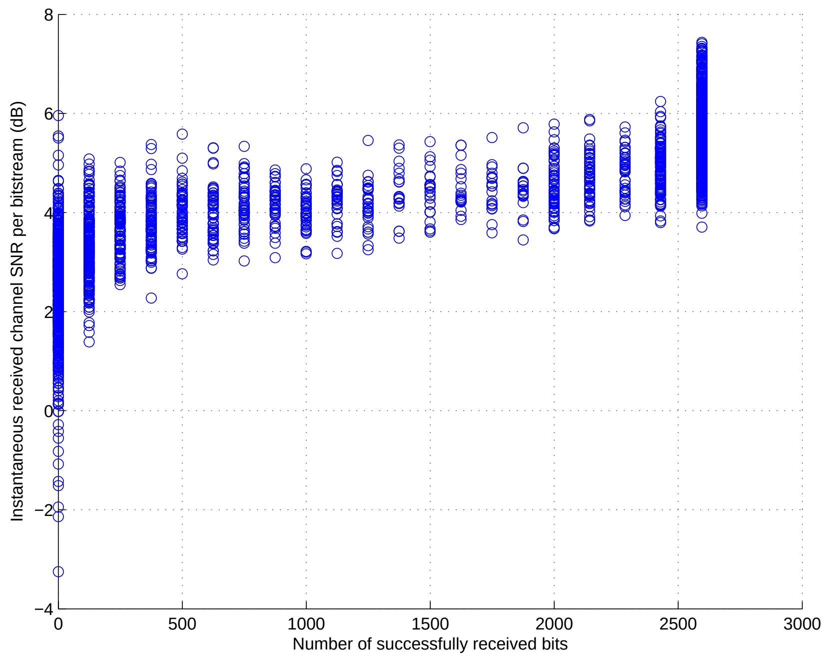

Figure IV.13: Distribution of the throughput and corresponding instantaneous received channel SNR per bitstream from the investigation of transmission of 2500 frames in a 4x4 MIMO system. $P_T/\sigma_n^2 = 0$ dB and ZF detection is used and $f_{nd} = 10^{-5}$.

after signal combining, and is presented in [53] and [57]. This will be possible by assuming that the transmitter knows the throughput profiles over the previous frames and corresponding instantaneous channel SNRs as shown in Fig. IV.13.

To compute the instantaneous received SNR per bitstream, we follow the expressions in [53] and [57], where the computation is different for each of the different MIMO modes. Due to the important role of the first packet in the progressive encoded EL, we compute the instantaneous received channel SNR per bitstream for the MIMO mode of the first packet.

We denote the probability mass function of the throughput by $P_T(T)$, where $0 \leq T \leq \sum_{j=1}^{N} r_j M_j$. Then we consider how to choose β from this information. Denote the average PSNR from frame n to $(N+n-1)$ by $PSNR_n(\underline{\beta}, \underline{T})$, where the vectors $\underline{\beta} = [\beta_n, \beta_{n+1}, \cdots, \beta_{N+n-1}]^T$ and $\underline{T} = [T_n, T_{n+1}, \cdots, T_{N+n-1}]^T$ represent the partial prediction parameter β and the throughput for N frames. We assume $PSNR_n(\underline{\beta}, \underline{T})$ is available at the encoder. We choose β to maximize the expected $PSNR_n$ when the instantaneous received channel SNR per bitstream is given. If β_n can be chosen from the set of $\{\beta^1, \beta^2, \cdots, \beta^K\}$, then for each possible value of β_n, the expected $PSNR_n$ is computed as follows using the probability mass function of the throughput:

$$
\begin{aligned}
&E[PSNR_n([\beta_n = \beta^i, \beta_{n+1}, \cdots, \beta_{N+n-1}], \underline{T})] \\
&= \sum_{t=0}^{r_j M_j} P_T(T_n = t) PSNR_n([\beta_n = \beta^i, \beta_{n+1}, \cdots, \beta_{N+n-1}], \\
&\cdot [T_n = t, T_{n+1}, \cdots, T_{N+n-1}]),
\end{aligned}
\tag{IV.17}
$$

where all elements in the vectors $\underline{\beta}$ and $\underline{T}$ except β_n and T_n are fixed at the specific value not to result in reference mismatch in the subsequent $N-1$ frames. That is,

$$
\begin{aligned}
&E[PSNR_n([\beta_n, \beta_{n+1}, \cdots, \beta_{N+n-1}], \underline{T})] \\
&= E[PSNR_n(\beta_n, T_n)].
\end{aligned}
$$

Then, β_n is chosen to satisfy the following :

$$
\max_{\beta_n \in \{\beta^1, \beta^2, \cdots, \beta^K\}} E[PSNR_n(\beta_n, T_n)]. \tag{IV.18}
$$

An example of adaptive choice of β is presented in Fig. IV.14(b) when the instantaneous channel is given as shown in Fig. IV.14(a) with $f_{nd} = 10^{-5}$, which makes the channel correlated over a time period of three frames. As can be seen, when β is selected adaptively, the possibility of reference mismatch is reduced. Note that α is fixed at unity for the case of adaptive selection of β due to the lack of reference mismatch, and less than unity to compensate for the propagated error when β is fixed. Their performances are compared in Fig. IV.14(c), where PSNR profiles for all strategies are presented.

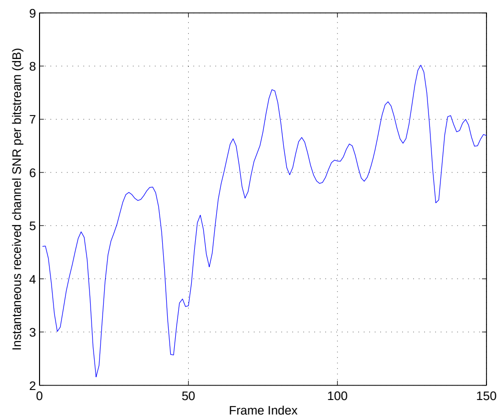

(a) Instantaneous channel received SNR

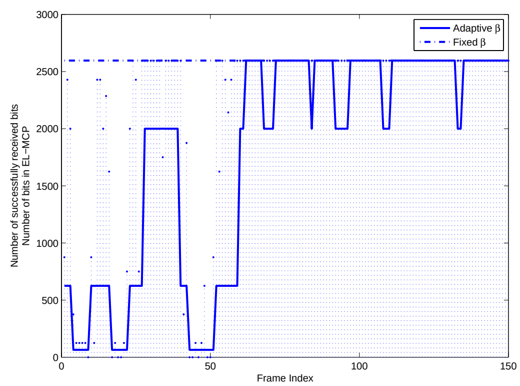

(b) Actual throughput and selected β

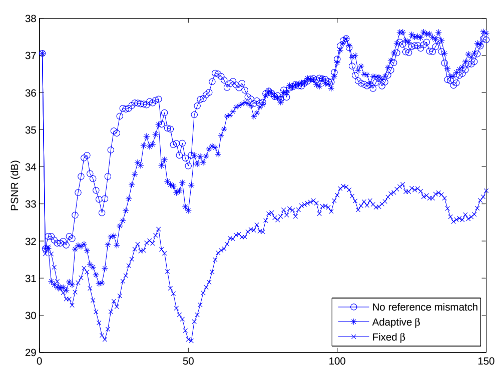

(c) PSNR profiles

Figure IV.14: $P_T/\sigma_n^2 = 0$ dB. For the video simulation, the *"Akiyo"* sequence is used.

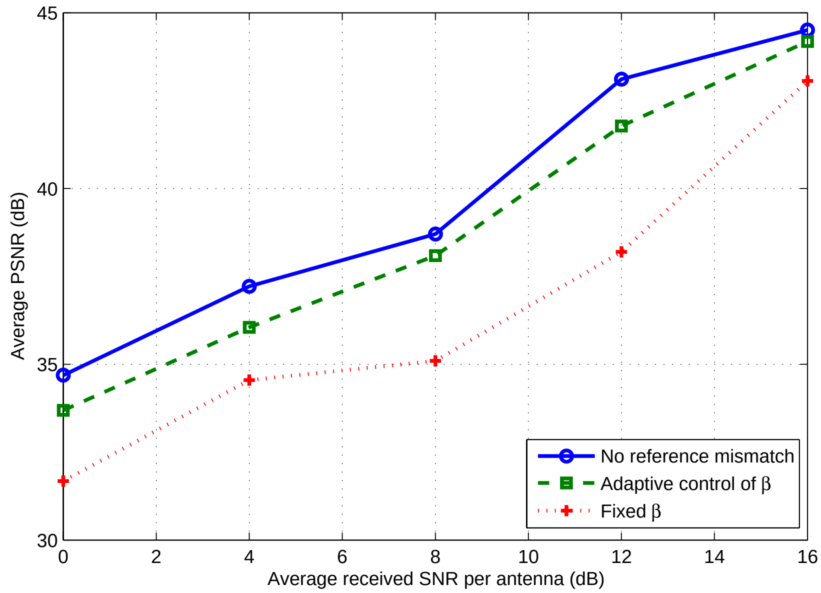

Figure IV.15: Performance comparison of different strategies to select β.

In Fig. IV.15, a performance comparison of different selection strategies for β is presented for *"Akiyo"*. To choose β for the current frame, we assume that the instantaneous channel information when the previous frame was transmitted is known at the transmitter before the encoding of the current frame. In the figure, the case of no reference mismatch represents the ideal case where the encoder knows the instantaneous throughput for every frame. By choosing β equal to the instantaneous throughput, reference mismatch never happens. In contrast, fixing β represents the case where both α and β are jointly selected for the whole video using average instead of instantaneous channel information. As can be seen, when β is fixed, the PSNR loss is more than 3 dB compared to the no reference mismatch case, especially in the low SNR region. However, based on the simulation, the adaptive approach to select β frame-by-frame showed less than 0.5 dB PSNR reduction compared to the no reference mismatch case. Note that we fixed $\alpha = 1$ when β is selected adaptively, since the probability of reference mismatch is reduced significantly.

IV.E Conclusion

In this chapter, we studied the transmission of an MC-FGS video bitstream over a MIMO wireless channel under the condition of imperfect channel estimation. We proposed a UEP policy consisting of FEC and MIMO mode selection per packet for the enhancement layer of MC-FGS by exploiting the fundamental tradeoff between multiplexing and diversity. To compensate for reference mismatch and the resulting error propagation, leaky and partial prediction schemes are applied in the MCP loop. Then we investigated the average PSNR performance with various choices of the leaky and partial prediction parameters for rapidly varying channels. Simulation results show that the joint control of prediction parameters and UEP can enhance the system performance significantly. In addition, we investigated the adaptive selection of the partial prediction parameter in a slow fading channel. If instantaneous channel information is available at the transmitter, the partial prediction parameter can be chosen based on the throughput which is estimated using the instantaneous channel information. Simulation results show that the adaptive selection of the partial prediction parameter is useful if the channel is varying slowly to allow the transmitter to obtain instantaneous channel information. Therefore, for the selection of prediction parameters, channel information such as the channel SNR as well as the coherence time needs to be considered.

IV.F Acknowledgements

This work was supported in part by the Center for Wireless Communications of UCSD, LG Electronics, and the UC Discovery Grant Program.

V

Conclusion

In this dissertation, we have proposed various cross-layer designs for wireless multimedia transmission. We discuss the performance analysis in terms of throughput and derive an algorithm to find the UEP to optimize either the throughput or PSNR.

In Chapter II, we discussed an information-theoretic framework to analyze the cross-layer design to transmit progressive images over cooperative relay channels. We derived an algorithm to find the throughput optimal UEP, and compared the average throughput and the rate-optimal UEP code rates found using the analysis with those obtained by simulations of a BPSK-based system to confirm that our information-theoretic framework yielded an approximate upper bound on the system performance.

In Chapter III, we discussed a relay protocol to deliver superposition-coded multimedia data. We used a layered Gaussian source to model the scalable multimedia stream, and quantified the performance in terms of distortion. We proposed a novel relay protocol to assign dedicated relays to the BL and the EL, instead of the conventional DF-based protocol. We compared the performance of the proposed protocol with conventional DF-based protocols both with and without superposition coding in both SISO and MIMO channels. In terms of throughput as well as distortion, the proposed protocol outperformed the DF-based protocols.

In Chapter IV, we discussed scalable video transmission over wireless MIMO channels. We used MC-FGS video coding with leaky and partial prediction schemes to achieve a tradeoff with respect to compression efficiency and error resilience. To implement UEP, we considered a spatial multiplexing-diversity tradeoff, where the appropriate MIMO mode was selected based on the packet's priority. We considered the control of leaky and partial prediction parameters based on either instantaneous or long-term average channel state information. The results showed that adaptive selection of leaky and partial prediction parameters enhances the performance significantly in a slow fading channel.

V.A Future work

Possible future work for cross-layer design in the transmission of multimedia includes:

- *Multiuser multimedia communication*: In this dissertation, we focused on point-to-point communication. However, in practical communication systems, multiuser multimedia communication is also possible, where the constrained resources should be shared by multiple users with different QoS and channel qualities. Cross-layer design for point-to-point multimedia communication can be extended to multiuser multimedia communication with multiuser resource allocation.

- *Channel adaptation*: In this dissertation, we considered video coding parameter adaptation in slow fading channels. However, it is possible to adapt channel coding parameters in the sense of adaptive modulation and coding (AMC). Joint control of AMC and video coding parameters can be considered under various Doppler spreads.

- *Cooperative relay protocol for multimedia communication*: Instead of DF-based protocol which was considered in this dissertation, amplify-and-forward

(AF) and compress-and-forward (CF) based protocols can be considered for multimedia communication.

Appendix A

Concavity of average throughput expression for the baseline system

In this appendix, we demonstrate the concavity of average throughput for the baseline system when the SNR >> 1. Ignoring constants, the average throughput expression of the baseline system is

$$\overline{\mathcal{T}}(\underline{r}_c) = \sum_{l=1}^{M}(\sum_{k=1}^{l}\tilde{r}_c(k))\mathsf{S}_l = \sum_{l=1}^{M}\tilde{r}_c(l)\prod_{k=1}^{l}(1-\pi_k). \tag{A.1}$$

As can be seen in [39], for the rate-optimal UEP solution of a progressive image, the following nondecreasing condition holds : $\tilde{r}_c(1) \leq \tilde{r}_c(2) \leq \cdots \leq \tilde{r}_c(M)$. Therefore, we can focus on the region of $\underline{r}_c$ which satisfies the nondecreasing condition for the concavity proof. To generate comparable results, we also restrict the range of $\underline{r}_c$ to be between $\min\{R\}$ and $\max\{R\}$, where $\{R\}$ is the set of possible rates for the RCPC and RCPT codes. For simplicity of notation, we replace $\overline{\mathcal{T}}(\underline{r}_c)$, $\tilde{r}_c(i)$, $\frac{d\pi_i}{dr_i}$, and $\frac{d^2\pi_i}{dr_i^2}$ by $\overline{\mathcal{T}}$, r_i, π_i' and π_i''. From (A.1), we can derive the second and cross partial derivatives of $\overline{\mathcal{T}}(\underline{r}_c)$. Since π_i is a function of r_i, the second order and cross partial derivatives of $\overline{\mathcal{T}}$ are

$$\frac{\partial^2\overline{\mathcal{T}}}{\partial {r_i}^2} = -2\pi_i'\prod_{k=1}^{i-1}(1-\pi_k) - \sum_{l=i}^{M} r_l\pi_i''\prod_{\substack{k=1\\k\neq i}}^{l}(1-\pi_k) \tag{A.2}$$

Table A.1: MI Outage Probabilities of Baseline System

General Form	$\pi_i = \gamma_{\text{inc}}(\frac{1}{\overline{\Gamma}} f(r_i), N)$
Gaussian Inputs	$f(r_i) = 2^{r_i} - 1$
BPSK Approx.	$f(r_i) = -\frac{\ln(1-r_i)}{2b}$
BPSK Upper Bound (UB)	$f(r_i) = -\frac{\ln(2^{1-r_i}-1)}{2}$

and

$$\frac{\partial^2 \overline{\mathcal{T}}}{\partial r_i \partial r_j} = -\pi_i' \prod_{\substack{k=1 \\ k\neq i}}^{j} (1-\pi_k) + \sum_{l=j}^{M} r_l \pi_i' \pi_j' \prod_{\substack{k=1 \\ k\neq i,j}}^{l} (1-\pi_k) \tag{A.3}$$

respectively, where $i < j$. The MI outage probabilities, π_i, for both Gaussian and BPSK inputs, are presented in Table A.1. Note that the MI outage probability for BPSK inputs is approximated to get a closed form expression. The first and second order derivatives of π_i, where

$$\pi_i = \frac{1}{(N-1)!} \int_0^{\frac{1}{\overline{\Gamma}} f(r_i)} e^{-u} u^{N-1} du, \tag{A.4}$$

are given by

$$\pi_i' = \left(\frac{1}{\overline{\Gamma}}\right)^N e^{-\frac{1}{\overline{\Gamma}} f(r_i)} \left(f(r_i)\right)^{N-1} f'(r_i) \frac{1}{(N-1)!} \tag{A.5}$$

$$\begin{aligned} \pi_i'' &= \left(\frac{1}{\overline{\Gamma}}\right)^N e^{-\frac{1}{\overline{\Gamma}} f(r_i)} \left(f(r_i)\right)^{N-2} \frac{1}{(N-1)!} \cdot \\ &\quad \left(-\frac{1}{\overline{\Gamma}} f(r_i) \left(f'(r_i)\right)^2 + (N-1)\left(f'(r_i)\right)^2 + f(r_i) f''(r_i) \right), \end{aligned} \tag{A.6}$$

respectively.

Since $f(r_i)$ and $f'(r_i)$ are positive for all inputs, π_i and π_i' are positive, too. Moreover, π_i'' is also positive if

$$\overline{\Gamma} > \begin{cases} \frac{2^{r_i}(2^{r_i}-1)}{N2^{r_i}-1}, & \text{for Gaussian inputs} \\ \frac{\ln(1-r_i)}{2b(\ln(1-r_i)-N+1)}, & \text{for BPSK approx} \\ \frac{\ln(2^{1-r_i}-1)}{2\left(2^{r_i-1}\ln(2^{1-r_i}-1)-N+1\right)}, & \text{for BPSK UB.} \end{cases}$$

From (A.3), the cross derivative of average throughput is given as

$$\begin{aligned}
\frac{\partial^2 \overline{\mathcal{T}}}{\partial r_i \partial r_j} &= -\left(\frac{1}{\overline{\overline{\Gamma}}}\right)^N \frac{1}{(N-1)!} e^{-\frac{1}{\overline{\Gamma}} f(r_i)} \left(f(r_i)\right)^{N-1} f'(r_i) \prod_{\substack{k=1 \\ k \neq i}}^{j} (1-\pi_k) \\
&+ \left(\frac{1}{\overline{\overline{\Gamma}}}\right)^{2N} \left(\frac{1}{(N-1)!}\right)^2 e^{-\frac{1}{\overline{\Gamma}}(f(r_i)+f(r_j))} \left(f(r_i) f(r_j)\right)^{N-1} \cdot \\
& f'(r_i) f'(r_j) \sum_{l=j}^{M} r_l \prod_{\substack{k=1 \\ k \neq i,j}}^{l} (1-\pi_k). \qquad (A.7)
\end{aligned}$$

Note that $f(r_i)$ and $f'(r_i)$ are limited by $f(\max\{R\})$ and $f'(\max\{R\})$. Therefore, if $\overline{\Gamma}$ is large enough, (A.3) will be negative since its first term will become dominant. Next, we prove the following inequalities :

$$-\frac{1}{2}\frac{\partial^2 \overline{\mathcal{T}}}{\partial {r_i}^2} + \frac{\partial^2 \overline{\mathcal{T}}}{\partial r_i \partial r_j} > 0 \qquad (A.8)$$

$$-\frac{1}{2}\frac{\partial^2 \overline{\mathcal{T}}}{\partial {r_j}^2} + \frac{\partial^2 \overline{\mathcal{T}}}{\partial r_i \partial r_j} > 0. \qquad (A.9)$$

Eqs. (A.8) and (A.9) can be shown as

$$\begin{aligned}
-\frac{1}{2}\frac{\partial^2 \overline{\mathcal{T}}}{\partial {r_i}^2} + \frac{\partial^2 \overline{\mathcal{T}}}{\partial r_i \partial r_j} &= \pi_i' \prod_{k=1}^{i-1} (1-\pi_k) \left(1 - \prod_{k=i+1}^{j} (1-\pi_k)\right) \\
&+ \frac{1}{2} \sum_{l=i}^{M} r_l \pi_i'' \prod_{\substack{k=1 \\ k \neq i}}^{l} (1-\pi_k) + \sum_{l=j}^{M} r_l \pi_i' \pi_j' \prod_{\substack{k=1 \\ k \neq i,j}}^{l} (1-\pi_k) > 0
\end{aligned} \qquad (A.10)$$

$$\begin{aligned}
-\frac{1}{2}\frac{\partial^2 \overline{\mathcal{T}}}{\partial {r_j}^2} + \frac{\partial^2 \overline{\mathcal{T}}}{\partial r_i \partial r_j} &= \left(\pi_j'(1-\pi_i) - \pi_i'(1-\pi_j)\right) \prod_{\substack{k=1 \\ k \neq i}}^{j-1} (1-\pi_k) \\
&+ \frac{1}{2} \sum_{l=j}^{M} r_l \pi_j'' \prod_{\substack{k=1 \\ k \neq j}}^{l} (1-\pi_k) + \sum_{l=j}^{M} r_l \pi_i' \pi_j' \prod_{\substack{k=1 \\ k \neq i,j}}^{l} (1-\pi_k) > 0,
\end{aligned} \qquad (A.11)$$

where π_j and π_j' are monotonic increasing functions of r_i and

$$\begin{aligned}
\pi_j'(1-\pi_i) - \pi_i'(1-\pi_j) &> (\pi_j' - \pi_i') + \pi_j(\pi_i' - \pi_j') \\
&= (1-\pi_j)(\pi_j' - \pi_i') > 0.
\end{aligned}$$

Now consider the Hessian matrix of the objective function. Note that the negative definiteness of the Hessian matrix implies the strict concavity of the objective function. Let H_m denote the mth principal submatrix of the Hessian matix, which is computed from the objective function, $\overline{\mathcal{T}}$. We have shown that all elements of the Hessian matrix, (A.2) and (A.3), are negative, and (A.8) and (A.9) hold. Therefore, for any positive integers i and j less than or equal to M, we can represent $-\frac{\partial^2\overline{\mathcal{T}}}{\partial {r_i}^2} = 2a_i > 0$ and $-\frac{\partial^2\overline{\mathcal{T}}}{\partial r_i \partial r_j} = a_i - \delta_{ij} > 0$, where $a_i > 0$ and $0 < \delta_{ij} < a_i$. Then, H_m can be simplified as

$$-H_m = \begin{pmatrix} 2a_1 & a_1-\delta_{12} & a_1-\delta_{13} & \dots & a_1-\delta_{1m} \\ a_1-\delta_{21} & 2a_2 & a_2-\delta_{23} & \dots & a_2-\delta_{2m} \\ a_1-\delta_{31} & a_2-\delta_{32} & 2a_3 & \dots & a_3-\delta_{3m} \\ \vdots & \vdots & \vdots & \ddots & \vdots \\ a_1-\delta_{m1} & a_2-\delta_{m2} & a_3-\delta_{m3} & \dots & 2a_m \end{pmatrix}. \quad \text{(A.12)}$$

If we define $-G_m$ as

$$-G_m = \begin{pmatrix} 2a_m & a_m-\eta_{12} & a_m-\eta_{13} & \dots & a_m-\eta_{1m} \\ a_m-\eta_{21} & 2a_m & a_m-\eta_{23} & \dots & a_m-\eta_{2m} \\ a_m-\eta_{31} & a_m-\eta_{32} & 2a_m & \dots & a_m-\eta_{3m} \\ \vdots & \vdots & \vdots & \ddots & \vdots \\ a_m-\eta_{m1} & a_m-\eta_{m2} & a_m-\eta_{m3} & \dots & 2a_m \end{pmatrix}, \quad \text{(A.13)}$$

where $\eta_{ij} = a_m - \frac{a_m}{a_j}(a_i - \delta_{ij}) > 0$, then

$$\det(-H_m) = \frac{a_1}{a_m}\frac{a_2}{a_m}\dots\frac{a_{m-1}}{a_m}\det(-G_m) \quad \text{(A.14)}$$

and the sign of $\det(-H_m)$ is equivalent to that of $\det(-G_m)$. To evaluate the sign of $\det(-G_m)$, we use the following theorem introduced in [58] and lemmas.

Theorem 1. *If all the principal minors of a matrix are positive and all the elements off its main diagonal are negative, then all the elements of its inverse are positive [58].*

Lemma 1. *If A is a positive definite matrix whose elements are all positive, and Z is an all-zero matrix except it has an off diagonal positive element in the ith row and jth column which is less than the (i, j)th element of A, then $A - Z$ is also a positive definite matrix.*

Proof. Let's consider all principal submatrices of $A - Z$. Since only the (i, j)th element differs between $(A - Z)$ and A, up to the $\max(i - 1, j - 1)$th principal submatrix, their determinants are unchanged. If we assume $i < j$, then the jth and subsequent principal submatrices will have different determinants. Denote the jth principal submatrix of A as A_j and that of Z as Z_j. Then, we can define a matrix, X_j, where X_j is an all zero matrix except for its ith row, and satisfies

$$X_j = Z_j A_j^{-1}. \tag{A.15}$$

From Theorem 1, all elements of A_j^{-1} are negative except its diagonal element. Since there is only one positive element in Z_j, the nonzero diagonal element of X_j, x_{ii}, is negative. Then,

$$A_j - Z_j = (I - X_j)A_j \tag{A.16}$$

and

$$\det(A_j - Z_j) = \det(I - X_j)\det(A_j) = (1 - x_{ii})\det(A_j) > 0. \tag{A.17}$$

Therefore, the determinant of the jth principal submatrix is positive. In the same way, we can show the positiveness of all submatrices' determinants. Since all submatrices have positive determinant, the new matrix, $A - Z$, is positive definite. □

Lemma 2. *The following matrix is positive definite for any positive number a_m :*

$$F = \begin{pmatrix} 2a_m & a_m & a_m & \dots & a_m \\ a_m & 2a_m & a_m & \dots & a_m \\ a_m & a_m & 2a_m & \dots & a_m \\ \vdots & \vdots & \vdots & \ddots & \vdots \\ a_m & a_m & a_m & \dots & 2a_m \end{pmatrix}.$$

Proof. For the ith principal submatrix of F, F_i,

$$\det(F_i) = (a_m)^m 2 \frac{3}{2} \frac{4}{3} \cdots \frac{i+1}{i} > 0 \tag{A.18}$$

$\square$

With Lemma 1 and 2, $-G_m$ is positive definite, which implies that both $\det(-G_m)$ and $\det(-H_m)$ are positive for all m. Therefore, the Hessian matrix is negative definite and the average throughput is a concave function over $\underline{r}$.

Appendix B

Concavity of average throughput expression for the half-duplex relay system

The average throughput expression for the half-duplex relay system is equivalent to that for the baseline system except for its packet error probability. Instead of following all steps in the previous appendix, we show the following inequalities for the half duplex relay system :

$$\frac{\partial^2 \overline{\mathcal{T}}}{\partial {r_i}^2} < 0 \tag{B.1}$$

$$\frac{\partial^2 \overline{\mathcal{T}}}{\partial r_i \partial r_j} < 0 \tag{B.2}$$

$$-\frac{1}{2}\frac{\partial^2 \overline{\mathcal{T}}}{\partial r_i \partial r_j} + \frac{\partial^2 \overline{\mathcal{T}}}{\partial {r_i}^2} > 0 \tag{B.3}$$

$$-\frac{1}{2}\frac{\partial^2 \overline{\mathcal{T}}}{\partial r_i \partial r_j} + \frac{\partial^2 \overline{\mathcal{T}}}{\partial {r_j}^2} > 0, \tag{B.4}$$

where the superscript $'\mathrm{CoOp}'$ was dropped throughout this appendix and $r_c^{\mathrm{CoOp}}(i)$, $\overline{\mathcal{T}}_{\mathrm{CoOp}}(\underline{r}_c^{\mathrm{CoOp}})$, and the first and second partial derivatives of π_i^{CoOp} are denoted by r_i, $\overline{\mathcal{T}}$, π_i', and π_i'', respectively. Then, the remainder of the proof is equivalent to that of the baseline system. As shown in (II.24), the average error probability for

Table B.1: Decoding Error Probability of Half-duplex Relay System

General Form	$q(i,j) = \gamma_{\text{inc}}(\frac{1}{\overline{\gamma}_{sr}^{i}(N)} f(r_i), 1)$
Gaussian Inputs	$f(r_i) = 2^{2r_i} - 1$
BPSK Approx.	$f(r_i) = -\frac{\ln(1-2r_i)}{2b}$
BPSK Upper Bound (UB)	$f(r_i) = -\frac{\ln(2^{1-2r_i}-1)}{2}$

the jth packet in the relay system is given by

$$\pi_j = \sum_{\mathcal{D}_j} \text{Prob}(\mathcal{D}_j)\pi_j(\mathcal{D}_j), \tag{B.5}$$

where $\text{Prob}(\mathcal{D}_j)$ is the probability that the relay nodes in a set, $\mathcal{D}_j$, decode the jth source packet successfully, and $\pi_j(\mathcal{D}_j)$ is the probability that the jth packet is in error at the destination, conditioned on $\mathcal{D}_j$. With the high SNR assumption and the fact that, for small x, $\exp(-x) \approx 1 - x$, $\text{Prob}(\mathcal{D}_j)$ and $\pi_j(\mathcal{D}_j)$ can be approximated as [59]

$$\begin{aligned} \text{Prob}(\mathcal{D}_j) &= \left\{ \prod_{i \in \mathcal{D}_j} \left(1 - \gamma_{\text{inc}} \left(\frac{f(r_j)}{\overline{\gamma}_{sr}^{i} N}, 1 \right) \right) \right\} \times \left\{ \prod_{k \notin \mathcal{D}_j} \gamma_{\text{inc}} \left(\frac{f(r_j)}{\overline{\gamma}_{sr}^{k} N}, 1 \right) \right\} \\ &\approx \prod_{k \notin \mathcal{D}_j} \frac{f(r_j)}{\overline{\gamma}_{sr}^{k} N} \end{aligned} \tag{B.6}$$

and

$$\begin{aligned} &\pi_j(\mathcal{D}_j) \\ &= \quad \text{Prob} \left(\frac{\overline{\gamma}_{sd}(\alpha_{sd,j})^2}{\Omega_{sd}} + \sum_{l \in \mathcal{D}_j} \frac{\overline{\gamma}_{rd}^{l}(\alpha_{rd,j}^{l})^2}{\Omega_{rd}^{l}} < \frac{f(r_j)}{N} \right) \\ &\approx \quad \frac{1}{(|\mathcal{D}_j| + 1)!} \left(\frac{f(r_j)}{N} \right)^{|\mathcal{D}_j|+1} \frac{1}{\overline{\gamma}_{sd}} \prod_{l \in \mathcal{D}_j} \frac{1}{\overline{\gamma}_{rd}^{l}}. \end{aligned} \tag{B.7}$$

With (B.6) and (B.7), π_j and its derivatives are approximated as

$$\pi_j \approx \sum_{\mathcal{D}_j} \frac{1}{(|\mathcal{D}_j|+1)!} \left(\frac{f(r_j)}{N}\right)^N \frac{1}{\overline{\gamma}_{sd}} \prod_{k\notin\mathcal{D}_j} \frac{1}{\overline{\gamma}_{sr}^k} \prod_{l\in\mathcal{D}_j} \frac{1}{\overline{\gamma}_{rd}^l} \tag{B.8}$$

$$\pi_j' \approx \left(\frac{f(r_j)}{N}\right)^{N-1} f'(r_j) \sum_{\mathcal{D}_j} \frac{1}{(|\mathcal{D}_j|+1)!} \frac{1}{\overline{\gamma}_{sd}} \prod_{k\notin\mathcal{D}_j} \frac{1}{\overline{\gamma}_{sr}^k} \prod_{l\in\mathcal{D}_j} \frac{1}{\overline{\gamma}_{rd}^l} \tag{B.9}$$

$$\pi_j'' \approx \frac{(f(r_j))^{N-2}}{N^{N-1}} \Big((N-1)(f'(r_j))^2 + f(r_j)f''(r_j)\Big) \cdot$$

$$\sum_{\mathcal{D}_j} \frac{1}{(|\mathcal{D}_j|+1)!} \frac{1}{\overline{\gamma}_{sd}} \prod_{k\notin\mathcal{D}_j} \frac{1}{\overline{\gamma}_{sr}^k} \prod_{l\in\mathcal{D}_j} \frac{1}{\overline{\gamma}_{rd}^l}. \tag{B.10}$$

(B.11)

Note that $f'(r_j)$ and $f''(r_j)$ are positive for any inputs. Therefore, the approximations of both π_j' and π_j'' are positive, and (B.1), (B.3), and (B.4) can be proved as shown in the previous appendix. To prove the remaining inequality, we define

$$L_j = \sum_{\mathcal{D}_j} \frac{1}{(|\mathcal{D}_j|+1)!} \frac{1}{\overline{\gamma}_{sd}} \prod_{k\notin\mathcal{D}_j} \frac{1}{\overline{\gamma}_{sr}^k} \prod_{l\in\mathcal{D}_j} \frac{1}{\overline{\gamma}_{rd}^l}.$$

Then, the approximation of $\frac{\partial^2\overline{\mathcal{T}}}{\partial r_i \partial r_j}$ is shown as

$$\begin{aligned}\frac{\partial^2\overline{\mathcal{T}}}{\partial r_i \partial r_j} \approx\ & -L_i \left(\frac{f(r_i)}{N}\right)^{N-1} f'(r_i) \prod_{k=1,k\neq i}^{j} (1-\pi_k) \\ & + L_i^2 \left(\frac{f(r_i)}{N}\right)^{N-1} f'(r_i) \left(\frac{f(r_j)}{N}\right)^{N-1} f'(r_j) \sum_{l=j}^{M} r_l \prod_{k=1,k\neq i,j}^{l} (1-\pi_k),\end{aligned} \tag{B.12}$$

where L_i is equivalent to L_j, since the possible sets of $\mathcal{D}_j$ are the same as the possible sets of $\mathcal{D}_i$. Since $f(r_i)$ and $f'(r_i)$ are limited by $f(\max\{R\})$ and $f'(\max\{R\})$, the second term will be relatively small if the SNR is high enough, and then

$$\frac{\partial^2\overline{\mathcal{T}}}{\partial r_i \partial r_j} \approx -L_i \left(\frac{f(r_i)}{N}\right)^{N-1} f'(r_i) \prod_{k=1,k\neq i}^{j} (1-\pi_k) < 0.$$

Appendix C

Optimization of source-channel rate allocation

Due to the concavity of the average throughput expression, the optimal UEP is the peak of the expression, if it exists. The peak can be found by M partial differentiations as follows :

$$\frac{\partial \overline{\mathcal{T}}}{\partial r_i} = 0 \quad i = 1, \ldots, M. \tag{C.1}$$

If there is no solution for the ith equation, then the ith element of the optimal UEP is $\min\{R\}$ or $\max\{R\}$. In particular, $\frac{\partial \overline{\mathcal{T}}}{\partial r_M}$ will be

$$\frac{\partial \overline{\mathcal{T}}}{\partial r_M} = (1 - \pi_M) - r_M \pi'_M = 0. \tag{C.2}$$

That is, we can find the optimum rate of the last packet first and then find the rate of the $(M-1)$th packet recursively. This recursive algorithm is equivalent to that introduced in [39].

Bibliography

[1] T. Yoo, E. Setton, X. Zhu, A. Goldsmith, and B. Girod. Cross-layer design for video streaming over wireless ad hoc networks. *IEEE Workshop on Multimedia Signal Processing*, 2004.

[2] van D. Schaar and N.S. Shankar. Cross-layer wireless multimedia transmission:challenges, principles, and new paradigms. *IEEE Transactions on Wireless Communications*, 12(4):350–358, Aug 2005.

[3] F. Foukalas, V. Gazis, and N. Alonistioti. Cross-layer design proposals for wireless networks: a survey and taxonomy. *IEEE Communicationns Survey Tutorials*, 10(1):70–85, 2008.

[4] H. Wang, W. Wang, S. Wu, and K. Hua. A survey on the cross-layer design for wireless multimedia sensor networks. *Mobile Wireless Middleware, Operating Systems, and Appplications*, 48:474–486, 2010.

[5] J. Park, H. Lee, S. Lee, and A.C. Bovik. Optimal channel adaptation of scalable video over a multicarrier-based multicell environment. *IEEE Transactions on Multimedia*, 11(6):1062–1071, Oct 2009.

[6] C.-M. Chen, Y.-R. Setton, C.-W. Lin, and Y.-C. Chen. Error resilience transcoding using prioritized intra-refresh for video multicast over wireless networks. *IEEE International Conference on Multimedia and Expo*, 2005.

[7] D. Taubman and M.W. Marcellin. *JPEG2000 : Image compression fundamentals, standards, and practice*. Kluwer Academic Publishers, Boston, 2002.

[8] J.M. Shapiro. Embedded image coding using zerotree of wavelet coefficients. *IEEE Transactions on Signal Processing*, 41(12):3445–3462, Dec 1993.

[9] A. Said and W.A. Pearlman. A new, fast and efficient image codec based on set partitioning in hierarchical trees. *IEEE Transactions on Circuits and Systems for Video Technology*, 6(3):243–250, Jun 1996.

[10] W. Li. Overview of fine granularity scalability in MPEG-4 video standard. *IEEE Transactions on Circuits and Systems for Video Technology*, 11(3):301–317, Mar 2001.

[11] T.-L. Lin, S. Kanumuri, Z. Yuan, D. Poole, P.C. Cosman, and A.R. Reibman. A versatile model for packet loss visibility and its application to packet prioritization. *IEEE Transactions on Image Processing*, 19(3):722–735, Mar 2010.

[12] P.G. Sherwood and K. Zeger. Progressive image coding for noisy channels. *IEEE Signal Processing Letters*, 4(7):189–191, Jul 1997.

[13] P.G. Sherwood, T. Xiaodong, and K. Zeger. Channel code blocklength and rate optimization for progressive image transmission. *Proceedings of the IEEE Wireless Communications and Networking Conference*, 1999.

[14] V. Chande and N. Farvardin. Progressive transmission of images over memoryless noisy channels. *IEEE Journal on Selected Areas in Communications*, 18(6):850–860, Jun 2000.

[15] A. Nosratinia, J. Lu, and B. Aazhang. Source-channel rate allocation for progressive transmission of images. *IEEE Transactions on Communications*, 51(2):186–196, Feb 2003.

[16] D. Gunduz and E. Erkip. Source and Channel Coding for Quasi-Static Fading Channels. *Asilomar Conference on Signals, Systems and Computers*, 2005.

[17] F. Etemadi and H. Jafarkhani. A Unified Framework for Layered Transmission Over Fading and Packet Erasure Channels. *IEEE Transactions on Communications*, 56(4):565–573, Apr 2008.

[18] D. Gunduz and E. Erkip. Joint source-channel codes for MIMO block-fading channels. *IEEE Transactions on Information Theory*, 54(1):116–134, Jan 2008.

[19] D. Gunduz and E. Erkip. Source and Channel Coding for Cooperative Relaying. *IEEE Transactions on Information Theory*, 53(10):3454–3475, Oct 2007.

[20] Y. Yang, H. Hu, and G. Mao. Relay technologies for WiMAX and LTE-advanced mobile systems. *IEEE Communications Magazine*, 47(10):100–105, Oct 2009.

[21] H. Kim, R. Annavajjalla, P.C. Cosman, and L.B. Milstein. Source-channel rate optimization for progressive image transmission over block fading relay channels. *IEEE Transactions on Communications*, 58(6):1631–1642, Jun 2010.

[22] H.Y. Shutoy, D. Gunduz, E. Erkip, and Y. Wang. Cooperative Source and Channel Coding for Wireless Multimedia Communications. *IEEE Journal of Selected Topics in Signal Processing*, 1(2):295–307, Aug 2007.

[23] O. Alay, T. Korakis, Y. Wang, E. Erkip, and S. Panwar. Layered wireless video multicast using omni-directional relays. *IEEE International Conference on Acoustics, Speech and Signal Processing*, 2008.

[24] K. Doppler, M. Rinne, C. Wijting, C. Ribeiro, and K. Hugl. Device-to-device communication as an underlay to LTE-advanced networks. *IEEE Communications Magazine*, 47(12):42–49, Dec 2009.

[25] M. Kornfeld and G. May. DVB-H and IP datacast-broadcast to handheld devices. *IEEE Transactions on Broadcasting*, 53(1):161–170, Mar 2007.

[26] M.R. Chari, F. Ling, A. Mantravadi, R. Krishnamoorthi, R. Vijayan, G.K. Walker, and R. Chandhok. FLO physical layer: an overview. *IEEE Transactions on Broadcasting*, 53(1):145–160, Mar 2007.

[27] P. Popovski and E. de Carvalho. Improving the rates in wireless relay systems through superposition coding. *IEEE Transactions on Wireless Communications*, 7(12):4831–4836, Dec 2008.

[28] A.K. Goparaju, S. Wei, and Y. Liu. On superposition coding based cooperative diversity schemes. *Asilomar Conference on Signals, Systems and Computers*, 2005.

[29] M. van der Schaar and H. Radha. Adaptive motion-compensation fine granular-scalability (AMC-FGS) for wireless video. *IEEE Transactions on Circuits and Systems for Video Technology*, 12(6):360–371, Jun 2002.

[30] H.-C. Huang, C.-N. Wang, and T. Chiang. A robust fine granularity scalability using Trellis-based predictive leak. *IEEE Transactions on Circuits and Systems for Video Technology*, 12(6):372–385, Jun 2002.

[31] Y.S. Chan, P.C. Cosman, and L.B. Milstein. A multiple description coding and delivery scheme for motion-compensated fine granularity scalable video. *IEEE Transactions on Image Processing*, 17(8):1353–1367, Aug 2008.

[32] R. Hamzaoui, V. Stankovic, and Z. Xiong. Optimized error protection of scalable image bit streams [advances in joint source-channel coding for images]. *IEEE Signal Processing Magazine*, 22(6):91–107, Nov 2005.

[33] T.M. Cover and J.A. Thomas. *Elements of Information Theory*. John Wiley, New York, 1990.

[34] W. He and C.N. Georghiades. Computing the capacity of a MIMO fading channel under PSK signaling. *IEEE Transactions on Information Theory*, 51(5):1794–1803, May 2005.

[35] E. Baccarelli. Evaluation of the reliable data rates supported by multiple-antenna coded wireless links for QAM transmissions. *IEEE Journal on Selected Areas in Communications*, 19(2):295–304, Feb 2001.

[36] W. Li, H. Yang, and D. Yang. Simple approximation formula for the symmetric capacity. *International Conference on Wireless and Mobile Communications*, 2007.

[37] T.F. Wong. Numerical calculation of symmetric capacity of Rayleigh fading channel with BPSK/QPSK. *IEEE Communications Letters*, 5(8):328–330, Aug 2001.

[38] W. He and C.N. Georghiades. Approximation to the symmetric capacity of Rayleigh fading channels with multi-level signals. *IEEE Communications Letters*, 10(3):129–131, Mar 2006.

[39] V. Stankovic, R. Hamzaoui, and D. Saupe. Fast algorithm for rate-based optimal error protection of embedded codes. *IEEE Transactions on Communications*, 51(11):1788–1795, Nov 2003.

[40] N. Prasad and M.K. Varanasi. Outage Theorems for MIMO Block-Fading Channels. *IEEE Transactions on Information Theory*, 52(12):5284–5296, Dec 2006.

[41] L.H. Ozarow, S. Shamai, and A.D. Wyner. Information theoretic considerations for cellular mobile radio. *IEEE Transactions on Vehicular Technology*, 43(2):359–378, May 1994.

[42] M. Abramowitz and I.A. Stegun. *Handbook of Mathematical Functions with Formulas, Graphs, and Mathematical Tables*. Dover, New York, 1990.

[43] S. Benedetto and G. Montorsi. Unveiling turbo codes: some results on parallel concatenated coding schemes. *IEEE Transactions on Information Theory*, 42(2):409–428, Mar 1995.

[44] ETSI. EN 300 744, V1.5.1, DIgital Video Broadcasting (DVB) : framing structure, channel coding and modulation for digital terrestrial television. 2004.

[45] M. Yuksel and E. Erkip. Broadcast strategies for the fading relay channel. *IEEE Military Communications Conference*, 2004.

[46] IEEE. 802.16m Evaluation Methodology Document (EMD), IEEE 802.16m-08/004r5. 2009.

[47] J.H. Winters. Optimum combining in digital mobile radio with cochannel interference. *IEEE Transactions on Vehicular Technology*, 33(3):144–155, Aug 1984.

[48] F. Wu, S. Li, and Y-Q. Zhang. A framework for efficient progressive fine granularity scalable video coding. *IEEE Transactions on Circuits and Systems for Video Technology*, 11(3):332–344, Mar 2001.

[49] A. Kwasinski and K.J.R. Liu. Optimal Unequal Error Protection with User Cooperation for Transmission of Embedded Source-Coded Images. *IEEE International Conference on Image Processing*, 2006.

[50] J.K. Cavers. An analysis of pilot symbol assisted modulation for Rayleigh fading channels. *IEEE Transactions on Vehicular Technology*, 40(4):686–693, Nov 1991.

[51] K. Lee and J. Chun. Symbol detection in V-BLAST architectures under channel estimation errors. *IEEE Transactions on Wireless Communications*, 6(2):593–597, Feb 2007.

[52] H. Jafarkhani. A quasi-orthogonal space-time block code. *IEEE Transactions on Communications*, 49(1):1–4, Jan 2001.

[53] A. Paulraj, R. Nabar, and D. Gore. *Introduction to Space-Time Wireless Communications*. Cambridge University Press, U.K., U.K., 2003.

[54] 3GPP. Technical specification group radio access network : multiple input multiple output in UTRA, 3GPP, Technical Report, 25.876 V1.7.0. 2004.

[55] J. Wu, J. Cai, and C. W. Chen. Rate-distortion analysis of leaky prediction based FGS video for constant quality constrained rate adaptation. *Journal of Visual Communications and Image Representation*, 18(14):45–58, Feb 2007.

[56] J. Sun, W. Gao, D. Zhao, and Q. Huang. Statistical model, analysis and approximation of rate-distortion function in MPEG-4 FGS videos. *IEEE Transactions on Circuits and Systems for Video Technology*, 16(4):535–539, Apr 2006.

[57] H. Lee, R.W. Heath, and E.J. Powers. Information outage probability and diversity order of Alamouti transmit diversity in time-selective fading channels. *IEEE Transactions on Vehicular Technology*, 57(6):3890–3895, Nov 2008.

[58] H.E. Goheen. On a lemma of Stieltjes on Matrices. *American Mathematical Monthly*, 43(5):359–378, May 1949.

[59] R. Annavajjala, P.C. Cosman, and L.B. Milstein. Statistical channel knowledge-based optimum power allocation for relaying protocols in the high SNR regime. *IEEE Journal on Selected Areas in Communications*, 25(2):292–305, Feb 2007.